Danish Meteorological Institute

Ministry of Transport

Scientific Report 06-07

EUCOS space/terrestrial OSE study using the DMI-HIRLAM 3D-Var data assimilation system. Part I: A winter period

Bjarne Amstrup

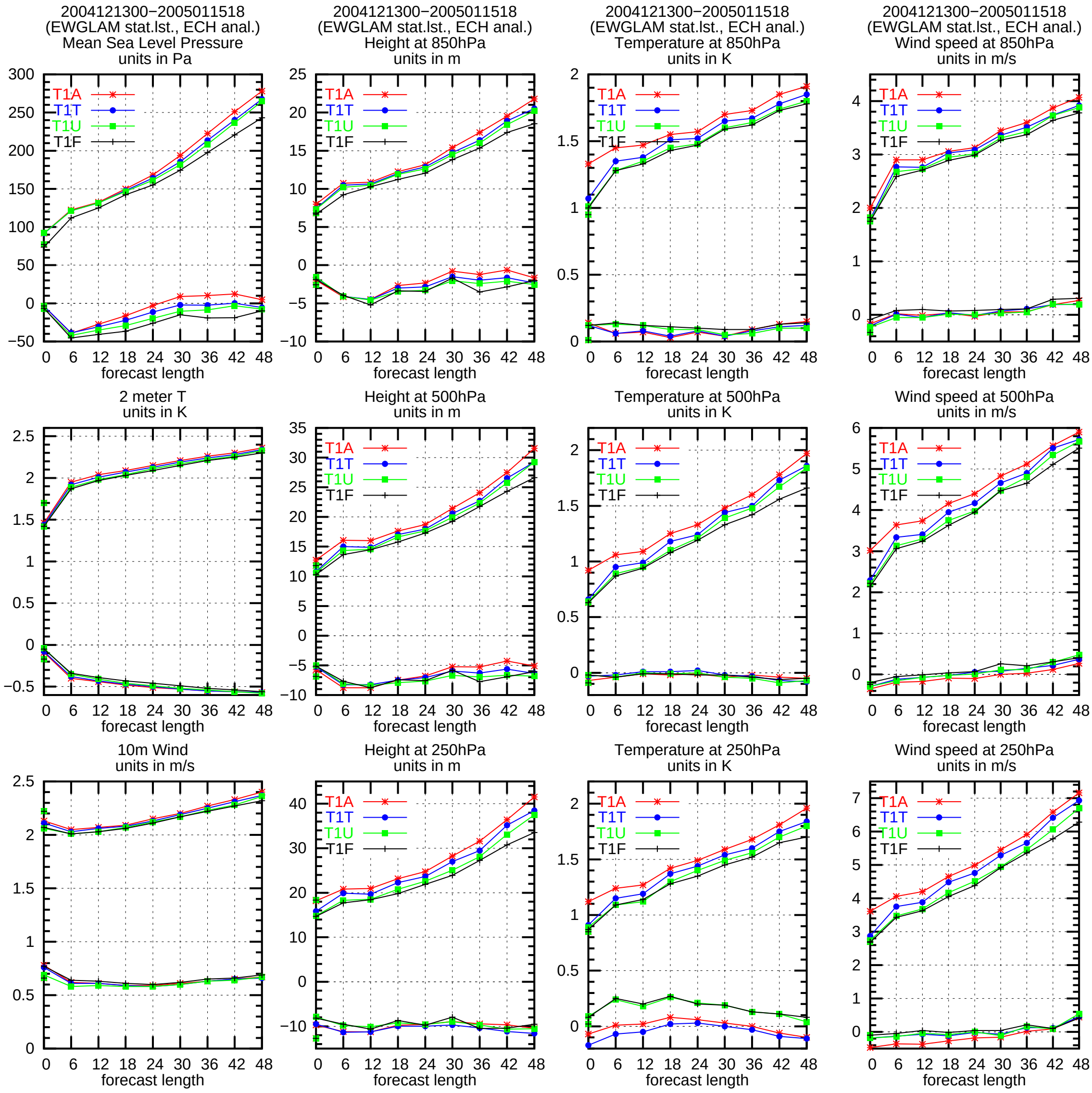

Colophone Serial title:
Scientific Report 06-07

Title:
EUCOS space/terrestrial OSE study using the DMI-HIRLAM 3D-Var data assimilation system. Part I: A winter period

Subtitle:

Authors:
Bjarne Amstrup

Other Contributers:

Responsible Institution:
Danish Meteorological Institute

Language:
English

Keywords:
HIRLAM, Observing System Experiments, EUCOS

Url:
www.dmi.dk/dmi/sr06-07

ISSN:
1399-1949

Version:

Link til hjemmeside:
www.dmi.dk

Contents

Abstract

EUCOS has decided to make an assessment of the impact on NWP forecasts of different components of the current observing systems in various combinations. As part of this a number of OSEs (Observing System Experiments) has to be executed by NWP centres. Both some running global models and by centres running limited area models. The Danish Meteorological Institute was one of the centres to make OSEs with a limited area model (HIRLAM). The lateral boundaries for these OSEs are provided by runs made by ECMWF (one of the centres to make OSEs with global models). Since the OSEs are to be made by the then operational HIRLAM model at DMI it is quite computer intensive. The following runs have been made by DMI (two periods one month each): 1) Baseline system (BL); 2) BL + all aircraft; 3) BL + non-GUAN wind; 4) BL + non-GUAN temp and wind; 5) BL + wind-profiler; 6) as (4) + aircraft; 7i) as (4) + non-GUAN humidity; 8) as BL + all in-situ data (full combined system); and 9) BL + E-AMDAR.

The results from the winter period run are presented in this report. The main conclusions are that the radiosonde data are the most important data, closely followed by the aircraft data; and that aircraft data and radiosonde data are complementary and not redundant data. Furthermore the results show that it is important to have both wind and temperature data – wind data alone give much poorer impact.

Resumé

I dette projekt, iværksat af EUCOS (EUMETNET (European Meteorological Network) Composite Observing System), undersøges indflydelsen af forskellige typer in situ ("terrestrial") vind- og temperaturmålinger på prognosemodellernes analyser og, via det, indflydelsen på prognosernes kvalitet. Denne undersøgelse, sammen med tilsvarende undersøgelser ved andre institutter, er iværksat med henblik på den fremtidige strategi for observationsnetværket.

I modsætning til normalt, hvor man bruger det fulde sæt af observationer som udgangspunkt, tager man her udgangspunkt i det fulde sæt af satellitobservationer som bruges i analyserne, samt et minimalt sæt af radiosonde- (GUAN (GCOS (Global Climate Observing System) Upper-Air Network) netværket) og SYNOP-målinger (GSN (GCOS Surface Network) netværket) samt alle overfladebøjemålinger. Der laves test i en vinterperiode (medio december 2004 til medio januar 2005) og i en sommermåned (august 2005). Indflydelsen af følgende observationer i forhold til det ovennævnte grundsæt undersøges: 1) Alle flyobservationer (vind og temperatur), 2) vindmålinger fra de øvrige (d.v.s. "non-GUAN") radiosonder, 3) vind- og temperaturmålinger fra de øvrige radiosonder, 4) vindmålinger fra windprofilers, 5) vind- og temperaturmålinger fra de øvrige radiosonder og fra fly, 6) vind-, temperatur- og fugtighedsmålinger fra de øvrige radiosonder, 7) vind- og temperaturmålinger fra EUCOS AMDAR (Aircraft Meteorological Data Relay), og 8) alle tidligere ekskluderede in situ data (dvs. det fulde observationssystem). Denne rapport indeholder resultaterne fra vinterperioden og de væsentligste konklusioner er, at radiosondedata stadig er de vigtigste in situ data til brug i prognosemodellernes analyser skarp forfulgt af data fra fly; og at data fra fly komplementerer radiosondedata og er således ikke redundante. Desuden viser resultaterne at det er vigtigt med både vind- og temperaturobservationer. Vindobservationer alene er ikke tilstrækkeligt for at få en effektiv virkning.

1 Introduction

Normally observing system experiments (OSEs) at DMI are made by either adding a new data type to or denying a data type from the *full* set of observations used in operations (see, e.g. Amstrup, 2000; Amstrup and Mogensen, 2000; Amstrup, 2001; Amstrup and Mogensen, 2004; Amstrup, 2004; Vedel and Huang, 2004; Guerrero and Amstrup, 2005. See also Vignes *et al.*, 2005). This large set of "basic" observations makes it difficult to identify a (significant) impact in an OSE from a particular type of observations. That DMI operational analyses are further improved by reanalyses twice (now four times) a day, in which 4D-Var ECMWF[1] analyses are blended (see next section) into the HIRLAM[2] analysis, makes it even more difficult. The same is to a certain extent the case in the European area for centers running global forecasting models (see, e.g., Graham *et al.*, 1998; Lacroix *et al.*, 1998; Gérard and Saunders, 1999; Deblonde, 1999; English *et al.*, 2000; Tomassini *et al.*, 1999; Bouttier and Kelly, 2001; Bormann *et al.*, 2003; Cardinali *et al.*, 2003; Köpken *et al.*, 2003; Marécal and Mahfouf, 2003; Isaksen and Janssen, 2004; Bormann and Thépaut, 2004; Langland and Baker, 2004; Fourrié *et al.*, 2006; Healy and Thépaut, 2006; McNally *et al.*, 2006; Andersson *et al.*, 2006; Okamoto and Derber, 2006).

In this study, initiated by EUCOS[3] and EUMETSAT[4], the impact of different terrestrial (in situ) observing systems is investigated by adding selected terrestrail datasets to the full set of satellite data used in operations and a very limited basic set of terrestrial observations.

The forecasting and analysis system used in these OSEs is based on the HIRLAM reference system including a 3D-Var analysis scheme (Gustafsson *et al.*, 2001; Lindskog *et al.*, 2001) and a forecast model (Undén *et al.*, 2002), both with some local DMI modifications.

The set of OSEs is briefly described in Table 1, including the model names used in the figures and tables in this report.

Table 1: OSE description with experiment names in the column "model". See section 2.4 for further details and comments.

model	Description
T1A	Control/baseline run (with GUAN radiosondes)
T1B	as T1A plus addition of all aircraft data
T1W	as T1A plus addition of all wind data from non-GUAN radiosondes
T1T	as T1A plus addition of all wind and temperature data from non-GUAN radiosondes
T1V	as T1A plus addition of wind profiler data
T1D	as T1A plus addition of data from non-GUAN radiosondes
T1X	as T1A plus addition of E-AMDAR data
T1Y	as T1X plus addition of E-AMDAR data from ECMWF archive
T1U	as T1T plus addition of all aircraft data
T1F	'all' observations and use of similar ECMWF run for lateral boundaries

The report is organized in the following way: Section 2 describes the setup used for these OSEs, section 3 gives the results obtained in terms of verification measures and other statistics, and finally the conclusions are given

[1] European Centre for Medium-Range Weather Forecasts
[2] High Resolution Limited Area Model
[3] EUMETNET Composite Observing System
[4] European Organisation for the Exploitation of Meteorological Satellites

in section 4.

2 Experimental set-up

The experimental set-up is based on the operational DMI-HIRLAM set-up in the summer 2005 (Yang *et al.*, 2005b), with some updates to the 3D-Var system applied to the operational set-up in November 2005. The model version DMI-HIRLAM-T15 (T15) was run in all the experiments. In addition the model version DMI-HIRLAM-S05 (S05) was run in two of the experiments, to illustrate that the impact from the observations to a large extent are carried over to S05, via analysis increments from T15 used as analysis increments in S05 (the results are not shown here).

2.1 Domain(s)

The operational DMI-HIRLAM model domains from late summer 2005 are shown in Figure 1. All domains are defined on a rotated grid. The polar coordinates $(P_{\rm lat}, P_{\rm lon})$, the starting coordinates (southwest corner) in the rotated coordinate system, and model resolutions for the two domains covering Denmark are given in Table 2.

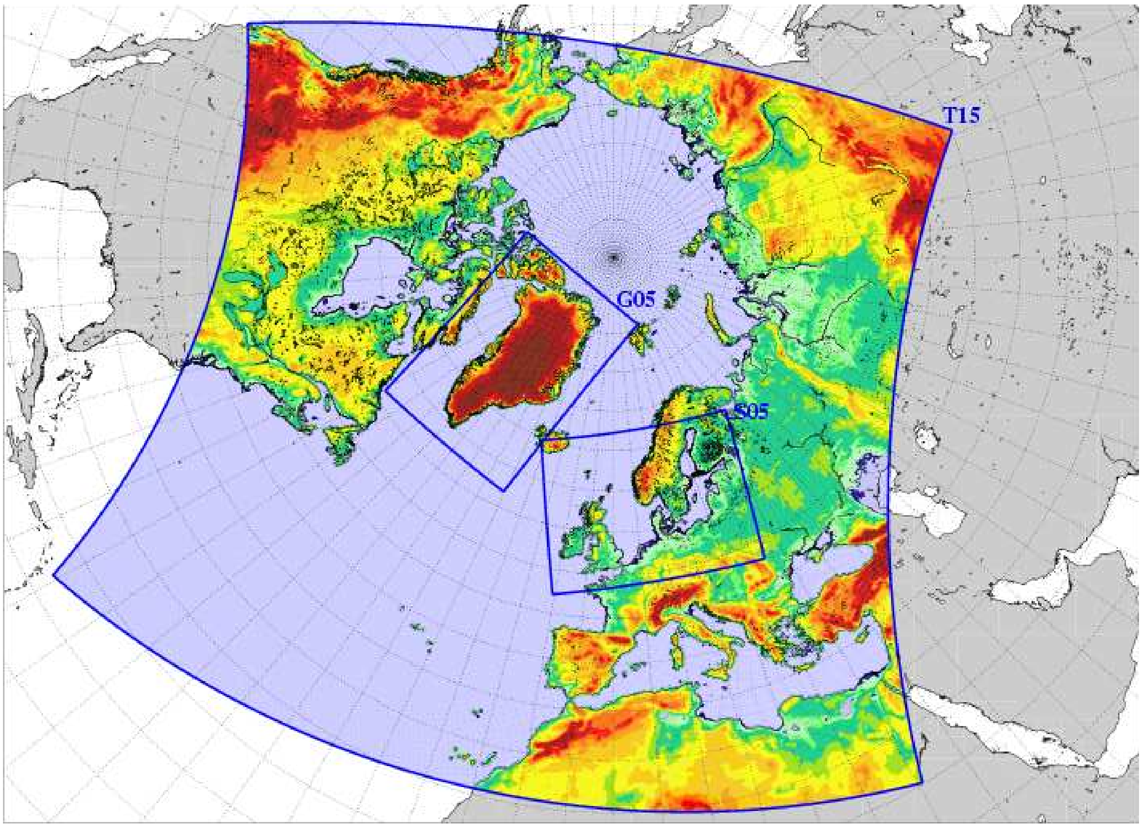

Figure 1: Operational DMI-HIRLAM areas from late August 2005. DMI-HIRLAM-T15 (large area), DMI-HIRLAM-Q05 (G05) and DMI-HIRLAM-S05 all have 40 vertical levels. The horizontal resolution of DMI-HIRLAM-T15 is $0.15° \times 0.15°$ and the horizontal resolution of DMI-HIRLAM-S05 and DMI-HIRLAM-Q05 is $0.05° \times 0.05°$.

2.2 Forecast model and lateral boundary files

The model grid is a rotated, regular lat.-lon. Arakawa C grid, with 40 vertical levels in the atmosphere and the model top at 10 hPa. The forecast system is based on HIRLAM reference version 6.2.3 (see Undén *et al.*, 2002 for a more detailed description of the reference system) with a number of modifications. The following options and specifications apply to the system:

Table 2: Model variables for DMI operational runs. $(P_{\rm lon}, P_{\rm lat})$ are the geographical coordinates of the rotated south pole. $(x_{\rm lon,1}, y_{\rm lat,1})$ are the coordinates of the southwest corner of the model area in the rotated grid. See text for changes to this in the present set-up used for the EUCOS OSEs.

Model Identification	T15	S05
grid points (mlon)	610	496
grid points (mlat)	568	372
no. of vertical levels	40	40
horizontal resolution	0.15°	0.05°
hor. res. (assimilation)	0.15°	—
$(P_{\rm lon}, P_{\rm lat})$	$(80°, 0°)$	$(10°, -40°)$
$x_{\rm lon,1}$	$-64.325°$	$-13.675°$
$y_{\rm lat,1}$	$-37.527°$	$-1.027°$
time step (dynamics)	360 s	120 s
time step (physics)	360 s	120 s
boundary age (in forec.)	6 h	0 h
boundary age (in ass.)	0 h–6 h	0 h
host model	ECMWF	T15
boundary frequency	1/(3 h)	1/(1 h)
data assimilation cycle	3 h	6 h
forecast length (long)	60	54
long forecasts per day	4	4

- HIRLAM 6.2.3 physics with recent extensions (of which some are mentioned below).
- Semi-Lagrangian dynamics option (SETTLS option is true, see Lindberg, 2005).
- Incremental digital filter initialization.
- Implicit 6'th order horizontal diffusion.
- The HIRLAM 6.2.5 experimental version of the CBR scheme is used. The parameterization of turbulence is based upon turbulent kinetic energy (TKE).
- ISBA[5] surface scheme and surface analysis is used. However, upgrades to the SST- and ice-analysis have been made. ECMWF disseminated SST-data and ice-data are used more efficiently to update sea surface temperature and for diagnosing fraction of ice. This is of particular importance close to coastal areas. In addition SSTs from the Ocean & Sea Ice SAF[6] are used.
- The STRACO convection scheme is used (Sass, 2002).
- Schedule: 3-hourly data assimilation cycles for T15. Long forecasts for 00 UTC, 06 UTC, 12 UTC and 18 UTC for T15 and S05. DMI-HIRLAM-T15 is restarted via blending from ECMWF 3D-Var analysis

[5] Integrated Soil Biosphere Atmosphere
[6] Satellite Application Facility

Table 3: Operational time schedule for T15 and S05 used in June 2005. The times in the left column indicate the start of the preprocessing of boundary data and ISBA. The 3D-Var analysis (for DMI-HIRLAM-T15) begins ca. 5-7 min later. T_E denotes reanalysis and blending from ECMWF analysis. See text for details.

UTC	T	S
1:37	T00+60 h	
2:29		S00+54 h
ECMWF 00 UTC		
7:37	T06+60 h	
8:29		S06+54 h
ECMWF 06 UTC		
11:45	T_E00+05 h T03+05 h T06+05 h T09+05 h	
12:43		S00+03 h S03+03 h S06+03 h S09+03 h
13:37	T12+60 h	
14:29		S12+54 h
ECMWF 12 UTC		
19:37	T18+60 h	
20:29		S18+54 h
ECMWF 18 UTC		
23:50	T_E12+05 h T15+05 h T18+05 h T21+05 h	
24:48		S12+03 h S15+03 h S18+03 h S21+03 h

(here the ECMWF 4D-Var analysis) (0.45° resolution) twice a day before the long 00 UTC and 12 UTC runs (see Yang *et al.*, 2005a for further details on the blending scheme). Normal HIRLAM cycles then follow (03 UTC, 06 UTC, 09 UTC) in the morning for T15 to produce an ‘up-to-date’ status of the atmosphere. In the evening the subsequent analyses are valid at 15 UTC, 18 UTC and 21 UTC respectively. Table 3 shows the operational schedule as of June 2005 for T15 and S05. As an example ‘T06+5 h’ denote a T15 analysis valid at 06 UTC followed by a 5 h forecast. For S05 6-hourly updates are made and no reassimilation.

▷ Adjustment of diagnostics for V10m, T2m and RH2m (see Geleyn, 1998) and an improved algorithm for calculation of msl pressure from surface pressure (Feddersen, 2004).

▷ The “vegetation” roughness and “thermal” roughness over land have been modified.

▷ Adaption of the analysis increment method for the high resolution model DMI-HIRLAM-S05 using analyses from DMI-HIRLAM-T15.

The basic model applied in the present OSE study is DMI-HIRLAM-T15, using the forecast model version operational June 2005. The resolution of the (disseminated) ECMWF sst- and ice-fields used is 0.5°. As listed in Table 2, the horizontal resolution of DMI-HIRLAM-T15 is $0.15°$, the number of vertical levels 40, the number of grid points is 610×568, the dynamics as well as the physics time step is 360 s and the lateral boundary values are updated every 3 hours from ECMWF (the so called "frames" boundaries) 00 UTC or 12 UTC forecasts (operationally ECMWF 06 UTC and 18 UTC forecasts are used as well). Long (48 hour) forecasts are made at the four major synoptic times (00, 06, 12 and 18 UTC).

As mentioned, the lateral boundaries for the operational T15 runs are 3 hourly so called FRAMES (with 0.45° horizontal resolution) disseminated from ECMWF. They are 6 h older than the forecasts for the long runs. However, the ECMWF baseline runs do not include 06 UTC and 18 UTC forecasts, and accordingly 12 h old lateral boundaries are used for the long 00 UTC and 12 UTC runs in these tests. The number of passive boundary points used for lateral boundary conditions in the forecasts is 12.

As mentioned, a reassimilation is made before the long 00 UTC and 12 UTC runs. This is done in order to take advantage of both the extra observations that arrive after the relative short cut off for the long runs, and also to take advantage of the ECMWF analyses. The ECMWF analyses are expected to be somewhat better on 'large scale', since they use much more observations than DMI (in particular satellite data), and are based on 4D-Var rather than 3D-Var. Therefore, a new analysis is made, and based on this analysis and large scale blending of the ECMWF analysis a short forecast is made. Subsequently, further analyses and short forecasts are made to make up-to-date first guess fields for the following long forecast run at 12 UTC or 00 UTC.

2.3 3D-Var and observation types used

The analysis version used here is the HIRLAM 3D-Var 6.3.6 MPI version, modified to use RTTOV8[7] developed in the Numerical Weather Prediction SAF[8] project set up by EUMETSAT (see Schyberg *et al.*, 2003 for further details on the use of ATOVS data in the HIRLAM 3D-Var system). The observation window covers a 6 h span around the analysis times 06 UTC and 18 UTC before the long forecasts starting from these. For the other runs the observation window covers a 3 h span around the analysis times (00, 03, 06, 09, 12, 15, 18, 21 UTC).

It should be noted that the background error statistics is based on rather old, non-separable structure functions made by "the NMC method" (See Berre, 2000; Gustafsson *et al.*, 2001 and references therein for further details), calculated from differences between $+24$ h and $+48$ h forecasts valid at the same time from the 1997-1998 operational SMHI forecast model with a horizontal resolution of $0.4° \times 0.4°$ and 31 vertical levels. This set of data has subsequently been interpolated to a set of data appropriate for the 40 vertical levels used here. In an upgrade in November 2005, this was changed to using a revised set, based on similar statistics made using recent operational T15 data instead. It is also being investigated how the relation between background errors and observation errors can be tuned (see Navascués *et al.*, 2006), since they are not optimal anymore.

Since November 2005 the following observation types have been used operationally in the DMI-HIRLAM system: SYNOP (surface pressure), SHIP (surface pressure), DRIBU (surface pressure), PILOT (wind at all levels), TEMP (wind, temperature and humidity at all observed levels), AIREP (wind and temperature; includes AMDAR[9] and ACARS[10]), NOAA15[11] and NOAA16 AMSU-A[12] brightness temperature data from channels 1-10 (effectively only channels 4-10 over open sea and channels 6-10 over sea ice) are included (from local

[7] Radiative Transfer model for TOVS, release 8
[8] Satellite Application Facility
[9] Aircraft Meteorological Data Relay
[10] Aircraft Communication Addressing and Reporting System
[11] NOAA: National Oceanic and Atmospheric Administration
[12] Advanced Microwave Sounding Unit-A

Table 4: Observation error standard deviations for AMV wind.

Pressure (hPa)	1000	850	700	500	400	300	250	200
u/v (m/s)	2.00	2.00	2.00	2.45	3.10	3.60	3.80	3.80
Pressure (hPa)		150	100	70	50	30	20	10
u/v (m/s)		5.00	5.00	5.00	5.00	5.00	5.00	5.70

Table 5: Diagonal elements of observation covariance matrix for NOAA15 and NOAA16 AMSU-A. Values (σ^2) are in kelvin squared. Non diagonal elements are set to 0.

Channel #:	1-3	4	5	6	7	8	9	10
Open sea	900	1.40	0.35	0.35	0.35	0.35	0.70	1.40
Sea ice	9×10^6	9×10^6	9×10^6	1.40	0.35	0.35	0.70	1.40

receiving stations and via EARS[13]), Meteosat-8 AMV[14] winds and QuikScat winds (near surface wind data from the SeaWinds scatterometer; see Portabella and Stoffelen, 2004, and references therein). The AMSU-A data are thinned to 0.9° for NOAA15 and NOAA16 data separately. The redundancy check of aircraft data is done in vertical intervals of 10 hPa: One of two measurements are discarded in the redundancy check if they differ by less than 10 hPa and a distance of less than half a grid point (see also Amstrup and Mogensen, 2000 for OSEs with different redundancy checks of AIREPs).

The Meteosat-8 AMV data are used over open sea and over land south of 30°N. Furthermore, the distributed data include two quality indices. Based on these two quality indices the data are rejected if the indices are below 20 or 30, respectively. The observation error standard deviations used in the analyses are given in Table 4. The first guess check of Meteosat-8 AMV data and other single level wind data is traditional and includes an "asymmetry check" (see Guerrero and Amstrup, 2005).

For bias-correction of AMSU-A brightness temperatures a Harris-Kelly (Harris and Kelly, 2001) scheme with 7 predictors from the background model (model first guess) is used. The initial examination that was done for NOAA16 data (Schyberg *et al.*, 2003) showed that the scatter of the difference between observed and modeled brightness temperature varied significantly with latitude. It was therefore decided to have separate bias correction coefficients for three latitude bands: 1) up to 50°N, 2) between 50°N and 65°N, and 3) north of 65°N. The AMSU-A bias correction for the 3D-Var version used here is based on a 5 month period from January 2005 through May 2005 using archived operational 3 h T15 forecast data as first guess files. The bias correction coefficients are calculated independently for data over sea-ice and for data over open sea.

At present a diagonal observation error covariance matrix is used for AMSU-A data. Based on the experience from the initial tests with RTTOV8 (Amstrup, 2005) the observation error for channel 4 data over open sea has been reduced compared to the error used in RTTOV7, so that the channel 4 data now have more weight than previously. The values for NOAA15 and NOAA16 are listed in Table 5. Some of the channels that 'see' the surface are given a large observation error so that they are effectively not used, that is in particular true for data over sea-ice. Since the model surface temperature over sea-ice can differ considerable from the real surface temperature, and due to uncertainties in the emissivity over sea-ice, an extra screening is done for these data. The data are discarded if the difference between the modelled and observed brightness temperatures for channels 4 and 5 disagree by more than 1.0 K and 0.8 K, respectively.

[13]EUMETSAT ATOVS/Advanced Retransmission Service
[14]Atmospheric Motion Vectors

The FGAT (First-Guess at the Appropriate Time) option is used (see Huang *et al.*, 2002 for further details).

The DMI EUCOS baseline run uses the following satellite data: i) NOAA15 and NOAA16 AMSU-A data over open sea and over sea-ice, ii) QuikScat surface winds, iii) Meteosat-8 AMV winds. In addition to the satellite data, the EUCOS baseline set-up consists of the following conventional data: i) the GUAN[15] radiosonde network, ii) the GSN[16] surface network and iii) buoy data. See Appendix A for a list of the WMO[17] station identification numbers in the GUAN and GSN networks.

An example of the coverage of the baseline radiosonde data and surface data is shown in Figure 2. The distribution, for 12 UTC as shown here, is reasonable except for a rather low number of radiosonde data in the Atlantic. The distances between stations are much higher than in a normal DMI-HIRLAM 12 UTC analysis. Similarly, the distribution of surface pressure data in the baseline set-up via buoys and SYNOPs is shown in the lower part of the figure. Figure 3 shows the available data for the T1F experiment (full observing system), and includes PILOTs and ship data as well at the same analyses time. Note that PILOTs are considered redundant if a TEMP is available from the same station position. For this particular analysis, T1F had data from 182 more radiosonde stations than the baseline experiment.

2.4 Short description and comments on different experiments

T1A Baseline run. This includes a fairly small amount of (GUAN) radiosonde and (GSN) SYNOP data (an example of the data coverage is shown in Figure 2), and in addition buoy data are included to ‘anchor’ the satellite data (studies at ECMWF have shown that AMSU-A data in their data assimilation system do not perform well in the absence of sea surface pressure data (Jean-Noël Thépaut, in a presentation at the “Alpbach workshop”, `http://www.wmo.ch/web/www/GOS/Alpbach2004/Agenda-index.html`)). No aircraft data, no ship data, and no PILOT data are included.

T1B Baseline plus all aircraft (AMDAR, ACARS and standard AIREP) data. This is not an optimal experiment since the DMI operational servers receiving and processing the GTS data sometimes could not cope with the relative high number of ACARS data, and the number of ACARS in these cases were fairly low. This is worst in the Christmas/New Year period, due to a very inadequate monitoring of the servers. Besides, a large number of AMDAR data from the Lufthansa fleet received in bufr[18]-format at DMI were not processed at the time, since they were unknown to DMI. Furthermore, the encoding implied that they were ASDAR[19] instead. However, the experiment **does** reflect the actual operational usage during the period.

T1X Baseline plus E-AMDAR data (AMDAR observations with station id starting with ‘EU’). The same deficiency as for the T1B run with respect to AMDAR (but the experiment does reflect the actual operational usage).

T1W Baseline plus wind from the non-GUAN radiosondes.

T1T Baseline plus wind and temperature from the non-GUAN radiosondes.

T1D Baseline plus all data (wind, temperature, humidity) from the non-GUAN radiosondes.

T1U Baseline plus wind and temperature from the non-GUAN radiosondes and from all aircraft. AMDAR data from the archive at ECMWF are included as well. The data which are doubled due to this are screened away in the redundancy check.

[15] GCOS (Global Climate Observing System) Upper-Air Network
[16] GCOS Surface Network
[17] World Meteorological Organization
[18] Binary Universal Form for the Representation of Meteorological Data (WMO, 1995)
[19] Aircraft to Satellite Data Relay

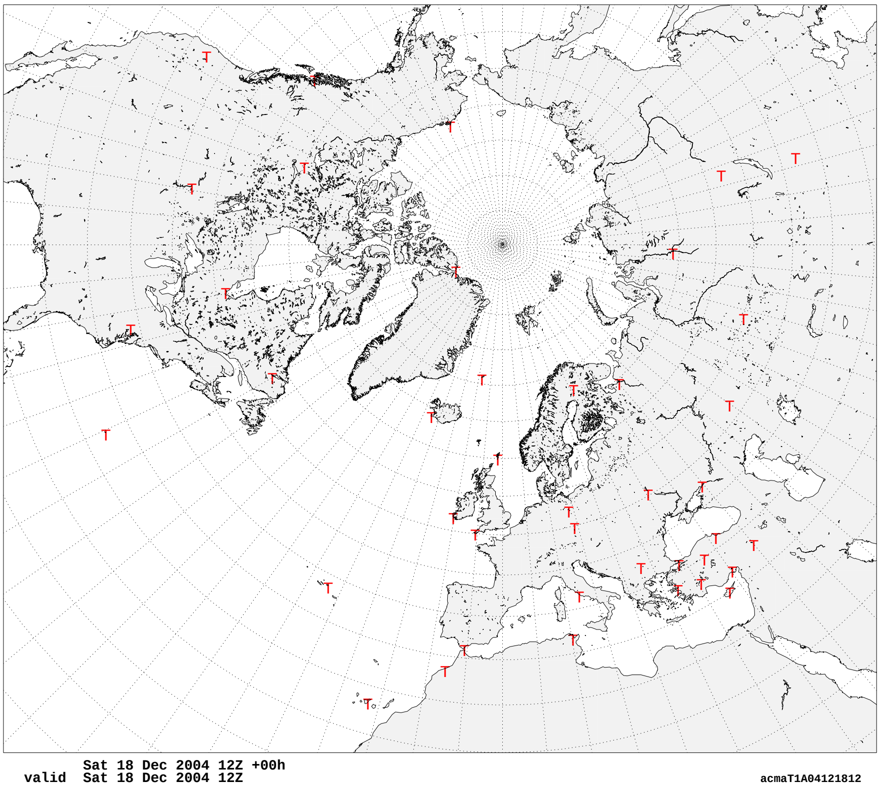

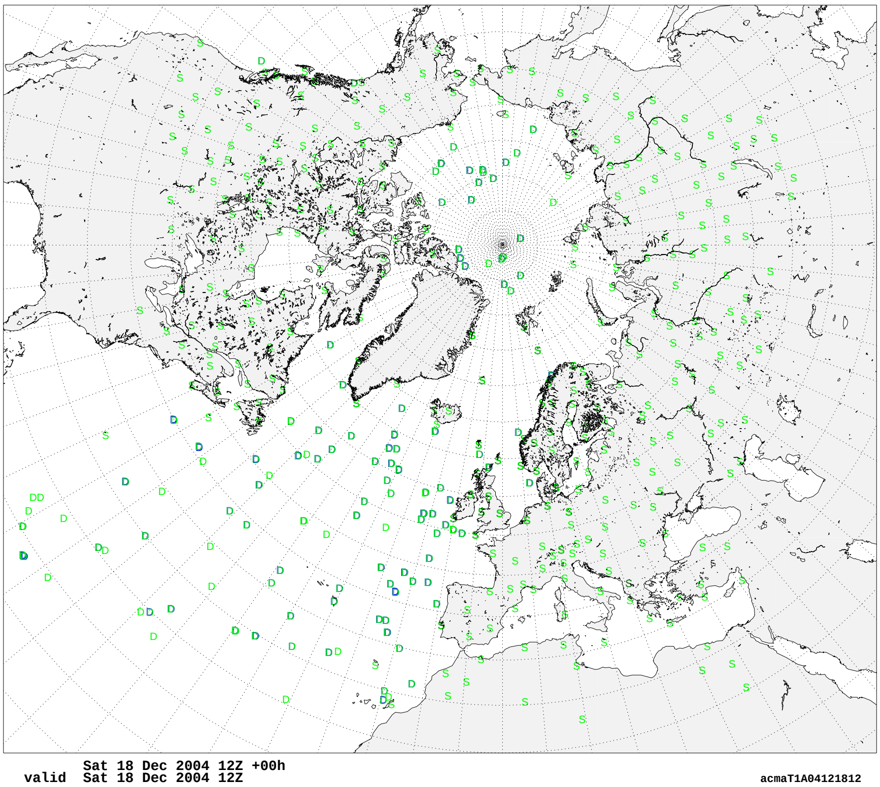

Figure 2: An example of the coverage of the “baseline” radiosondes (upper, red ’T’s) and surface (lower, green ’S’s for SYNOP, ’D’s for buoys) data available on 12 UTC December 18, 2004. The radiosonde stations are GUAN stations and the SYNOP stations are GSN stations.

T1V Baseline plus wind profiler data extracted from the ECMWF archive. The ECMWF white list has been used to specify which wind profilers to use. These data are not used operational at DMI and, accordingly, they have been used with the analysis system as is. Some data may therefore not have been used as they were supposed to, and some may not have been used at all even if they were supposed to. In this

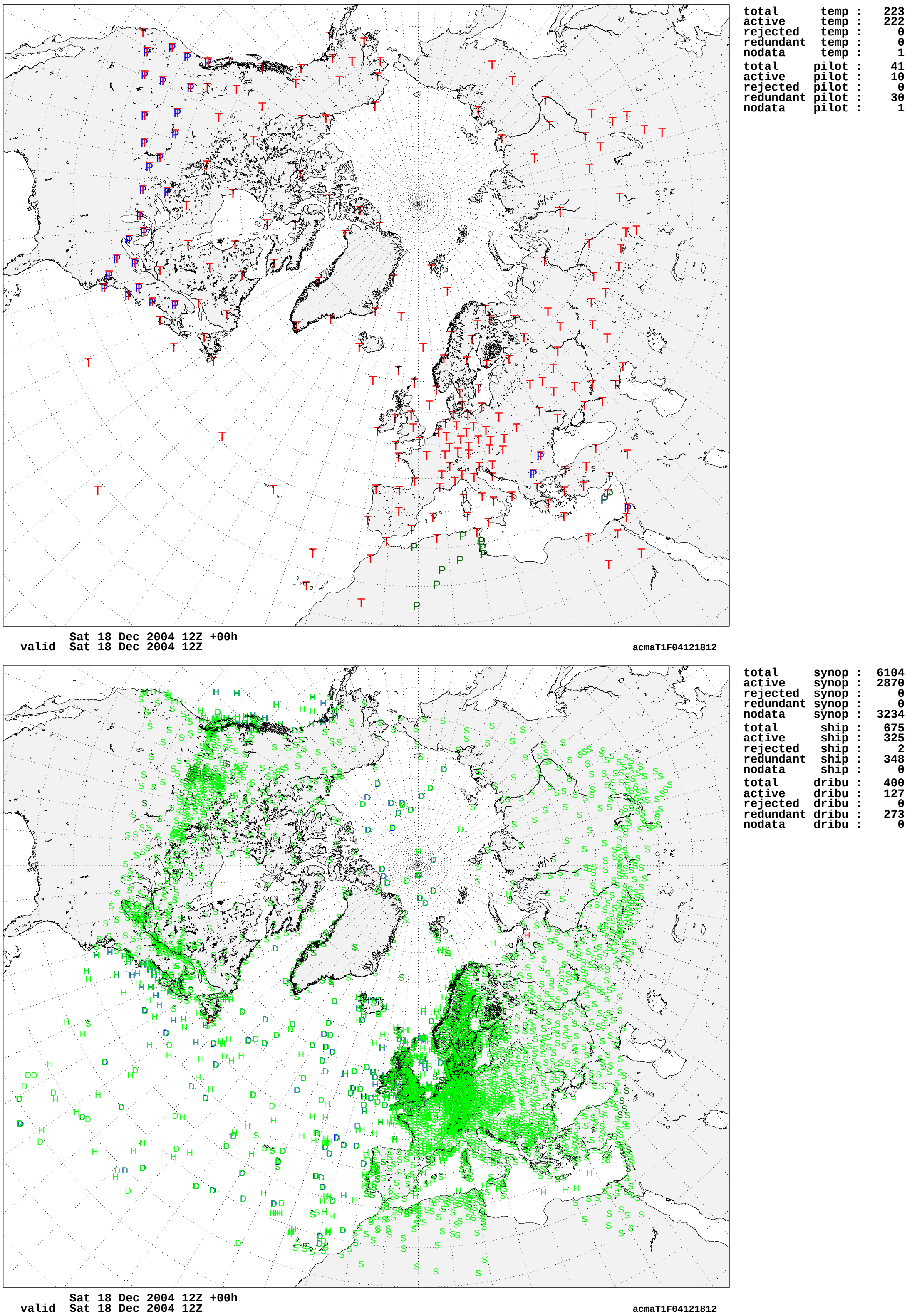

Figure 3: An example of the coverage of the radiosondes (upper, red ’T’s) and PILOTs (upper, blue ’P’s for redundant, green ’P’s for active) and surface (lower, green ’S’s for SYNOP, ’D’s for buoys and ’H’s for ships) data available on 12 UTC December 18, 2004. From the T1F run.

experiment data from 6 stations have been used. Wind profiler data are not included in the real time DMI bufr-database and have therefore not been monitored at all at DMI for a long time.

T1F The control run including all observations (including extra AMDAR from the ECMWF archive). Boundaries are from the similar ECMWF control run instead of their baseline run. But more important: the analyses from the ECMWF run are used in the reassimilation scheme as shortly described in section 2.

T1Y Baseline plus E-AMDAR data (AMDAR observations with station id starting with 'EU'). This experiment also includes AMDAR data from the archive at ECMWF which make the difference from the T1X experiment.

Figures 4 and 5 show the number of observation reports used in the main analyses at 00 UTC, 06 UTC, 12 UTC and 18 UTC for the baseline experiment (T1A) versus the 'all observations included' (T1F) experiment. With respect to aircraft data, the number of reports used for the 'all aircraft' (T1B) experiment, and the 'E-AMDAR' (T1X) experiment are shown as well. Note the extra number of aircraft reports used in T1F (and T1U as well!) compared to T1B. These are the extra E-AMDAR data extracted from the ECMWF archive and most of these reports are over Europe. Furthermore, due to the above mentioned problems with the DMI server, the number of aircraft data were relatively low during Christmas and until early January. The T1U and T1F experiments were done later than the T1X and T1B experiments, and it was decided to use the data in the ECMWF archive for the T1U and T1F experiments after a meeting at ECMWF in January 2006. Despite the computational costs a rerun of T1X, named T1Y, including the extra data has been done. It can also be noted that Meteosat-8 AMV data were missing for some days in January 2005, due to problems with another DMI server receiving the data from EUMETCast[20].

3 Results

The results are compared in different ways. A standard observation verification, where forecast results are compared to standard SYNOP and radiosonde observations using an EWGLAM[21] station list, is done and the results are shown and commented upon in section 3.1. Furthermore, significance tests by use of students t-test, with 90 % two sided significance interval, are shown (Mike Fisher, memorandum ECMWF research department, May 2001). Results of forecasted 12 h precipitation amounts against observations from SYNOP stations at 06 UTC and 18 UTC are given in terms of standard contingency tables as well as in the form of equitable threat scores in section 3.2. Results from field verification, where forecasts are compared to the control experiment (T1F) verifying analyses, are given in section 3.3. Section 3.4 contains some case studies. Finally, in section 3.5, the statistics of wind speed data observations from Meteosat-8 AMV, aircrafts, and radiosondes are compared with similar model data.

At the last pages, Figures 50-53 show daily statistics of the difference between actual observed brightness temperatures modeled from the background field for NOAA15 and NOAA16 over open sea and over sea ice for the baseline experiment (T1A) and the control experiment (T1F). These plots illustrate the effect of bias correction besides being examples of the daily variance in the number of data used and the statistics.

3.1 Observation verification

The experiments are verified by calculation of bias (forecast value minus observed value) and root mean square (rms) for the surface variables 10 m wind, mslp (mean sea level pressure), and 2 m temperature; for the upper level variables temperature, wind speed, and geopotential height at 850 hPa, 500 hPa and 250 hPa; and for

[20] a EUMETSAT distribution system
[21] European Working Group on Limited Area Model

relative humidity at 850 hPa, 700 hPa and 500 hPa, as function of forecast length in one set of figures (Figures 6-10). Using a second type of figures (Figures 12-20), the vertical structure of temperature and geopotential height offsets is illustrated, by plotting the rms scores for a test experiment on the left hand side and differences in rms scores between the experiment and the baseline experiment on the right hand side. Also some inter comparisons between experiments are made. The scores are shown at analysis time and for the 12, 24, 36 and 48 hour forecasts as a function of pressure. Figure 11 shows bias and rms scores for the full combined system, to illustrate the general trends of the bias behavior. Figures 21-23 show daily scores of 48 h forecasts of mslp, 850 hPa temperature, and 500 hPa geopotential height. Figures 24-29 show differences in root mean square errors from obs-verification based on daily scores of 00 UTC and 12 UTC forecasts for the variables: Mslp, 300 hPa temperature and wind, 850 hPa temperature, 700 hPa relative humidity, and 500 hPa geopotential height. Furthermore, results for mslp based on daily scores of 06 UTC and 18 UTC forecasts are shown in Figure 30. Some other results based daily scores of 06 UTC and 18 UTC forecasts are shown in Figure 31 for experiments using additional wind and temperature from aircraft or non-GUAN radiosondes. Overlayed is the 90 % two sided confidence intervals. These plots (Figures 24-31) are additional to the previous and made to see the significance of the differences for some of the parameters; they are the ones referred to when comments about significance of the results are made later in the report.

A comment about the verification of upper air temperatures at analysis time is appropriate. Some of the experiments (T1T, T1D, T1U and T1F) use radiosonde temperature data in the analyses, and as some of these data are used for verification these experiments are bound to have better upper air temperature scores for the analyses (0 h forecast lengths) than the experiments not including these data.

Figure 6 shows the verification scores for T1X (wind and temperature from E-AMDAR), T1B (all aircraft) and T1T (wind and temperature from the additional radiosondes). Figures 12, 13, and 14 provide additional profile information. For short forecast lead times it is expected that the impact from E-AMDAR dominate the scores for T1B since the large majority of EWGLAM stations are located in the area in which most of the E-AMDAR data originate, while most of the other aircraft data come from areas somewhat away from the EWGLAM stations. For long forecast lead times the ACARS coming mainly from over USA are expected to have an important impact, in particular for a relative large, limited area model, such as T15, that covers a large part of USA. With the typical easterly flow the air masses for which E-AMDAR have contributed to a given analysis may have moved outside the main verification area during a forecast. Contrary to this, the air masses for which ACARS (over North America) have contributed to a given analysis may have moved into the main verification area over Europe during a forecast. Therefore, the impact from all aircraft data is expected to be somewhat larger than the impact from E-AMDAR data alone.

In general, T1T and T1B have the better scores. In comparison T1X has lower scores but better than the baseline experiment. For reasons mentioned above, T1T naturally has somewhat better analyses temperature scores than T1B and T1X. The upper air wind, temperature, and geopotential scores are in general significantly better than the comparable baseline experiment scores. The inter comparison between T1B and T1X show that the 300 hPa wind and temperature scores (Figures 25 and 26) are significantly better for T1B and that the 00 UTC/12 UTC mslp scores (Figure 24) for long forecast lead times are better for T1B. However, the significance plots show that there are large day to day variances in some of the scores for 48 h forecasts. The inter comparison between T1T and T1B show that aircraft data have almost as big an impact as the additional wind and temperature data from radiosondes. However, the impact on 850 hPa temperature (Figure 27) and 500 hPa geopotential (Figure 29) is significantly higher from the radiosonde data than from the aircraft data. Since aircraft data in principle are available at any time (though presently only few over Europe in the hours after 00 UTC), and only very few radiosonde data are available for analyses except for the 00 UTC and 12 UTC analyses, some additional significance plots based on 06 UTC and 18 UTC forecasts are shown in Figure 31 for T1T, T1B and T1X. The verifications are done against 00 UTC and 12 UTC radiosonde data and therefore results are shown for the forecast lengths 6 h, 18 h, 30 h and 42 h. The figure shows that T1B has significantly better 500 hPa geopotential height, 300 hPa wind and temperature scores than both T1T and T1X for most of the forecast lengths. The differences in the T1T and T1X scores are insignificant for the 06 UTC and 18 UTC forecasts.

Figure 7 shows the verification scores for impact of additional non-GUAN radiosonde data information: additional wind data (T1W), additional wind and temperature data (T1T) and all data (T1D). Figures 15, 16 and 17 show additional profile information. In general T1D and T1T have the better scores and T1W scores in between these scores and the scores from the baseline experiment. In general the upper air wind, temperature and geopotential scores as well as the long lead forecast time 00 UTC/12 UTC mslp scores are significantly better than the comparable baseline experiment scores. The differences between T1T and T1D scores are insignificant. In general T1T has significantly better upper air wind, temperature and geopotential scores than the corresponding T1W scores. So the additional temperature data do have a significant positive impact over adding only the wind observations.

Figure 8 shows the verification scores for impact of wind and temperature from additional non-GUAN radiosondes (T1T), further adding wind and temperature from aircraft data (T1U) and for the full observing system in addition to better boundary data and large scale analyses from ECMWF (T1F). Figures 18, 19 and 20 show additional profile information. In general T1F has much better scores than T1U that has somewhat better scores than T1T. The baseline (T1A) has the worst scores. For most variables except humidity these tendencies are significant.

Finally, Figure 9 shows that the impact from the few wind profiler data are insignificant. This may to some extent be caused by the very few stations from which data are used (6). Preliminary results (not shown) showed a very weak positive impact from the first half of the period, so a larger number of wind profiler data may have an impact. In addition, wind profiler data are normally not used operationally in any country using the HIRLAM data analysis and forecasting system, wherefore no attempt to optimize the usage of these data have been made since the original implementation of the assimilation software. This should of course be done to obtain proper use of the data, in particular if hourly data could be used in connection to using 4D-Var analyses. However, as the simulations with adding just wind (T1W) and both wind and temperature (T1T) show that impact of wind only is less than from both wind and temperature.

Figures 32, 33 and 34 show that the impact from the additional E-AMDAR from the ECMWF archive are in general positive or neutral on most parameters (and some of them a significantly positive impact) for the first 18 h to 24 h. One exemption is the bias of 250 hPa temperature which is more positive for the experiment using the additional E-AMDAR data. One of the purposes of the E-AMDAR programme is to make temperature and wind profiles around airports in connection to take off and landing. Figure 33 does indeed show that the rms error of the temperature analysis is better for the T1Y experiment in the lower atmosphere due to the additional data. For unknown reasons this is not the case above the 250 hPa level but this is probably linked to the extra positive temperature bias seen at 250 hPa.

3.2 Precipitation verification

Precipitation is verified by two means: By producing contingency tables, and by calculating equitable threat scores, both for 12 h periods.

Tables 8 to 13 show contingency tables of precipitation accumulated over 12 hours (from 6 to 18 hour forecasts, 18 to 30 hour forecasts, and 30 to 42 hour forecasts) for the given period, using either EWGLAM stations that do report 12 hours accumulated precipitation, or Danish stations. The numbers in these tables are obtained by counting the number of observed and predicted precipitation amounts in each of five classes. The five precipitation classes are: $P1 < 0.2$, $0.2 \leq P2 < 1.0$, $1.0 \leq P3 < 5$, $5 \leq P4 < 10$ and $P5 \geq 10$ (precipitation amounts in mm). P is either F (forecast) or O (observation) in the tables. The "sum" rows and columns are the sums of the numbers in the given observation classes or forecast classes, respectively. Note that the observed values are uncorrected values. Thus, small observed precipitation values are most likely underestimated, and some "observed" 0 mm/12 h values may not be a real measurement at all, but a default number used (this occasionally do happen for some Danish stations). The results based on this kind of comparisons are very mixed, and it is not possible to make any solid conclusions. Two noteworthy results are: 1) for the Danish station list the baseline experiment has the poorest results for the short range (6 h-18 h lead forecast time); 2) for the short forecast range (6 h-18 h lead forecast time) the experiments including aircraft data (T1B, T1X, T1U and T1F) have the best overall scores in terms of highest numbers in the diagonal.

The equitable threat score (ETS) measures the fraction of observed and/or forecast events that were correctly predicted, adjusted for hits associated with random change (see, e.g. `http://www.bom.gov.au/bmrc/wefor/staff/eee/verif/verif_web_page.html`). By use of the following table

	observed	
	no event	event
forecast no event	A	B
forecast event	C	D

we have ETS=(D−chance)/(B+C+D−chance) with chance=(C+D)*(B+D)/(A+B+C+D). This is sometimes written as: ETS=(R−chance)/(T−chance) where R is the total number of observed **and** forecasted events, T is total number of events observed **or** forecasted and chance is given by chance=F*O/N where F is number of forecasted events, O the number of observed events and N is the total number of events plus non-events. The ETS score is between $-1/3$ and 1, 1 being the perfect score and 0 indicating no skill.

Tables 14 and 15 show the results by use of a Danish station list and an EWGLAM station list, respectively. Results for 6-18 h, 18-30 h and for 30-42 h are given for limits of very low precipitation amounts (0.3 mm/12 h), low precipitation amounts (1.5 mm/12 h) and for larger precipitation amounts (5 mm/12 h).

Both of these comparisons indicate a deficiency in the present humidity analysis. The model seems to act in a negative manner to the humidity increments, which may be in imbalance with the overall fields.

The results for the Danish station list are very mixed. Part of this may be due to the relative small area compared to the full model area, a single bad case may have a relative larger impact on the result. However, for the EWGLAM stations, the ETS scores show a clear benefit from using the full observing system for precipitation forecasts.

3.3 Field verification

Results from field verification, for which forecasts are compared to verifying analyses valid at the same time, are summarized for selected parameters in Table 6 for 36 h and 48 h forecasts. The verifying analyses are the T1F initialized analyses for all the cases. The results are averages of the 4 daily forecasts over the period examined. The averages given are averages over grid points for the full area as well as for grid points in a European area defined by the southwest corner 12.5°W,35°N and northeast corner 35°E,75°N which is an area often used by ECMWF. The results support the findings in obs-verification, in the sense that T1A (baseline) and T1V (baseline plus wind profilers) have the worst scores for most parameters, and that the full system (T1F) has the superior rms-scores. T1U (baseline plus wind and temperature from other radiosondes as well as aircrafts) typically has

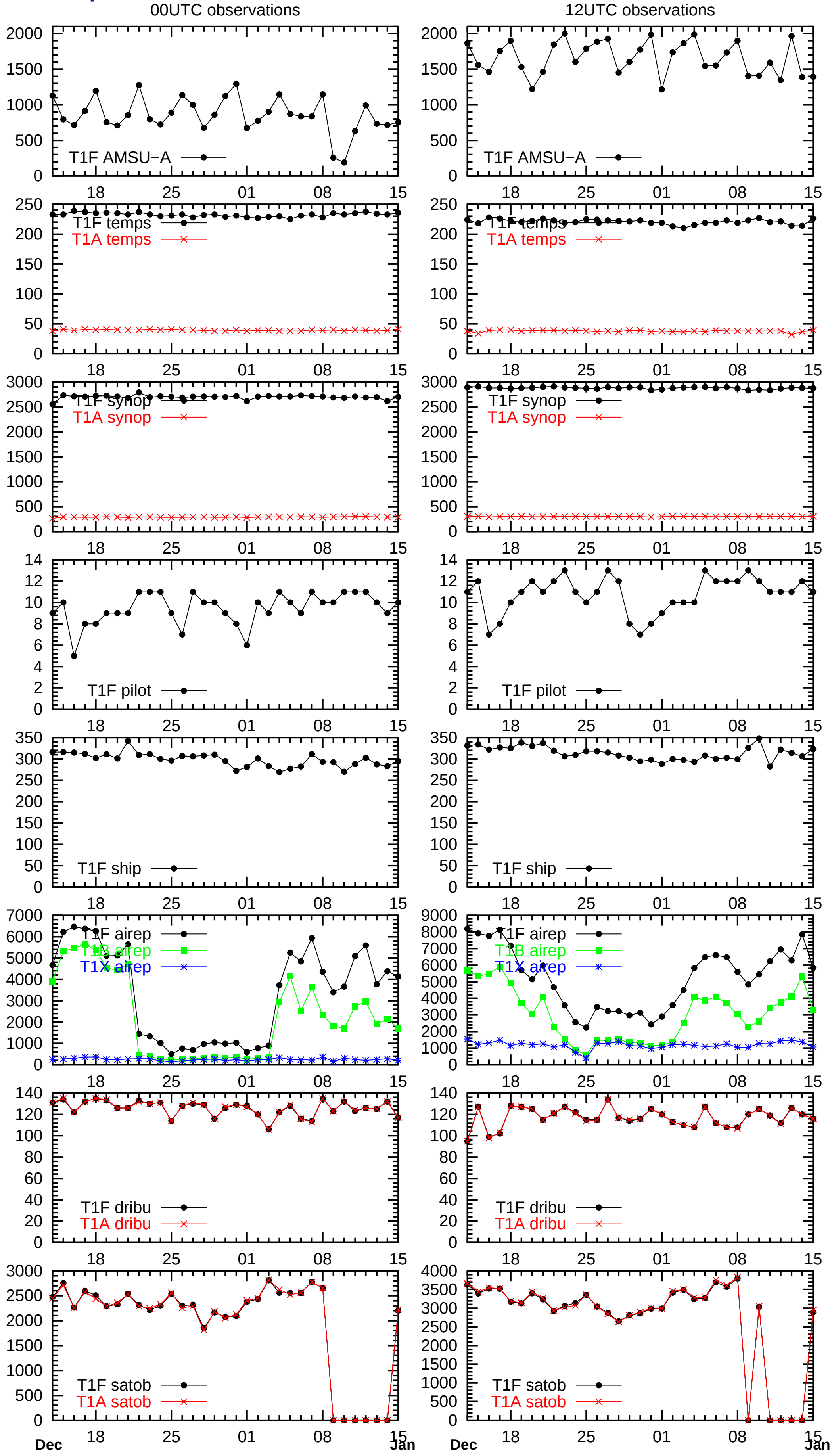

Figure 4: Observation usage for 00 UTC analyses (left) and 12 UTC analyses (right). Note that PILOT and SHIP data are used in the T1F experiment only.

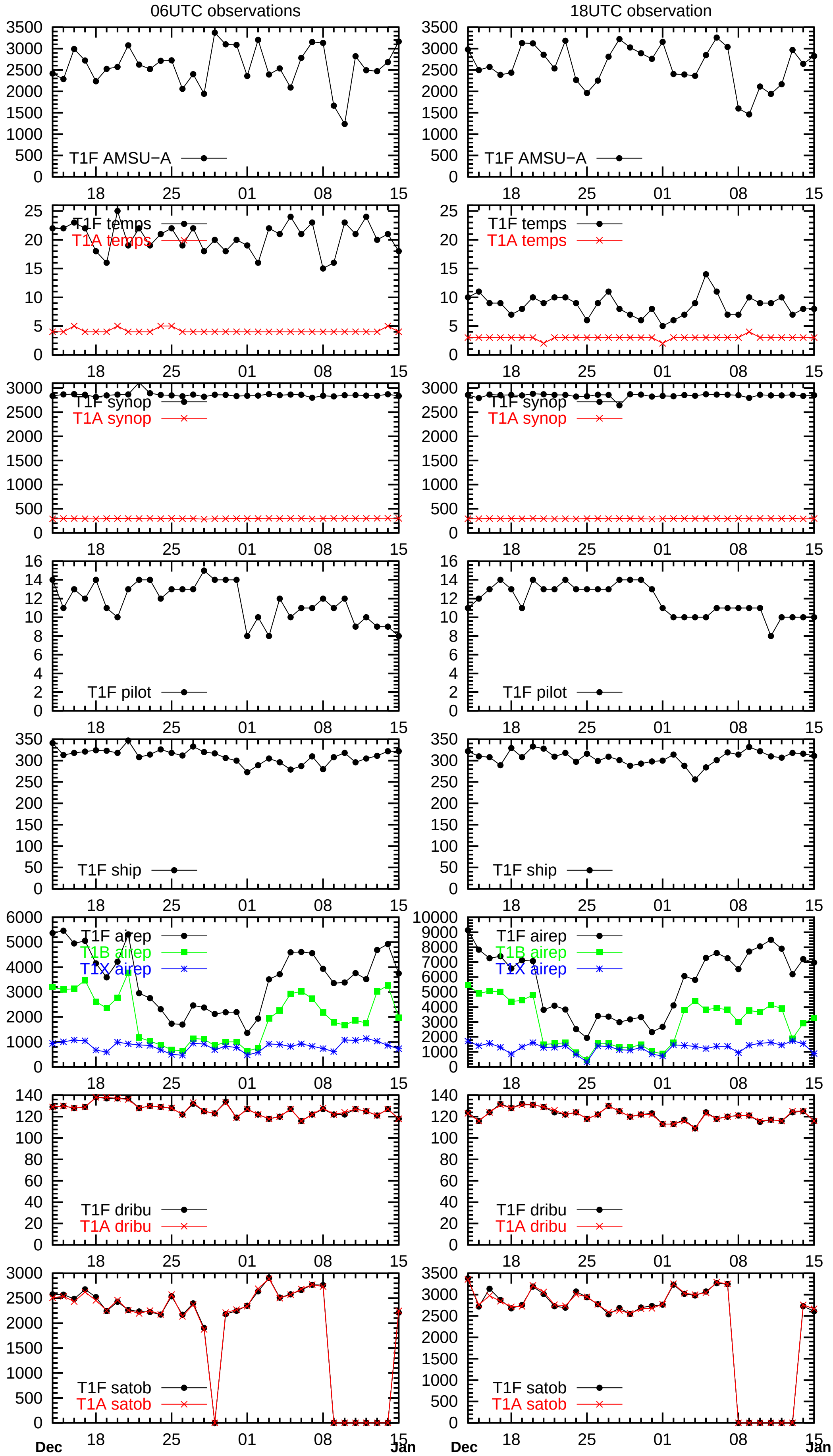

Figure 5: Observation usage for 06 UTC analyses (left) and 18 UTC analyses (right). Note that PILOT and SHIP data are used in the T1F experiment only.

Table 6: Results from field verification. Top part is for averages over the full domain and the bottom part is for averages over a European area. The verifying analyses are T1F initialised analyses. The worse scores are marked in a bold, red font. The best scores are given with a bold, black font. The FCL column indicates the forecast length.

		T1A		T1V		T1W		T1T		T1D		T1X		T1B		T1U		T1F	
type	FCL	bias	rms	bias	rms	bias	rms	bias	rms	bias	rms	bias	rms	bias	rms	bias	rms	bias	rms
mslp	36	−0.10	**2.69**	−0.10	**2.69**	−0.08	2.63	**−0.04**	2.59	−0.05	2.58	−0.08	2.63	−0.09	2.60	**−0.05**	2.53	**−0.15**	**2.35**
mslp	48	**−0.07**	**3.32**	**−0.07**	**3.33**	−0.06	3.25	**−0.02**	3.20	−0.03	3.20	−0.06	3.26	−0.06	3.22	**−0.03**	3.14	**−0.09**	**2.89**
H500	36	**1.9**	**23.8**	**1.9**	**23.8**	**1.9**	22.9	1.4	22.2	1.4	22.2	1.4	22.7	1.2	22.3	1.0	21.3	**−0.1**	**19.3**
H500	48	**2.1**	**30.2**	**2.1**	**30.3**	**2.1**	29.4	1.7	28.6	1.7	28.7	1.7	29.3	1.5	28.8	1.3	27.8	**0.6**	**25.1**
T850	36	**0.33**	**1.96**	**0.33**	**1.97**	**0.33**	1.93	0.26	1.87	0.27	1.87	0.31	1.92	0.30	1.91	0.25	1.83	**0.19**	**1.71**
T850	48	**0.34**	**2.23**	**0.34**	**2.23**	**0.33**	2.19	0.27	2.14	0.28	2.15	0.32	2.19	0.31	2.17	0.26	2.11	**0.21**	**1.97**
T500	36	−0.05	**1.47**	−0.05	**1.46**	−0.05	1.43	−0.05	1.39	−0.04	1.39	−0.07	1.42	−0.07	1.41	−0.06	1.36	−0.03	**1.25**
T500	48	−0.06	**1.77**	−0.06	**1.77**	−0.06	1.73	−0.07	1.70	−0.06	1.70	−0.08	1.74	−0.09	1.72	−0.08	1.67	−0.05	**1.53**
T300	36	**−0.25**	**1.29**	**−0.25**	**1.30**	**−0.24**	1.27	−0.21	1.23	−0.21	1.23	−0.22	1.26	−0.20	1.24	−0.17	1.19	**−0.06**	**1.11**
T300	48	**−0.25**	**1.49**	**−0.25**	**1.49**	**−0.24**	1.47	−0.22	1.44	−0.21	1.44	−0.23	1.46	−0.21	1.45	−0.18	1.41	**−0.07**	**1.31**
RH850	36	−0.9	19.8	−0.8	19.7	−0.9	19.6	−0.9	19.4	−0.9	19.4	−0.9	19.6	−0.9	19.5	−1.0	19.2	−0.0	18.1
RH850	48	−0.6	21.4	−0.6	21.4	−0.7	21.2	−0.7	21.1	−0.6	21.1	−0.6	21.3	−0.7	21.2	−0.7	21.0	0.1	19.9
Average over European area (lon,lat): $(-12.5, 35) \rightarrow (35, 75)$																			
mslp	36	**−0.03**	**2.77**	**−0.03**	**2.78**	0.09	2.70	0.22	2.68	0.18	2.67	0.08	2.73	0.09	2.70	**0.27**	2.62	0.16	**2.49**
mslp	48	0.08	3.61	**0.06**	**3.63**	0.18	3.53	0.29	3.52	0.24	3.51	0.18	3.55	0.17	3.52	**0.34**	3.41	**0.34**	**3.21**
H500	36	1.9	**23.6**	1.8	**23.7**	2.7	22.7	1.6	22.5	1.8	22.4	**2.2**	23.0	2.2	22.5	1.8	21.7	**−0.1**	**20.4**
H500	48	2.1	31.6	1.9	**31.9**	**2.8**	30.8	1.6	30.4	1.7	30.4	2.4	30.9	2.3	30.3	1.9	29.2	**1.3**	**27.1**
T850	36	**0.23**	**1.84**	**0.22**	**1.84**	**0.22**	1.78	0.10	1.73	0.12	1.73	0.20	1.81	0.19	1.79	0.10	1.70	**−0.03**	**1.59**
T850	48	**0.21**	**2.10**	**0.20**	**2.10**	**0.20**	2.04	0.08	1.99	0.11	1.99	0.18	2.06	0.17	2.05	0.09	1.96	**−0.02**	**1.84**
T500	36	−0.07	**1.52**	−0.07	**1.52**	−0.06	1.46	−0.12	1.45	−0.10	1.44	−0.09	1.48	−0.09	1.46	−0.13	1.41	−0.13	**1.34**
T500	48	−0.10	**1.86**	−0.10	**1.87**	−0.09	1.81	−0.14	1.80	−0.12	1.79	−0.11	1.84	−0.10	1.80	−0.14	1.73	−0.14	**1.64**
T300	36	0.01	**1.25**	0.01	**1.25**	0.01	1.21	0.01	1.19	0.03	1.19	0.02	1.21	0.05	1.20	0.04	1.16	0.06	**1.12**
T300	48	0.02	**1.47**	0.02	**1.47**	0.02	1.45	0.02	1.43	0.04	1.43	0.04	1.45	0.06	1.44	0.06	1.40	0.08	**1.34**
RH850	36	−1.9	19.8	−1.9	19.7	−2.0	19.5	−2.2	19.5	−2.2	19.5	−1.9	19.5	−2.0	19.5	−2.3	19.3	−0.2	17.6
RH850	48	−2.0	21.7	−2.0	21.7	−2.0	21.5	−2.2	21.4	−2.1	21.4	−2.1	21.5	−2.1	21.5	−2.3	21.3	−0.4	19.8

the second best rms-scores. It should be noted that T1F may have a small advantage since this verification uses the T1F analyses, but the effect of this is believed to be only marginal.

3.4 Case studies

In the period January 7 to January 14 2005 a number of storms hit the Scandinavian area. Here, we focus on two of those. Firstly, the storm named Edwin or Gudrun (see, e.g., `http://www.dmi.dk/dmi/8januarstormguycarprapport.pdf` by Guy Carpenter & Company Lmt.) that heavily affected Northern Europe from Ireland to Russia. Here, we focus on 15 UTC and 18 UTC January 8, when the storm peaked over Denmark. Secondly, a low passing Faeroe Islands and a little north of Shetland Islands affecting these islands, Scotland and Norway. Here we focus on the wind and pressure on 06 UTC January 12, 2005. This is a time at which the pressure was close to the minimum. Furthermore, a low close to Iceland on 00 UTC January 1, 2005, is also studied since the comparable met.no (Norwegian Meteorological Institute) results showed large variations in the analyses at this time.

The first storm was the best ever (operational, real time) predicted storm over Denmark. It is therefore of interest whether the different OSEs have similar quality. Figures 35, 36 and 37 show the verifying analyses for each simulation, the 30 h forecasts, and the 42 h forecasts, respectively, valid 18 UTC January 8. Figure 38 shows 27 h forecasts valid 15 UTC January 8. Table 7 list the mslp of the center low for the analyses and for the forecasts. For the analyses, T1F has the best center low pressure when compared to available observations. This is a natural consequence of the many additional SYNOP data in Scandinavia which are available for the T1F analysis compared to the number of SYNOP data available in the other experiments. Compared to the other analyses, the T1F analysis has larger areas with wind speeds above 20 m/s in the North Sea and in general higher wind speeds over Danish land areas and in the Baltic Sea. The higher wind speeds over land areas agree well with observations. For the 30 h and 42 h forecasts valid at 18 UTC T1A (baseline) and T1V (baseline plus wind profilers) seem to underestimate the wind speed and furthermore has the maximum wind speed areas in the Baltic Sea too far to the north when compared with the analyses. In both cases T1U (baseline plus wind and temperature from aircrafts) and T1F (full system) are among the experiments that have the highest wind speeds in the Skagerrak/Kattegat. For the 30 h forecasts the experiments including radiosonde data (T1W, T1T and T1D) underestimates the wind speed in this area. This is not the case for the 42 h for the experiments (T1T and T1D) including both wind and temperature data from the non-GUAN radiosondes. However, they seem to underestimate the wind speed in the Baltic Sea. The T1B (baseline plus all aircraft data) forecasts look reasonable in both cases.

Most of the 27 h forecasts (Figure 38) have the maximum 10 m wind speeds located just north of the “top of Jutland” (Skagen) in opposition to the observations (not shown). In that respect the best forecasts are T1F (full system) and T1U (baseline plus upper air wind and temperature from non-GUAN radiosondes and from aircraft). T1B (baseline plus wind and temperature from aircrafts) also has the correct place for the maximum 10 m wind speed but it is slightly underestimated as compared to the other forecasts. However, it is not clear from the available observations whether the higher wind speeds is better or not. T1W (baseline plus wind from non-GUAN radiosondes) has the position a little more to the north than the above mentioned but still better than the others.

It is difficult to state a “best performance” based on these plots for this storm. For that, a test with a storm surge model used operational or pre-operational for the water level in the Danish waters would be beneficial. Such a test may be performed at a later stage.

For the second storm the analyses and 30 h forecasts valid on 06 UTC January 12, 2005, are shown in Figures 39 and 40. Differences between the 30 h mslp forecasts and the T1F mslp analysis are shown in Figure 41. The mslp of the center low in the analyses and 30 h forecasts are given in the following table:

Table 7: Mslp pressure in the center low for the analyses, 30 h, and 42 h forecasts valid at 18 UTC January 8, 2005, and (bottom row) mslp pressure in the center low for the 27 h forecasts valid at 15 UTC January 8, 2005. The T1F analysis valid at 15 UTC January 8, 2005, has a center low mslp of 961.6 hPa.

experiment	T1A	T1V	T1W	T1T	T1D	T1X	T1B	T1U	T1F
analysis (hPa)	961.5	961.5	961.2	961.8	961.5	961.5	961.6	961.7	960.5
30 h forecast (hPa)	959.5	959.6	960.2	960.3	959.2	960.1	960.1	960.0	960.6
42 h forecast (hPa)	957.6	958.0	956.6	954.6	954.9	958.5	958.5	953.9	957.5
27 h forecast (hPa)	959.6	959.7	960.7	960.0	959.2	959.8	960.9	961.8	961.4

experiment	T1A	T1V	T1W	T1T	T1D	T1X	T1B	T1U	T1F
analysis (hPa)	943.6	943.7	944.5	945.8	945.7	944.0	944.7	946.3	945.9
30 h forecast (hPa)	951.7	947.4	948.7	950.5	950.3	948.4	946.7	946.3	945.6

As expected there are some variations in the pressure of the low in the analyses since there are no observations close to the center in this case. For the 30 h forecasts some forecasts predicts the pressure of the center low very well and some have the center low 4 hPa to 6 hPa too high. However, the combination of the position and the center pressure of the center low is not very well predicted except in the T1V (baseline plus wind profiler) experiment. This is a case in which this experiment do very well compared to the other experiments despite the overall bad scores. Difference plots of mslp for the analyses between T1A and T1V show only very small differences and is not shown here. Figure 42 show difference plots of 500 hPa geopotential height between T1A and T1V around Alaska where 3 wind profilers have been assimilated in the T1V experiment. These wind profilers do make a difference in this analysis. Since the control run also includes these wind profilers it could be expected that this experiment also should have a good impact from them. However, as the other plot in the figure show, the additional radiosondes in Alaska and Canada 'degrade' the good impact from the wind profilers in this case.

For the third case, the analyses, 36 h forecasts, and 48 h forecasts valid on 00 UTC January 1, 2005, are shown in Figures 43-45. The analyses agree quite well except for a small difference in the T1F analysis. It is likely that the reassimilation from 12 UTC 31 December, 2004, using the same ECMWF baseline analysis for large scale blending, with T1F as an exception, is the reason for this. The different observational data sets used in the subsequent analyses to prepare for the first guess field for the 00 UTC analysis may not be sufficient to make the surface pressure first guess fields in this area differ and neither are the observations available for the 00 UTC analysis. But as Figures 44 and 45 show, the 36 h and 48 h forecasts valid at 00 UTC 1 January 2005 are rather poor, except for the T1F forecasts being the best and fairly good. Figures 46 and 47 that show differences between the validating (T1F) analysis and the 36 h and 48 h forecasts clearly demonstrate the superior performance of the full system for both the 36 h and 48 h forecasts. Figure 45 also shows that the false alarm of a deep low between Iceland and Greenland for the other experiments is a little less pronounced for T1T, T1D and T1U than the others for the 48 h forecasts. Thus, the experiments including radiosonde wind and temperature data are a little better than the other experiments in this case. This is not the case for the 36 h forecasts.

3.5 Comparisons of wind speed observations with first guess fields

For the use of observations in an analysis system such as the HIRLAM 3D-Var system it is important that the background (or first guess) and observation error statistics are specified correctly. Recently, a study by Navascués *et al.* (2006)) based on the method of Desrozier *et al.* (2005), was initiated within the HIRLAM community in order to tune these errors. One of the assumptions made in the assimilation system, is that the observations are bias-free and that the error distributions of the background and observations are Gaussian. Figures 48 and 49 show the statistics of wind speed data from Meteosat-8, aircraft, and radiosondes compared with the first guess fields (from the control experiment, T1F) interpolated to the observation points. The statistics are shown for three vertical ‘layers’. The observational data are the data used in the analyses, data rejected in the data assimilation are not used for making the statistics. The figures show that the “quality” of the observations – as compared to the model fields – are similar for the 3 data types. If anything, the radiosonde wind speeds are a little worse. However, only few AMV and aircraft winds are available above ca. 200 hPa, in opposition to radiosonde wind data.

4 Discussion and conclusions

The present study has resulted in a number of interesting results. Besides showing that radiosonde data are still a core part of the present observation systems some of the major conclusions are:

- The baseline set-up has rather poor overall scores compared to most other set-ups.
- Addition of the (very few) additional wind profiler data give an insignificant impact. Nevertheless, one case study gave a very positive impact on a high impact weather situation. Regular monitoring of the data from the different stations should be made, and based on this a revised list of observation errors and which stations to be included in the whitelist can be estimated. Furthermore, restrictions such as is done in Aladin (between 400 hPa and 700 hPa; Roger Randriamampianina (OMSZ), private communication) to which part of the atmosphere where the data are used could be considered as well.
- The use of E-AMDAR data give only approximately half the impact (over Europe) compared to use of all aircraft data for the long forecast lead times. For short forecast lead times the impact is almost the same and essentially as big as the impact of radiosonde wind and temperature.
- The use of wind data alone from the additional non-GUAN radiosondes give approximately half the impact from using both wind and temperature from the additional radiosonde data.
- Additional use of humidity from the additional non-GUAN radiosondes give an insignificant impact. However, this is probably due to deficiencies in the assimilation system. Work is being done within the HIRLAM cooperation (and elsewhere as well) to improve this in the future.
- The radiosonde wind and temperature data are the most important part of the terrestrial network in this study.
- However, the use of aircraft wind and temperature data gives almost the same impact as the additional radiosonde wind and temperature data. For a few parameters the impact is smaller.
- The use of both aircraft and the additional radiosonde wind and temperature data leads to significantly better scores compared to using only the wind data.
- For the long 06 UTC and 18 UTC forecasts for which the analyses have data available from only **very few** radiosonde stations, the impact from aircraft data are significantly larger than data from the non-GUAN radiosonde stations.

Thus, aircraft data and the extra radiosonde data are complementary data, not redundant data, in the DMI-HIRLAM analysis and forecasting system. Besides being extremely important now, radiosonde data may also in the future be very important data. Besides being important by themselves in the data assimilation, they will likely play a strong role in anchoring the bias correction of satellite radiances in a set-up with adaptive bias correction, and of course for verification/validation purposes.

It seems important to have temperature information in addition to wind data, as the radiosonde data experiments show. In a future study it would be interesting to have an additional experiment with temperature data (and no wind data) from non-GUAN radiosonde stations.

Figures 4 and 5 show that occasionally some satellite data are missing. They also show that the number of available AMSU-A data is smaller within the DMI-HIRLAM-T15 area over open sea and sea ice for the 00 UTC runs compared to the other cycles with the present satellite configuration. Plots (not shown here) of the position of the AMSU-A data in the 00 UTC data analyses show that very few data are available in the Atlantic. This results in a baseline set-up that may be more sensitive to additional data than for a set-up using more satellite data, as we expect to have in the future. It should also be noted that in general the amount of AMSU-A data over sea and sea-ice are somewhat lower for the 00 UTC analyses than for other analyses times with the present satellite configuration. This is also the case for aircraft data in Europe during night since many airports do not allow aircrafts to land or depart during the night. This could be important if aircraft data are supposed to replace some radiosonde stations.

The present study has two important weak points beside the ones described in section 2.4: 1) lack of short cut off data for the long runs and therefore long cut off data have been used in stead; and 2) lack of the corresponding ECMWF test runs for lateral boundaries and use of the analyses in the reassimilation steps. ECMWF decided to make all tests (except for the AMDAR experiment) after the first DMI tests were done. The computational costs prohibited reruns of the first experiments and therefore all experiments, except for the control experiments, have used the ECMWF baseline run. The real importance of 1) is uncertain. Most likely it is not very important in comparison to 2). The difference between the results from the experiment with the second best scores and the experiment with the full system **and** use of the corresponding ECMWF run for lateral boundaries and analyses in the reassimilation part suggests that it may be a very important part in a more realistic assessment of the importance of the different terrestrial components of the global observing system in the DMI-HIRLAM system. It is expected that some of the impacts found here are *underestimated* compared to impact found if the ECMWF runs had been available for the study. For the next (a summer period) part of this EUCOS OSE study, the corresponding ECMWF test runs are available.

Studies like this should be repeated in the future, when more satellite data become available (with the above remark about the 00 UTC in mind), and when the assimilation system undergoes a large change such as the expected in the near future introduction of 4D-Var analyses, that can take advantage of more of the data that are available at least hourly.

Acknowledgments

This study has been supported by EUCOS. The simulations have been run at ECMWF, partly via allocation of computer resources to a Special Project entitled ’EUCOS/EUMETSAT Data Impact Studies’. Thanks to Roger Randriamampianina (OMSZ) for providing the revised diagnostic tool from ECMWF for the significance test. Discussions at the EUCOS meetings in connection to this project have also been very valuable. Henrik Vedel is acknowledged for careful reading of the manuscript and for useful suggestions for improving it.

References

Amstrup, Bjarne. 2000. *EUCOS observing systems experiments with the DMI-HIRLAM Optimum Interpolation analysis and forecasting system*. DMI Scientific Report 00-19. Danish Meteorological Institute.

Amstrup, Bjarne. 2001. *Impact of ATOVS AMSU-A radiance data in the DMI-HIRLAM 3D-Var analysis and forecasting system*. DMI Scientific Report 01-06. Danish Meteorological Institute.

Amstrup, Bjarne. 2004. Impact of NOAA15 and NOAA16 ATOVS AMSU-A radiance data in the DMI-HIRLAM 3D-VAR data assimilation system – November and December 2003. *Hirlam Newsletter*, **45**, 235–247.

Amstrup, Bjarne. 2005. *First experiences with RTTOV8 for assimilating AMSU-A data in the DMI 3D-Var data assimilation system*. `http://cimss.ssec.wisc.edu/itwg/itsc/itsc14/proceedings/`.

Amstrup, Bjarne and Mogensen, Kristian S. 2000. Observing system experiments with the DMI HIRLAM Optimum Interpolation analysis/three-dimensional variational analysis and forecasting system. *HIRLAM Technical Report*, **46**.

Amstrup, Bjarne and Mogensen, Kristian S. 2004. Observing system experiments with the DMI HIRLAM 3D-VAR data assimilation system in a winter and summer period in 2002. *Unpublised results*.

Andersson, E., Hólm, E., Bauer, P., Beljaars, A., Kelly, G. A., McNally, A. P., Simmons, A. J., Thépaut, J-N. and Tompkins, A. M. 2006. *Analysis and forecast impact of the main humidity observing systems*. Technical Memorandum 493. ECMWF.

Berre, Loïk. 2000. Estimation of Synoptic and Mesoscale Forecast Error Covariances in a Limited-Area Model. *Mon. Weather Rev.*, **128**, 644–667.

Bormann, Niels and Thépaut, Jean-Noël. 2004. Impact of MODIS Polar Winds in ECMWF's 4DVAR Data Assimilation System. *Monthly Weather Review*, **132**, 929–940.

Bormann, Niels, Saarinen, Sami, Kelly, Graeme and Thépaut, Jean-Noël. 2003. The Spatial Structure of Observation Errors in Atmospheric Motion Vectors from Geostationary Satellite Data. *Mon. Weather Rev.*, **131**, 706–718.

Bouttier, F. and Kelly, G. 2001. Observing-system experiments in the ECMWF 4D-Var data assimilation system. *Quart. J. Roy. Meteorol. Soc.*, **127**, 1469–1488.

Cardinali, Carla, Isaksen, Lars and Andersson, Erik. 2003. Use and Impact of Automated Aircraft Data in a Global 4DVAR Data Assimilation System. *Mon. Weather Rev.*, **131**, 1865–1877.

Deblonde, Godelieve. 1999. Variational Assimilation of SSM/I Total Precipitable Water Retrievals in the CMC Analysis System. *Mon. Weather Rev.*, **127**, 1458–1476.

Desroziers, G., Berre, L., Chapnik, B. and Poli, P. 2005. Diagnosis of observation, background and analysis-error statistics in observation space. *Quart. J. Roy. Meteorol. Soc.*, **131**, 3385–3396.

English, S. J., Renshaw, R. J., Dibben, P. C., Smith, A. J., Rayer, P. J., Poulsen, C., Saunders, R. W. and Eyre, J. R. 2000. A comparison of the impact of TOVS and ATOVS satellite sounding data on the acuracy of numerical weather forecasts. *Quart. J. Roy. Meteorol. Soc.*, **126**, 2911–2931.

Feddersen, Henrik. 2004. "Horizontal" reduction of pressure to mean sea level. *Hirlam Newsletter*, **46**, 73–77.

Fourrié, Nadia, Marchal, David, Rabier, Florence, Chapnik, Bernard and Desroziers, Gerald. 2006. Impact study of the 2003 North Atlantic THORPEX Regional Campaign. *Quart. J. Roy. Meteorol. Soc.*, **132**, 275–295.

Geleyn, J.-F. 1998. Interpolation of wind, temperature and humidity values from the model levels to the height of measurement. *Tellus*, **40A**, 347–351.

Gérard, E. and Saunders, R. W. 1999. Four-dimensional variational assimilation of Special Sensor Microwave/Imager total column water vapour in the ECMWF model. *Quart. J. Roy. Meteorol. Soc.*, **125**, 3077–3101.

Graham, Richard, Anderson, Simon, Grant, Roger and Bader, Michael. 1998. Recent Data Impact Studies at UKMO - a review. *Pages 55–69 of: Proceedings of CGC/WMO workshop. Impact of various observing systems on numerical weather prediction. WMO/TD No. 868*.

Guerrero, C. Geijo and Amstrup, B. 2005. Assimilation of M8-AMV data in the HIRLAM-NWP model. *Hirlam Newsletter*, **49**, 12–21.

Gustafsson, N., Berre, L., Hörnquist, S., Huang, X.-Y., Lindskog, M., Navascués, B., Mogensen, K. S. and Thorsteinsson, S. 2001. Three-dimensional variational data assimilation for a limited area model. Part I: General formulation and the background error constraint. *Tellus*, **53A**, 425–446.

Harris, B. A. and Kelly, G. 2001. A satellite radiance-bias correction scheme for data assimilation. *Quart. J. Roy. Meteorol. Soc.*, **127**, 1453–1468.

Healy, S. B. and Thépaut, J.-N. 2006. Assimilation experiments with CHAMP GPS radio occultation measurements. *Quart. J. Roy. Meteorol. Soc.*, **132**, 605–623.

Huang, Xiang-Yu, Mogensen, Kristian Sten and Yang, Xiaohua. 2002 (March). First-Guess at the Appropriate Time: the HIRLAM Implementation and Experiments. *Pages 28–43 of: HIRLAM Workshop Report of HIRLAM Workshop on Variational Data Assimilation and Remote Sensing*.

Isaksen, Lars and Janssen, Peter A.E.M. 2004. Impact of ERS scatterometer winds in ECMWF's assimilation system. *Quart. J. Roy. Meteorol. Soc.*, **130**, 1793–1814.

Köpken, Christina, Thépaut, Jean-Noël and Kelly, Graeme. 2003. *Assimilation of Geostationary WV Radiances from GOES and Meteosat at ECMWF*. EUMETSAT/ECMWF Fellowship Programme, Research Report No. 14. ECMWF.

Lacroix, Bruno, Randriamamoianina, Roger and Charpentier, Etienne. 1998. Most recent impact studies at Metéo-France. *Pages 107–113 of: Proceedings of CGC/WMO workshop. Impact of various observing systems on numerical weather prediction. WMO/TD No. 868*.

Langland, Rolf H. and Baker, Nancy L. 2004. Estimation of observation impact using the NRL atmospheric variational data assimilation adjoint system. *Tellus*, **56A**, 189–201.

Lindberg, Karina. 2005. The effects of the modifications aimed to reduce noise in the semi-Lagrangian scheme in DMI-HIRLAM and the first preliminary tests of the SETTLS scheme in HIRLAM. *Hirlam Newsletter*, **48**, 128–134.

Lindskog, M., Gustafsson, N., Navascués, B., Mogensen, K. S., Huang, X.-Y., Yang, X., Andræ, U., Berre, L., Thorsteinsson, S. and Rantakokko, J. 2001. Three-dimensional variational data assimilation for a limited area model. Part II: Observation handling and assimilation experiments. *Tellus*, **53A**, 447–468.

Marécal, Virginie and Mahfouf, Jean-François. 2003. Experiments on 4D-Var assimilation of rainfall data using an incremental formulation. *Quart. J. Roy. Meteorol. Soc.*, **129**, 3137–3160.

McNally, A. P., Watts, P. D., Smith, J. A., Engelen, R., Kelly, G. A., Thépaut, J. N. and Matricardi, M. 2006. The assimilation of AIRS radiance data at ECMWF. *Quart. J. Roy. Meteorol. Soc.*, **132**, 935–957.

Navascués, Beatriz, Lindskog, Magnus, Yang, Xiaohua and Amstrup, Bjarne. 2006. Diagnosis of error statistics in the HIRLAM 3D-VAR. *HIRLAM Technical Report*, **66**.

Okamoto, Kozo and Derber, John C. 2006. Assimilation of SSM/I Radiances in the NCEP Global Data Assimilation System. *Monthly Weather Review*, **134**, 2612–2631.

Portabella, M. and Stoffelen, A. 2004. A probabilistic approach for SeaWinds data assimilation. *Quart. J. Roy. Meteorol. Soc.*, **130**, 127–152.

Sass, B. H. 2002. *A research version of the STRACO cloud scheme*. DMI Technical Report 02-10. Danish Meteorological Institute.

Schyberg, Harald, Landelius, Tomas, Thorsteinsson, Sigurdur, Tveter, Frank Thomas, Vignes, Ole, Amstrup, Bjarne, Gustafsson, Nils, Järvinen, Heikki and Lindskog, Magnus. 2003. Assimilation of ATOVS data in the HIRLAM 3D-VAR System. *HIRLAM Technical Report*, **60**.

Tomassini, M., Kelly, G. and Saunders, R. 1999. Use and Impact of Satellite Atmospheric Motion Winds on ECMWF Analyses and Forecasts. *Mon. Wea. Rew.*, **127**, 971–986.

Undén, Per, Rontu, Laura, Järvinen, Heikki, Lynch, Peter, Calvo, Javier, Cats, Gerard, Cuxart, Joan, Eerola, Kalle, Fortelius, Carl, Garcia-Moya, Jose Antonio, Jones, Colin, Lenderlink, Geert, McDonald, Aidan, McGrath, Ray, Navascues, Beatrix, Nielsen, Niels Woetmann, Ødegaard, Viel, Rodriguez, Ernesto, Rummukainen, Markku, Rõõm, Rein, Sattler, Kai, Sass, Bent Hansen, Savijärvi, Hannu, Schreuer, Ben Wichers, Sigg, Robert, The, Han and Tijm, Aleksander. 2002. *HIRLAM-5 Scientific Documentation*. HIRLAM Scientific Report.

Vedel, Henrik and Huang, Xiang-Yu. 2004. Impact of Ground Based GPS data on Numerical Weather Prediction. *J. Meteorol. Soc. Japan*, **82**, 459–472.

Vignes, Ole, Tveter, Frank Thomas and Schyberg, Harald. 2005. *Results from the Winter 2003/2004 HIRLAM Analysis Impact Study*. met.no report 06. Norwegian Meteorological Institute.

WMO. 1995. *Manual on codes, Volume I, International codes, Part B - Binary codes*. No 306, fm-94-ix, ext. bufr edn.

Yang, Xiaohua, Pedersen, Claus, Amstrup, Bjarne, Andersen, Bjarne, Feddersen, Henrik, Kmit, Maryanne, Korsholm, Ulrik, Lindberg, Karina, Mogensen, Kristian S., Sass, Bent Hansen, Sattler, Kai and Nielsen, Niels Woetmann. 2005a. *The DMI-HIRLAM upgrade in June 2004*. DMI Technical Report 05-09. Danish Meteorological Institute.

Yang, Xiaohua, Kmit, Maryanne, Sass, Bent Hansen, Amstrup, Bjarne, Lindberg, Karina, Pedersen, Claus, Korsholm, Ulrik and Nielsen, Niels Woetmann. 2005b. *The DMI-HIRLAM upgrade in May 2005*. DMI Technical Report 05-10. Danish Meteorological Institute.

Appendix A: GUAN and GSN station lists

The GUAN station list used here has the following WMO station identification numbers:

01001	02836	03005	03808	03953	04018	08495	08508	08594	10393
11520	15614	16245	17030	17062	17130	17220	17240	17280	17351
17351	17607	20674	21982	22550	23472	24266	26629	28698	30230
32540	33345	34731	35121	38880	41170	41217	41923	43599	44212
44231	44259	44277	44288	44292	44373	45004	47412	47646	47827
47936	47971	47991	48698	48820	48855	48900	50527	51709	52681
53068	55299	56778	57461	60018	60155	60191	60252	60715	60760
61052	61641	61901	61902	61976	61996	61998	62414	63450	63741
63985	64910	65578	67197	67774	68110	68588	68816	68906	70026
70308	70398	71082	71816	71836	71934	72201	72261	72293	72403
72597	72764	76654	78016	78397	78526	78583	78762	78954	80222
81405	82193	82332	82397	83378	83779	84628	85442	85469	85799
87155	87155	87860	88889	89002	89009	89022	89055	89512	89532
89564	89571	89592	89611	89642	89664	91165	91212	91217	91285
91334	91376	91408	91517	91557	91592	91610	91643	91765	91801
91802	91812	91824	91831	91843	91925	91938	91958	92035	92044
93417	93844	93986	93997	94120	94203	94294	94302	94461	94510
94610	94659	94975	94995	94996	94998	96935	96996		

At most 40 of these stations were within the DMI-HIRLAM-T15 model area in the winter runs. The GSN station list used here has the following WMO station identification numbers:

01001	01008	01026	01028	01098	01152	01212	01238	01403	01465
02120	02196	02226	02288	02410	02584	02836	02935	02963	03005
03026	03162	03302	03377	03808	03953	03980	04013	04048	04063
04210	04250	04320	04360	04390	06011	06186	06260	06680	06717
07130	07190	07255	07560	07630	07650	08027	08181	08202	08215
08280	08410	08506	08513	08522	08535	08583	10147	10393	10962
11012	11035	11146	11464	11934	12120	12385	12942	13577	14652
15085	15280	15360	16022	16134	16224	16258	16550	16597	16641
16723	16734	16746	17040	17062	17074	17090	17170	17240	17375
20069	20087	20292	20667	20674	20744	20891	20982	21432	21802
21921	21931	21946	21982	22113	22217	22471	22522	22550	22602
22802	22837	23074	23205	23330	23383	23405	23472	23552	23631
23678	23711	23724	23884	23891	23914	23933	23955	24125	24143
24266	24329	24343	24382	24507	24641	24671	24688	24738	24817
24908	24959	24966	25173	25248	25325	25356	25399	25400	25538
25551	25563	25594	25705	25744	25927	25954	26063	26242	26359
26406	26781	26997	27037	27051	27595	27612	27648	27995	28009
28064	28138	28224	28275	28418	28493	28552	28698	28722	28952
29231	29263	29282	29570	29612	29789	29807	29866	29939	30054
30230	30309	30372	30433	30554	30636	30673	30710	30758	30879
30925	30949	30965	31004	31088	31168	31253	31329	31369	31416
31707	31829	31873	31960	32061	32098	32150	32252	32389	32618
33038	33317	33377	33587	33915	33998	34123	34163	34186	34866
34880	34927	35011	35078	35108	35394	35416	35796	35849	35925
36177	36259	36535	36859	36870	36974	37470	37549	37989	38001
38262	38353	38413	38457	38507	38750	38763	38895	38915	38933

38954	40001	40022	40061	40199	40361	40394	40430	40438	40582
40665	40706	40745	40754	40766	40841	40848	40856	40930	41024
41140	41150	41196	41254	41288	41316	41560	41620	41640	41712
41759	41764	42027	42083	42165	42182	42295	42410	42515	42539
42587	42671	42731	42779	43041	43063	43128	43279	43295	43333
43339	43363	43369	43473	43497	43555	44212	44218	44231	44239
44259	44272	44288	44317	44341	44373	44454	47014	47112	47115
47165	47401	47420	47582	47600	47648	47778	47815	47817	47927
47936	47945	47971	47991	48042	48062	48097	48303	48400	48407
48462	48500	48568	48620	48657	48855	48900	50527	50745	51076
51463	51709	51777	51828	52203	52533	52836	52889	53068	53614
53772	54342	54511	54857	55591	56137	56294	56571	56739	56985
57036	57083	57461	57745	57993	58362	58606	59287	59316	59431
59758	60010	60040	60156	60195	60265	60338	60390	60590	60611
60680	60725	60765	61017	61024	61043	61096	61202	61223	61250
61270	61297	61401	61415	61421	61450	61497	61612	61641	61687
61856	61901	61902	61972	61974	61986	61988	61990	61996	61997
61998	62010	62053	62124	62131	62271	62306	62414	62417	62420
62432	62463	62600	62640	62641	62650	62730	62760	62762	62770
62781	62840	62880	62941	63021	63403	63450	63453	63533	63612
63624	63661	63723	63740	63820	63832	63862	63894	63962	63980
64040	64146	64282	64397	64459	64503	64552	64700	64706	64751
64753	64754	64870	65123	65167	65306	65335	65352	65501	65516
65528	65585	65599	66152	66160	66270	66390	66410	66422	66447
66460	67005	67009	67019	67025	67073	67083	67095	67143	67161
67197	67215	67283	67297	67323	67441	67475	67581	67633	67666
67693	67743	67775	67983	68014	68032	68106	68110	68174	68296
68312	68370	68424	68438	68496	68580	68618	68712	68858	68906
68920	68938	68994	70026	70086	70133	70200	70219	70231	70251
70261	70308	70316	70326	70341	70361	70398	71017	71018	71026
71029	71043	71049	71051	71066	71069	71074	71078	71079	71095
71101	71109	71120	71122	71158	71160	71185	71197	71199	71279
71288	71299	71320	71321	71322	71338	71350	71355	71356	71358
71361	71362	71363	71364	71365	71434	71446	71490	71550	71585
71586	71592	71600	71603	71713	71721	71727	71733	71803	71813
71816	71818	71822	71823	71827	71828	71836	71842	71844	71862
71867	71869	71887	71894	71905	71906	71907	71910	71913	71915
71917	71923	71938	71945	71950	71964	71966	71984	71989	71990
72201	72208	72211	72231	72234	72248	72253	72266	72270	72278
72290	72304	72306	72312	72324	72344	72353	72360	72365	72386
72389	72405	72422	72432	72445	72451	72458	72476	72486	72519
72520	72532	72556	72562	72576	72578	72583	72594	72613	72617
72654	72658	72666	72681	72688	72712	72743	72764	72768	72772
72792	74492	76311	76393	76405	76458	76577	76644	76654	76680
76833	78016	78073	78367	78384	78388	78526	78650	78767	78897
78954	80001	80222	80241	80259	80342	80405	80423	80425	80438
80450	80453	80462	81202	81405	82024	82106	82113	82193	82331
82353	82400	82410	82425	82571	82586	82704	82825	83064	83229

83236	83264	83361	83481	83488	83498	83566	83618	83650	83746
83781	83827	83842	83881	84008	84088	84140	84270	84279	84377
84444	84455	84721	84752	85041	85043	85114	85141	85207	85223
85230	85289	85364	85365	85406	85442	85469	85488	85543	85585
85629	85743	85799	85874	85934	86086	86297	86330	86440	86490
86565	87007	87047	87065	87078	87129	87155	87217	87257	87270
87305	87344	87374	87418	87534	87544	87623	87692	87715	87750
87803	87828	87860	87925	88963	88968	89002	89009	89022	89050
89055	89056	89062	89063	89065	89262	89266	89272	89324	89327
89345	89377	89512	89532	89564	89571	89573	89592	89606	89611
89642	89662	89664	89757	89828	89879	91165	91212	91285	91334
91348	91366	91376	91408	91413	91490	91503	91517	91554	91568
91577	91592	91610	91631	91643	91650	91652	91680	91699	91701
91724	91753	91765	91780	91789	91802	91812	91824	91831	91843
91925	91929	91938	91943	91945	91948	91954	91958	91964	92014
92035	92044	93012	93292	93309	93417	93615	93747	93844	93947
93987	93994	94101	94120	94131	94150	94170	94203	94212	94238
94259	94275	94287	94299	94300	94302	94312	94317	94326	94332
94340	94346	94367	94380	94403	94430	94461	94476	94480	94482
94485	94492	94510	94517	94541	94570	94589	94601	94626	94637
94638	94653	94689	94693	94711	94784	94802	94805	94821	94842
94907	94910	94937	94967	94995	94996	94998	95322	95646	95670
95719	95753	95916	95964	96073	96145	96163	96413	96441	96465
96491	96745	96805	96925	96995	96996	97014	97146	97240	97340
97372	97395	97502	97560	97686	97690	97724	97900	97980	98232
98429	98430	98444	98755	98836	98851				

At most 303 of these stations were within the DMI-HIRLAM-T15 area and reported surface pressure in the winter runs.

Table 8: Contingency tables for 20041213-20050115 (6–18 h forecasts). Danish station list.

T1A 20041213-20050115 (60.5 %)						
obs→ ↓for	O1	O2	O3	O4	O5	sum
F1	**311**	22	12	0	0	345
F2	190	**54**	33	2	0	279
F3	157	126	**185**	33	11	512
F4	3	13	52	**25**	8	101
F5	0	0	3	2	**2**	7
sum	661	215	285	62	21	1244
%FO	47	25	65	40	10	46

T1B 20041213-20050115 (62.7 %)						
obs→ ↓for	O1	O2	O3	O4	O5	sum
F1	**325**	20	9	1	0	355
F2	184	**67**	31	1	0	283
F3	144	120	**198**	39	12	513
F4	7	8	45	**19**	7	86
F5	**1**	0	2	2	**2**	7
sum	661	215	285	62	21	1244
%FO	49	31	69	31	10	49

T1W 20041213-20050115 (63.4 %)						
obs→ ↓for	O1	O2	O3	O4	O5	sum
F1	**310**	18	6	0	0	334
F2	199	**61**	36	2	0	298
F3	148	130	**199**	34	12	523
F4	4	6	41	**25**	7	83
F5	0	0	3	1	**2**	6
sum	661	215	285	62	21	1244
%FO	47	28	70	40	10	48

T1T 20041213-20050115 (64.5 %)						
obs→ ↓for	O1	O2	O3	O4	O5	sum
F1	**319**	20	10	0	0	349
F2	197	**65**	31	2	0	295
F3	142	124	**201**	33	13	513
F4	3	6	40	**25**	6	80
F5	0	0	3	2	**2**	7
sum	661	215	285	62	21	1244
%FO	48	30	71	40	10	49

T1D 20041213-20050115 (63.4 %)						
obs→ ↓for	O1	O2	O3	O4	O5	sum
F1	**325**	25	9	0	0	359
F2	186	**54**	26	2	0	268
F3	145	130	**208**	29	12	524
F4	5	6	40	**30**	7	88
F5	0	0	2	1	**2**	5
sum	661	215	285	62	21	1244
%FO	49	25	73	48	10	50

T1X 20041213-20050115 (62.7 %)						
obs→ ↓for	O1	O2	O3	O4	O5	sum
F1	**321**	21	10	1	0	353
F2	182	**61**	34	1	0	278
F3	151	126	**199**	38	12	526
F4	7	7	39	**20**	7	80
F5	0	0	3	2	**2**	7
sum	661	215	285	62	21	1244
%FO	49	28	70	32	10	48

T1U 20041213-20050115 (64.6 %)						
obs→ ↓for	O1	O2	O3	O4	O5	sum
F1	**327**	17	10	1	0	355
F2	184	**69**	30	1	0	284
F3	146	123	**207**	27	12	515
F4	4	6	36	**32**	7	85
F5	0	0	2	1	**2**	5
sum	661	215	285	62	21	1244
%FO	49	32	73	52	10	51

T1F 20041213-20050115 (63.4 %)						
obs→ ↓for	O1	O2	O3	O4	O5	sum
F1	**315**	21	8	0	0	344
F2	210	**63**	37	3	0	313
F3	131	123	**198**	32	10	494
F4	5	7	38	**26**	9	85
F5	0	1	4	1	**2**	8
sum	661	215	285	62	21	1244
%FO	48	29	69	42	10	49

T1A 20041213-20050115 (60.5 %)						
obs→ ↓for	O1	O2	O3	O4	O5	sum
F1	**311**	22	12	0	0	345
F2	190	**54**	33	2	0	279
F3	157	126	**185**	33	11	512
F4	3	13	52	**25**	8	101
F5	0	0	3	2	**2**	7
sum	661	215	285	62	21	1244
%FO	47	25	65	40	10	46

T1V 20041213-20050115 (62.6 %)						
obs→ ↓for	O1	O2	O3	O4	O5	sum
F1	**318**	21	8	0	0	347
F2	187	**58**	46	2	0	293
F3	150	129	**178**	33	11	501
F4	6	7	50	**26**	8	97
F5	0	0	3	1	**2**	6
sum	661	215	285	62	21	1244
%FO	48	27	62	42	10	47

Table 9: Contingency tables for 20041213-20050115 (18–30 h forecasts). Danish station list.

T1A 20041213-20050115 (60.3 %)						
obs→ ↓for	O1	O2	O3	O4	O5	sum
F1	**300**	17	13	0	0	330
F2	195	**53**	23	2	1	274
F3	152	130	**204**	42	15	543
F4	13	13	44	**18**	2	90
F5	1	0	2	0	**3**	6
sum	661	213	286	62	21	1243
%FO	45	25	71	29	14	47

T1B 20041213-20050115 (60.0 %)						
obs→ ↓for	O1	O2	O3	O4	O5	sum
F1	**307**	21	13	0	0	341
F2	199	**52**	31	3	0	285
F3	145	119	**194**	41	15	514
F4	9	21	45	**18**	4	97
F5	1	0	3	0	**2**	6
sum	661	213	286	62	21	1243
%FO	46	24	68	29	10	46

T1W 20041213-20050115 (59.7 %)						
obs→ ↓for	O1	O2	O3	O4	O5	sum
F1	**292**	21	10	0	0	323
F2	197	**43**	25	2	0	267
F3	161	137	**202**	43	15	558
F4	11	12	47	**17**	3	90
F5	0	0	2	0	**3**	5
sum	661	213	286	62	21	1243
%FO	44	20	71	27	14	45

T1T 20041213-20050115 (60.5 %)						
obs→ ↓for	O1	O2	O3	O4	O5	sum
F1	**298**	16	15	0	0	329
F2	193	**53**	19	1	0	266
F3	160	134	**205**	37	15	551
F4	9	10	44	**24**	3	90
F5	1	0	3	0	**3**	7
sum	661	213	286	62	21	1243
%FO	45	25	72	39	14	47

T1D 20041213-20050115 (59.9 %)						
obs→ ↓for	O1	O2	O3	O4	O5	sum
F1	**297**	18	11	0	0	326
F2	197	**47**	23	2	0	269
F3	158	136	**207**	37	16	554
F4	8	12	41	**23**	2	86
F5	1	0	4	0	**3**	8
sum	661	213	286	62	21	1243
%FO	45	22	72	37	14	46

T1X 20041213-20050115 (60.1 %)						
obs→ ↓for	O1	O2	O3	O4	O5	sum
F1	**298**	17	13	0	0	328
F2	199	**50**	27	2	0	278
F3	149	131	**204**	41	14	539
F4	13	15	40	**19**	4	91
F5	2	0	2	0	**3**	7
sum	661	213	286	62	21	1243
%FO	45	23	71	31	14	46

T1U 20041213-20050115 (61.3 %)						
obs→ ↓for	O1	O2	O3	O4	O5	sum
F1	**324**	21	12	1	0	358
F2	182	**56**	33	3	1	275
F3	144	119	**194**	37	13	507
F4	10	17	44	**21**	4	96
F5	1	0	3	0	**3**	7
sum	661	213	286	62	21	1243
%FO	49	26	68	34	14	48

T1F 20041213-20050115 (59.0 %)						
obs→ ↓for	O1	O2	O3	O4	O5	sum
F1	**328**	22	10	0	0	360
F2	169	**60**	37	4	0	270
F3	149	112	**177**	40	13	491
F4	14	19	60	**18**	5	116
F5	1	0	2	0	**3**	6
sum	661	213	286	62	21	1243
%FO	50	28	62	29	14	47

T1A 20041213-20050115 (60.3 %)						
obs→ ↓for	O1	O2	O3	O4	O5	sum
F1	**300**	17	13	0	0	330
F2	195	**53**	23	2	1	274
F3	152	130	**204**	42	15	543
F4	13	13	44	**18**	2	90
F5	1	0	2	0	**3**	6
sum	661	213	286	62	21	1243
%FO	45	25	71	29	14	47

T1V 20041213-20050115 (60.6 %)						
obs→ ↓for	O1	O2	O3	O4	O5	sum
F1	**300**	20	10	0	0	330
F2	191	**52**	29	2	0	274
F3	160	126	**210**	43	14	553
F4	9	15	34	**17**	4	79
F5	1	0	3	0	**3**	7
sum	661	213	286	62	21	1243
%FO	45	24	73	27	14	47

Table 10: Contingency tables for 20041213-20050115 (30–42 h forecasts). Danish station list.

T1A 20041213-20050115 (58.9 %)						
obs→ ↓for	O1	O2	O3	O4	O5	sum
F1	**287**	15	7	1	0	310
F2	181	**59**	36	12	2	290
F3	150	116	**194**	35	12	507
F4	9	17	48	**12**	7	93
F5	2	1	1	2	**0**	6
sum	629	208	286	62	21	1206
%FO	46	28	68	19	0	46

T1B 20041213-20050115 (60.6 %)						
obs→ ↓for	O1	O2	O3	O4	O5	sum
F1	**295**	20	11	2	0	328
F2	178	**56**	28	8	1	271
F3	146	117	**201**	35	11	510
F4	10	15	45	**16**	8	94
F5	0	0	1	1	**1**	3
sum	629	208	286	62	21	1206
%FO	47	27	70	26	5	47

T1W 20041213-20050115 (58.6 %)						
obs→ ↓for	O1	O2	O3	O4	O5	sum
F1	**280**	16	11	3	0	310
F2	194	**56**	33	9	4	296
F3	148	124	**189**	36	11	508
F4	7	12	46	**12**	6	83
F5	0	0	7	2	**0**	9
sum	629	208	286	62	21	1206
%FO	45	27	66	19	0	45

T1T 20041213-20050115 (58.7 %)						
obs→ ↓for	O1	O2	O3	O4	O5	sum
F1	**300**	21	12	2	0	335
F2	178	**60**	38	6	1	283
F3	144	108	**188**	40	14	494
F4	7	19	48	**13**	6	93
F5	0	0	0	1	**0**	1
sum	629	208	286	62	21	1206
%FO	48	29	66	21	0	47

T1D 20041213-20050115 (59.6 %)						
obs→ ↓for	O1	O2	O3	O4	O5	sum
F1	**292**	18	8	2	0	320
F2	192	**66**	44	4	2	308
F3	138	110	**187**	42	13	490
F4	7	14	46	**13**	6	86
F5	0	0	1	1	**0**	2
sum	629	208	286	62	21	1206
%FO	46	32	65	21	0	46

T1X 20041213-20050115 (58.2 %)						
obs→ ↓for	O1	O2	O3	O4	O5	sum
F1	**291**	22	15	4	0	332
F2	170	**57**	29	6	0	262
F3	156	109	**189**	36	13	503
F4	11	19	52	**15**	7	104
F5	**1**	1	1	1	**1**	5
sum	629	208	286	62	21	1206
%FO	46	27	66	24	5	46

T1U 20041213-20050115 (58.0 %)						
obs→ ↓for	O1	O2	O3	O4	O5	sum
F1	**299**	19	9	2	0	329
F2	180	**63**	35	2	0	280
F3	141	109	**178**	42	13	483
F4	9	17	61	**13**	6	106
F5	0	0	3	3	**2**	8
sum	629	208	286	62	21	1206
%FO	48	30	62	21	10	46

T1F 20041213-20050115 (57.5 %)						
obs→ ↓for	O1	O2	O3	O4	O5	sum
F1	**292**	25	12	1	0	330
F2	180	**56**	39	7	2	284
F3	148	111	**178**	40	15	492
F4	8	15	56	**14**	3	96
F5	**1**	1	1	0	**1**	4
sum	629	208	286	62	21	1206
%FO	46	27	62	23	5	45

T1A 20041213-20050115 (58.9 %)						
obs→ ↓for	O1	O2	O3	O4	O5	sum
F1	**287**	15	7	1	0	310
F2	181	**59**	36	12	2	290
F3	150	116	**194**	35	12	507
F4	9	17	48	**12**	7	93
F5	**2**	1	1	2	**0**	6
sum	629	208	286	62	21	1206
%FO	46	28	68	19	0	46

T1V 20041213-20050115 (58.3 %)						
obs→ ↓for	O1	O2	O3	O4	O5	sum
F1	**286**	16	12	2	0	316
F2	180	**64**	35	8	0	287
F3	149	108	**187**	35	13	492
F4	13	19	49	**15**	8	104
F5	**1**	1	3	2	**0**	7
sum	629	208	286	62	21	1206
%FO	45	31	65	24	0	46

Table 11: Contingency tables for 20041213-20050115 (6–18 h forecasts). EWGLAM station list.

T1A 20041213-20050115						
obs→ ↓for	O1	O2	O3	O4	O5	sum
F1	**8793**	382	105	12	**3**	9295
F2	2821	**992**	504	40	10	4367
F3	1109	1106	**1820**	411	92	4538
F4	60	63	343	**342**	170	978
F5	**4**	7	44	72	**169**	296
sum	12787	2550	2816	877	444	19474
%FO	69	39	65	39	38	62

T1B 20041213-20050115						
obs→ ↓for	O1	O2	O3	O4	O5	sum
F1	**8813**	375	108	9	**2**	9307
F2	2786	**1015**	466	41	12	4320
F3	1126	1094	**1865**	397	80	4562
F4	56	64	331	**367**	179	997
F5	**6**	2	46	63	**171**	288
sum	12787	2550	2816	877	444	19474
%FO	69	40	66	42	39	63

T1W 20041213-20050115						
obs→ ↓for	O1	O2	O3	O4	O5	sum
F1	**8774**	372	99	11	**1**	9257
F2	2829	**1019**	493	40	13	4394
F3	1116	1092	**1841**	406	83	4538
F4	59	60	339	**350**	181	989
F5	**9**	7	44	70	**166**	296
sum	12787	2550	2816	877	444	19474
%FO	69	40	65	40	37	62

T1T 20041213-20050115						
obs→ ↓for	O1	O2	O3	O4	O5	sum
F1	**8763**	369	82	10	**2**	9226
F2	2841	**995**	475	38	11	4360
F3	1114	1120	**1891**	409	90	4624
F4	64	58	322	**353**	175	972
F5	**5**	8	46	67	**166**	292
sum	12787	2550	2816	877	444	19474
%FO	69	39	67	40	37	62

T1D 20041213-20050115						
obs→ ↓for	O1	O2	O3	O4	O5	sum
F1	**8781**	369	88	9	**3**	9250
F2	2843	**990**	480	33	12	4358
F3	1098	1130	**1877**	410	83	4598
F4	58	52	323	**358**	184	975
F5	**7**	9	48	67	**162**	293
sum	12787	2550	2816	877	444	19474
%FO	69	39	67	41	36	62

T1X 20041213-20050115						
obs→ ↓for	O1	O2	O3	O4	O5	sum
F1	**8824**	365	95	10	**1**	9295
F2	2775	**1030**	501	41	12	4359
F3	1125	1089	**1847**	394	80	4535
F4	56	61	327	**364**	181	989
F5	**7**	5	46	68	**170**	296
sum	12787	2550	2816	877	444	19474
%FO	69	40	66	42	38	63

T1U 20041213-20050115						
obs→ ↓for	O1	O2	O3	O4	O5	sum
F1	**8867**	369	84	13	**2**	9335
F2	2773	**999**	459	29	19	4279
F3	1077	1116	**1881**	413	74	4561
F4	65	57	348	**351**	186	1007
F5	**5**	9	44	71	**163**	292
sum	12787	2550	2816	877	444	19474
%FO	69	39	67	40	37	63

T1F 20041213-20050115						
obs→ ↓for	O1	O2	O3	O4	O5	sum
F1	**8854**	364	76	8	**3**	9305
F2	2809	**996**	463	26	7	4301
F3	1060	1128	**1874**	411	79	4552
F4	54	59	365	**362**	175	1015
F5	**10**	3	38	70	**180**	301
sum	12787	2550	2816	877	444	19474
%FO	69	39	67	41	41	63

T1A 20041213-20050115						
obs→ ↓for	O1	O2	O3	O4	O5	sum
F1	**8793**	382	105	12	**3**	9295
F2	2821	**992**	504	40	10	4367
F3	1109	1106	**1820**	411	92	4538
F4	60	63	343	**342**	170	978
F5	**4**	7	44	72	**169**	296
sum	12787	2550	2816	877	444	19474
%FO	69	39	65	39	38	62

T1V 20041213-20050115						
obs→ ↓for	O1	O2	O3	O4	O5	sum
F1	**8793**	377	105	11	**1**	9287
F2	2828	**997**	496	43	10	4374
F3	1097	1103	**1830**	404	93	4527
F4	65	66	333	**356**	172	992
F5	**4**	7	52	63	**168**	294
sum	12787	2550	2816	877	444	19474
%FO	69	39	65	41	38	62

Table 12: Contingency tables for 20041213-20050115 (18–30 h forecasts). EWGLAM station list.

T1A 20041213-20050115						
obs→ ↓for	O1	O2	O3	O4	O5	sum
F1	**8684**	409	147	21	**3**	9264
F2	2764	**997**	521	48	13	4343
F3	1230	1068	**1797**	428	112	4635
F4	76	65	320	**320**	174	955
F5	**9**	11	45	64	**144**	273
sum	12763	2550	2830	881	446	19470
%FO	68	39	63	36	32	61

T1B 20041213-20050115						
obs→ ↓for	O1	O2	O3	O4	O5	sum
F1	**8702**	423	145	17	**2**	9289
F2	2718	**981**	503	53	15	4270
F3	1246	1069	**1823**	414	107	4659
F4	90	68	315	**329**	176	978
F5	**7**	9	44	68	**146**	274
sum	12763	2550	2830	881	446	19470
%FO	68	38	64	37	33	62

T1W 20041213-20050115						
obs→ ↓for	O1	O2	O3	O4	O5	sum
F1	**8696**	403	123	14	**2**	9238
F2	2762	**1005**	546	44	12	4369
F3	1231	1077	**1793**	440	109	4650
F4	64	60	324	**315**	180	943
F5	**10**	5	44	68	**143**	270
sum	12763	2550	2830	881	446	19470
%FO	68	39	63	36	32	61

T1T 20041213-20050115						
obs→ ↓for	O1	O2	O3	O4	O5	sum
F1	**8654**	403	143	17	**3**	9220
F2	2768	**993**	475	49	9	4294
F3	1258	1084	**1837**	433	111	4723
F4	72	63	327	**317**	178	957
F5	**11**	7	48	65	**145**	276
sum	12763	2550	2830	881	446	19470
%FO	68	39	65	36	33	61

T1D 20041213-20050115						
obs→ ↓for	O1	O2	O3	O4	O5	sum
F1	**8653**	409	126	12	**3**	9203
F2	2791	**983**	527	50	10	4361
F3	1235	1079	**1807**	436	105	4662
F4	73	71	324	**326**	180	974
F5	**11**	8	46	57	**148**	270
sum	12763	2550	2830	881	446	19470
%FO	68	39	64	37	33	61

T1X 20041213-20050115						
obs→ ↓for	O1	O2	O3	O4	O5	sum
F1	**8709**	408	145	18	**2**	9282
F2	2714	**1009**	504	48	16	4291
F3	1259	1053	**1830**	417	115	4674
F4	74	72	312	**325**	162	945
F5	**7**	8	39	73	**151**	278
sum	12763	2550	2830	881	446	19470
%FO	68	40	65	37	34	62

T1U 20041213-20050115						
obs→ ↓for	O1	O2	O3	O4	O5	sum
F1	**8680**	413	115	16	**1**	9225
F2	2761	**991**	520	46	20	4338
F3	1234	1069	**1836**	431	93	4663
F4	79	67	316	**317**	176	955
F5	**9**	10	43	71	**156**	289
sum	12763	2550	2830	881	446	19470
%FO	68	39	65	36	35	62

T1F 20041213-20050115						
obs→ ↓for	O1	O2	O3	O4	O5	sum
F1	**8644**	415	98	13	**3**	9173
F2	2822	**983**	516	40	12	4373
F3	1213	1070	**1834**	417	90	4624
F4	76	75	339	**335**	179	1004
F5	**8**	7	43	76	**162**	296
sum	12763	2550	2830	881	446	19470
%FO	68	39	65	38	36	61

T1A 20041213-20050115						
obs→ ↓for	O1	O2	O3	O4	O5	sum
F1	**8684**	409	147	21	**3**	9264
F2	2764	**997**	521	48	13	4343
F3	1230	1068	**1797**	428	112	4635
F4	76	65	320	**320**	174	955
F5	**9**	11	45	64	**144**	273
sum	12763	2550	2830	881	446	19470
%FO	68	39	63	36	32	61

T1V 20041213-20050115						
obs→ ↓for	O1	O2	O3	O4	O5	sum
F1	**8700**	410	149	14	**3**	9276
F2	2757	**985**	517	56	14	4329
F3	1220	1065	**1790**	427	110	4612
F4	80	82	329	**317**	172	980
F5	**6**	8	45	67	**147**	273
sum	12763	2550	2830	881	446	19470
%FO	68	39	63	36	33	61

Table 13: Contingency tables for 20041213-20050115 (30–42 h forecasts). EWGLAM station list.

T1A 20041213-20050115						
obs→ ↓for	O1	O2	O3	O4	O5	sum
F1	**8298**	436	188	20	**11**	8953
F2	2665	**922**	592	75	30	4284
F3	1264	1024	**1605**	442	112	4447
F4	97	87	335	**263**	154	936
F5	**22**	10	50	72	**131**	285
sum	12346	2479	2770	872	438	18905
%FO	67	37	58	30	30	59

T1B 20041213-20050115						
obs→ ↓for	O1	O2	O3	O4	O5	sum
F1	**8330**	448	180	18	**5**	8981
F2	2652	**924**	573	64	29	4242
F3	1247	999	**1632**	461	116	4455
F4	92	94	330	**255**	142	913
F5	**25**	14	55	74	**146**	314
sum	12346	2479	2770	872	438	18905
%FO	67	37	59	29	33	60

T1W 20041213-20050115						
obs→ ↓for	O1	O2	O3	O4	O5	sum
F1	**8279**	440	182	24	**8**	8933
F2	2698	**926**	565	66	29	4284
F3	1260	1017	**1639**	439	110	4465
F4	88	82	335	**272**	146	923
F5	**21**	14	49	71	**145**	300
sum	12346	2479	2770	872	438	18905
%FO	67	37	59	31	33	60

T1T 20041213-20050115						
obs→ ↓for	O1	O2	O3	O4	O5	sum
F1	**8259**	437	177	21	**6**	8900
F2	2709	**897**	552	71	25	4254
F3	1265	1043	**1633**	432	120	4493
F4	93	88	360	**279**	146	966
F5	**20**	14	48	69	**141**	292
sum	12346	2479	2770	872	438	18905
%FO	67	36	59	32	32	59

T1D 20041213-20050115						
obs→ ↓for	O1	O2	O3	O4	O5	sum
F1	**8292**	439	167	20	**7**	8925
F2	2673	**907**	573	73	28	4254
F3	1276	1040	**1643**	434	120	4513
F4	84	80	337	**276**	147	924
F5	**21**	13	50	69	**136**	289
sum	12346	2479	2770	872	438	18905
%FO	67	37	59	32	31	60

T1X 20041213-20050115						
obs→ ↓for	O1	O2	O3	O4	O5	sum
F1	**8318**	446	184	22	**12**	8982
F2	2653	**895**	547	65	19	4179
F3	1268	1049	**1625**	450	125	4517
F4	86	79	361	**259**	137	922
F5	**21**	10	53	76	**145**	305
sum	12346	2479	2770	872	438	18905
%FO	67	36	59	30	33	59

T1U 20041213-20050115						
obs→ ↓for	O1	O2	O3	O4	O5	sum
F1	**8303**	450	173	19	**5**	8950
F2	2687	**891**	561	51	27	4217
F3	1242	1033	**1636**	445	128	4484
F4	91	93	335	**271**	140	930
F5	**23**	12	65	86	**138**	324
sum	12346	2479	2770	872	438	18905
%FO	67	36	59	31	32	59

T1F 20041213-20050115						
obs→ ↓for	O1	O2	O3	O4	O5	sum
F1	**8339**	425	149	14	**5**	8932
F2	2660	**916**	548	57	14	4195
F3	1235	1046	**1679**	412	113	4485
F4	94	80	341	**314**	162	991
F5	**18**	12	53	75	**144**	302
sum	12346	2479	2770	872	438	18905
%FO	68	37	61	36	33	60

T1A 20041213-20050115						
obs→ ↓for	O1	O2	O3	O4	O5	sum
F1	**8298**	436	188	20	**11**	8953
F2	2665	**922**	592	75	30	4284
F3	1264	1024	**1605**	442	112	4447
F4	97	87	335	**263**	154	936
F5	**22**	10	50	72	**131**	285
sum	12346	2479	2770	872	438	18905
%FO	67	37	58	30	30	59

T1V 20041213-20050115						
obs→ ↓for	O1	O2	O3	O4	O5	sum
F1	**8294**	439	192	26	**7**	8958
F2	2675	**914**	576	83	37	4285
F3	1252	1037	**1598**	438	109	4434
F4	98	76	354	**252**	151	931
F5	**27**	13	50	73	**134**	297
sum	12346	2479	2770	872	438	18905
%FO	67	37	58	29	31	59

Table 14: Equitable threat scores (ETS) against Danish stations for the December/January period runs. ETS1 is for a limit of 0.3 mm/12 h, ETS2 is for a limit of 1.5 mm/12 h and ETS3 is for a limit of 5.0 mm/12 h. The smallest value and values within 0.0025 of this value for a given forecast range and limit is shown in red. The best value as well as values within 0.0025 of this value for a given forecast range and limit is marked with bold black font.

Danish stations									
	6–18 h			18–30 h			30–42 h		
model	ETS1	ETS2	ETS3	ETS1	ETS2	ETS3	ETS1	ETS2	ETS3
T1A	0.272	**0.305**	0.203	0.273	0.277	0.111	0.264	0.273	0.092
T1B	0.297	0.300	0.170	0.282	**0.294**	0.110	**0.271**	0.271	**0.131**
T1D	0.289	**0.305**	0.260	0.259	0.276	0.152	**0.272**	**0.291**	0.096
T1T	**0.308**	0.285	0.226	0.264	0.281	**0.157**	0.261	0.264	0.090
T1U	0.301	**0.306**	**0.288**	**0.288**	0.286	0.140	0.266	0.261	0.098
T1W	0.295	0.297	0.222	0.264	0.265	0.112	0.251	0.269	0.092
T1V	0.294	0.295	0.212	0.264	0.257	0.131	0.253	0.267	0.108
T1X	0.282	0.297	0.189	0.266	0.258	0.131	0.251	0.250	0.103
T1F	0.297	0.286	0.241	0.275	0.285	0.104	0.263	0.269	0.070

Table 15: Equitable threat scores (ETS) against EWGLAM stations for the December/January period runs. ETS1 is for a limit of 0.3 mm/12 h, ETS2 is for a limit of 1.5 mm/12 h and ETS3 is for a limit of 5.0 mm/12 h. The smallest value and values within 0.0025 of this value for a given forecast range and limit is shown in red. The best value as well as values within 0.0025 of this value for a given forecast range and limit is marked with bold black font.

EWGLAM stations									
	6–18 h			18–30 h			30–42 h		
model	ETS1	ETS2	ETS3	ETS1	ETS2	ETS3	ETS1	ETS2	ETS3
T1A	0.396	0.428	0.382	0.382	0.391	0.352	0.357	0.355	0.295
T1B	0.407	0.427	**0.401**	0.381	0.400	0.361	0.367	0.368	0.293
T1D	0.400	0.437	0.398	**0.387**	0.407	0.356	0.364	0.367	0.302
T1T	0.404	0.434	0.391	0.385	0.401	0.354	0.363	0.369	0.299
T1U	**0.410**	0.438	0.391	**0.385**	0.407	0.362	0.361	0.376	0.298
T1W	0.396	0.429	0.392	**0.387**	0.401	0.358	0.359	0.374	0.305
T1V	0.396	0.427	0.384	0.382	0.386	0.347	0.359	0.359	0.289
T1X	0.403	0.429	**0.403**	0.381	0.395	0.358	0.365	0.369	0.292
T1F	**0.409**	**0.448**	0.398	**0.386**	**0.416**	**0.374**	**0.371**	**0.380**	**0.335**

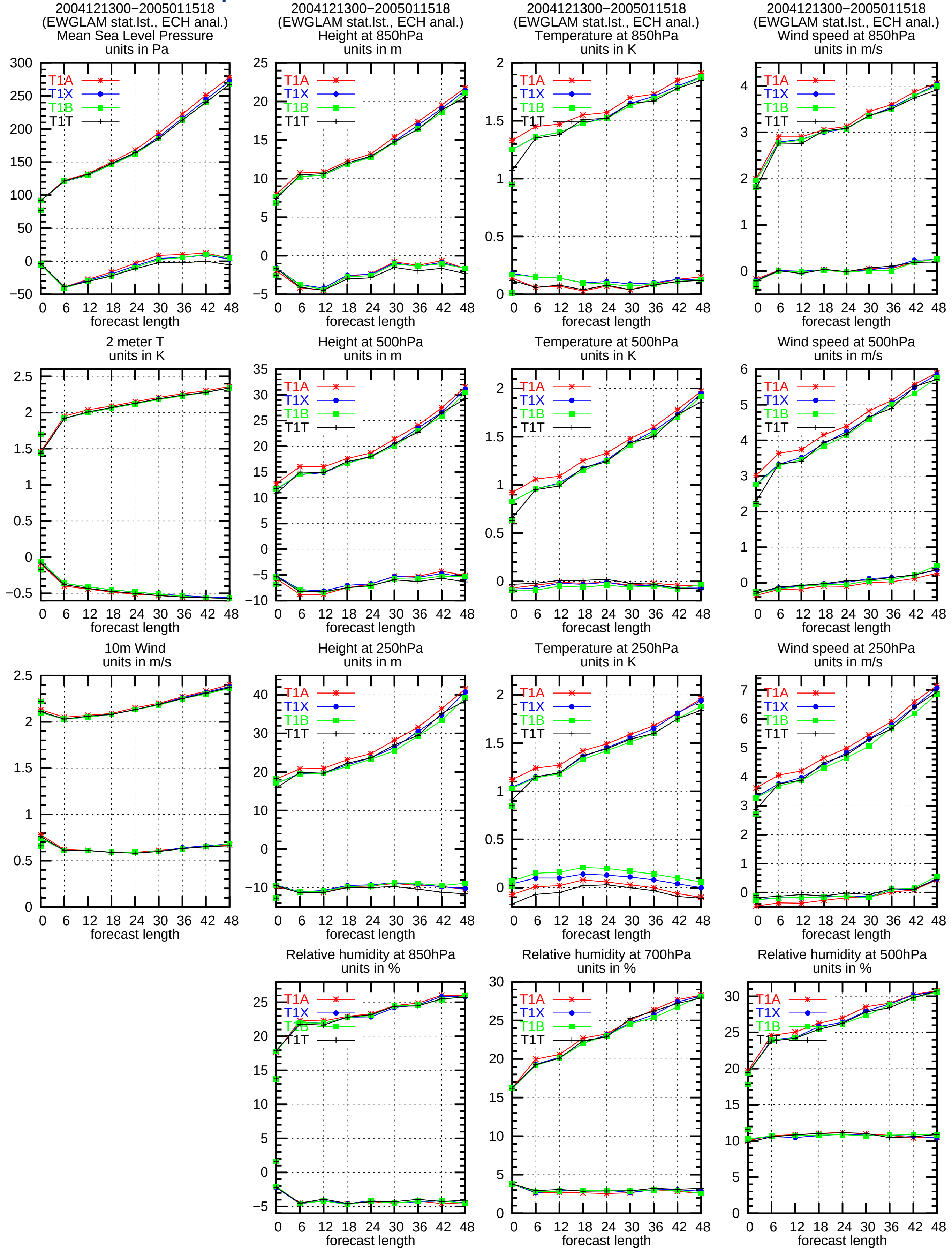

Figure 6: Obs-verification of control run (T1A), ‘additional radiosonde wind and temperature’ (T1T) run, ’all aircraft’ (T1B) run, and ‘E-AMDAR’ (T1X) run. EWGLAM station list.

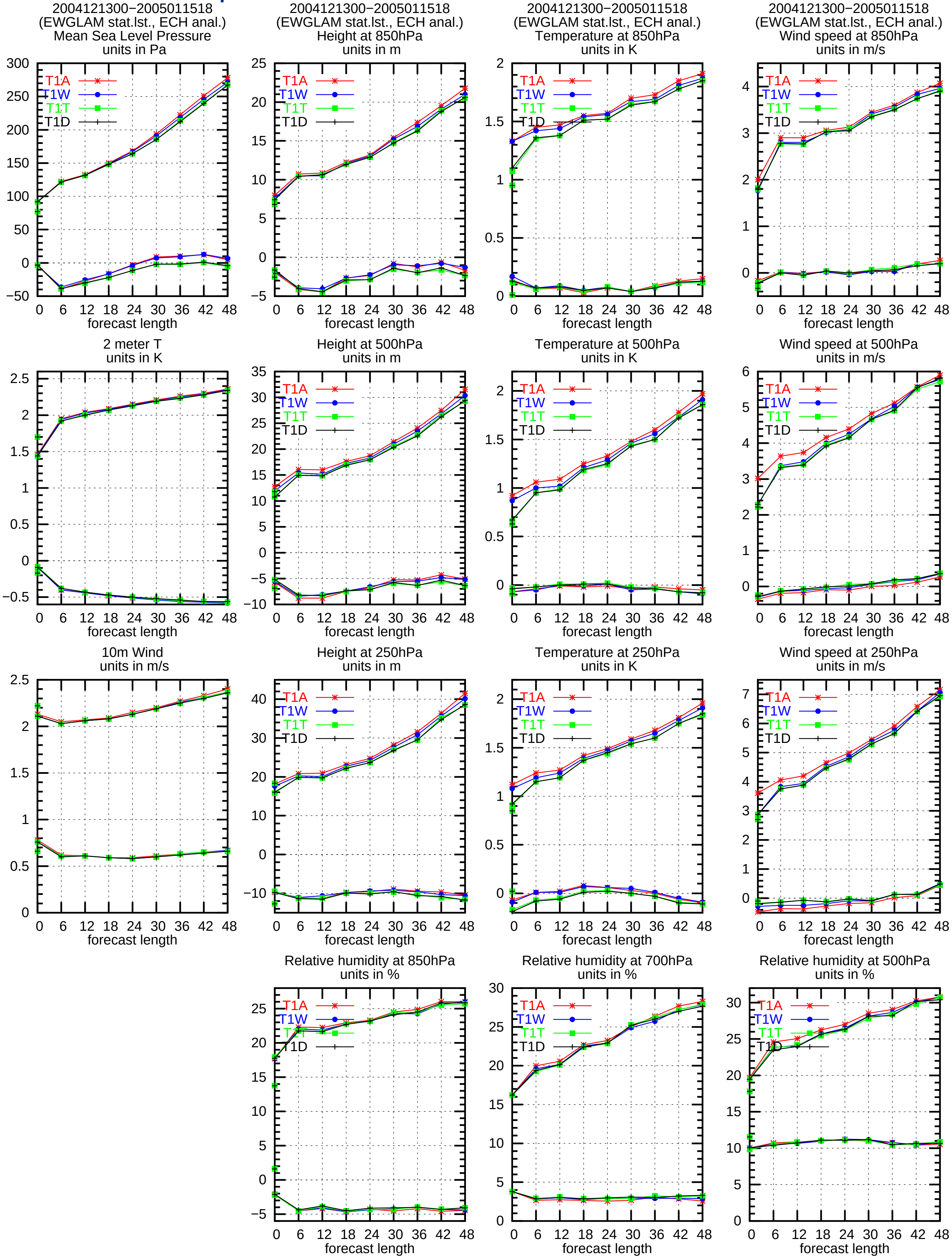

Figure 7: Obs-verification of control run (T1A), ‘additional radiosonde wind’ (T1W) run, ‘additional radiosonde wind and temperature’ (T1T) run, and ‘all TEMP’ run (T1D). EWGLAM station list.

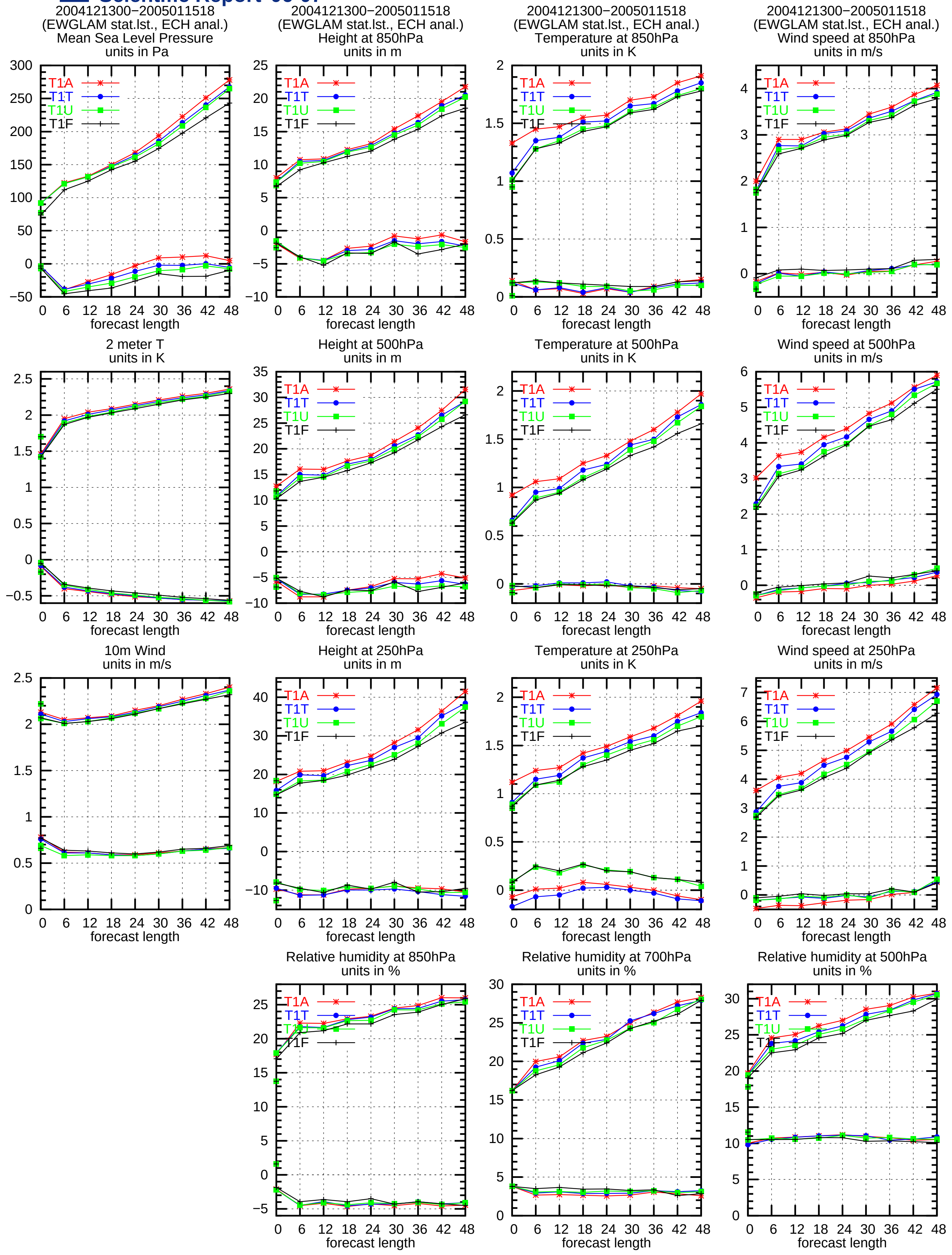

Figure 8: Obs-verification of the control run (T1A), the ‘additional radiosonde wind and temperature’ (T1T) run, ‘additional radiosonde and aircraft wind and temperature’ (T1U) run, and the ‘full system’ (T1F) run. EWGLAM station list.

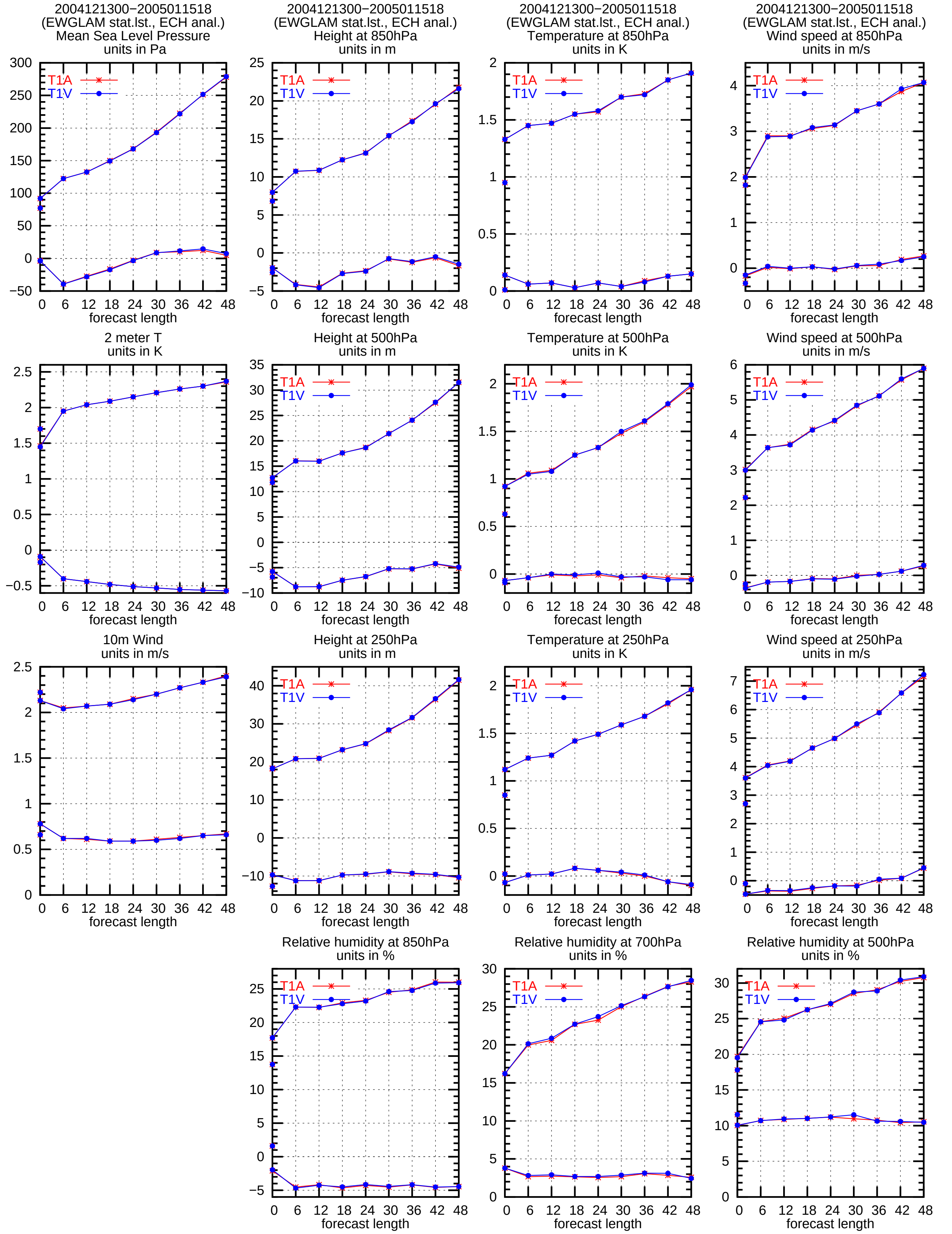

Figure 9: Obs-verification of the baseline (T1A) run and the 'wind profiler' (T1V) run. EWGLAM station list.

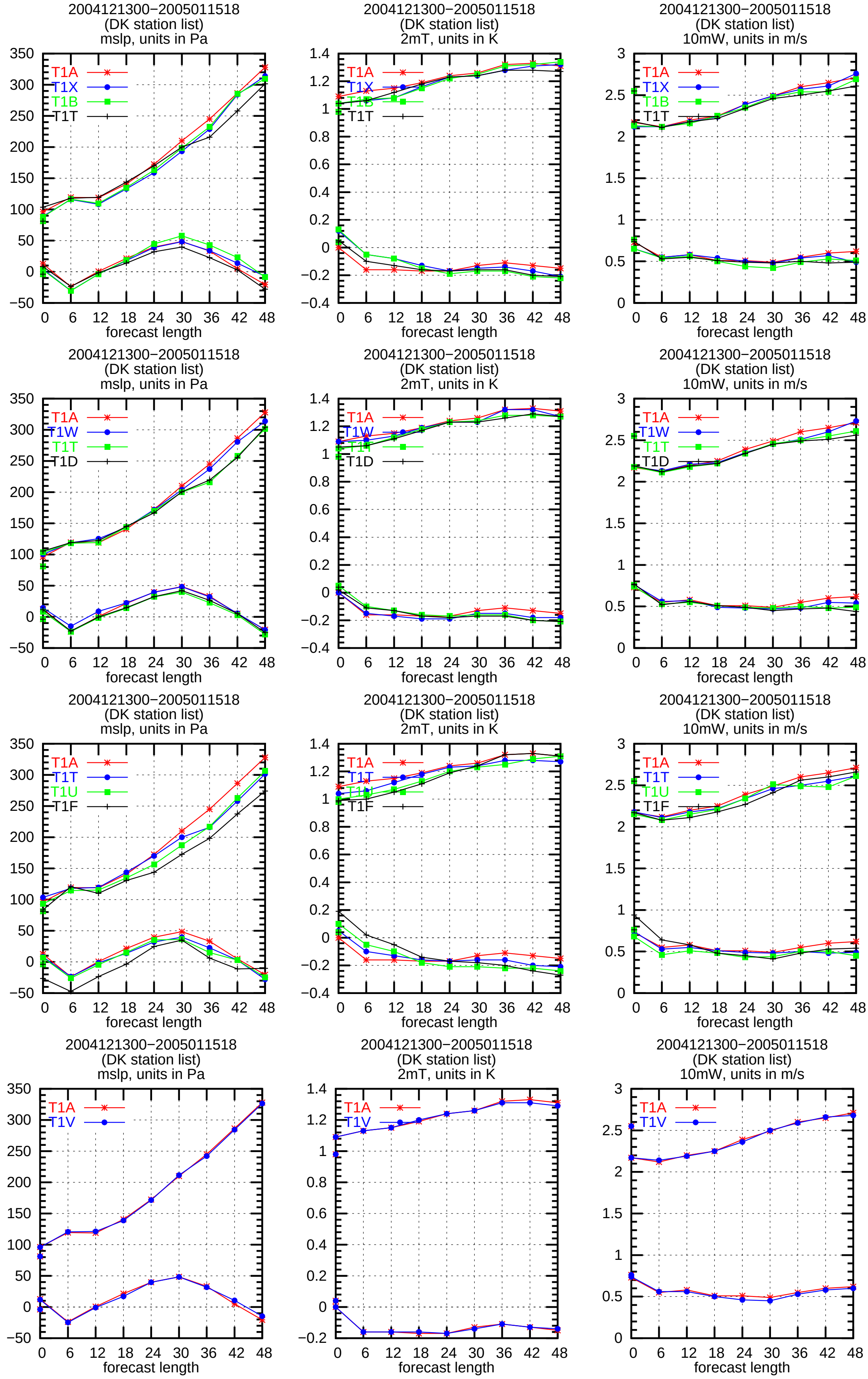

Figure 10: Obs-verification of surface parameters using a Danish station list. (T1F: all observations used; T1A: baseline run; T1B: T1A + aircraft; T1W: T1A + wind from other radiosondes; T1T: T1A + wind and temperature data from other radiosondes; T1D: T1A + data from all other radiosondes; T1X: T1A + E-AMDAR data; T1V: T1A + wind profiler data).

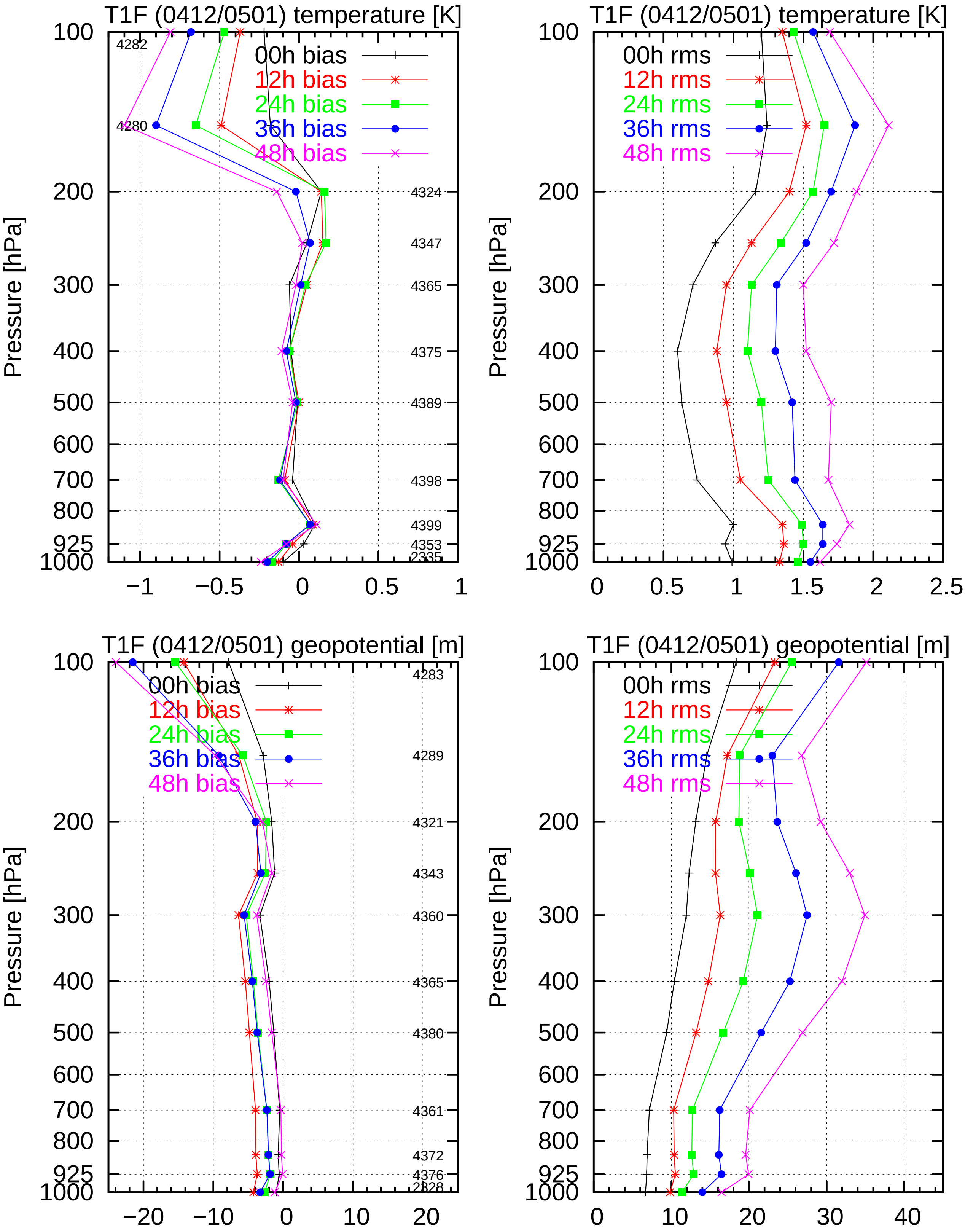

Figure 11: Bias (left) and rms scores at analysis time and for the 12, 24, 36 and 48 hour forecasts of the full system (T1F) experiment as a function of pressure in the December 2004/January 2005 period. Top row is for temperature and bottom row is geopotential. (The numbers in small print in the bias plots indicate the number of observations used).

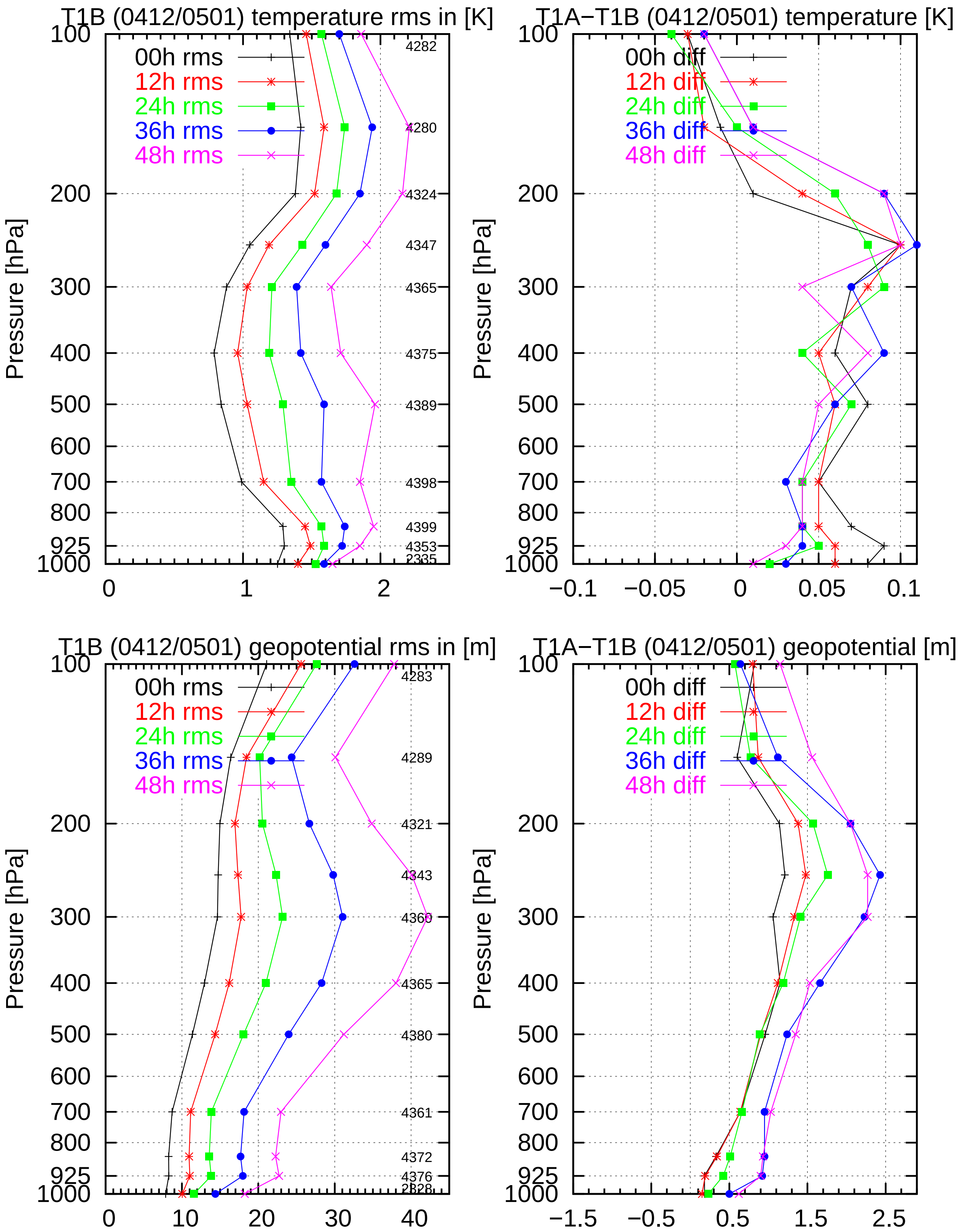

Figure 12: Rms scores for T1B (all AIREPs, left) and differences in rms-scores between T1A (baseline experiment) and T1B (right) at analysis time and for the 12, 24, 36 and 48 hour forecasts as a function of pressure in the December 2004/January 2005 period. Top row is for temperature and bottom row is for geopotential. Positive values in the difference plots indicate T1B has better rms-scores.

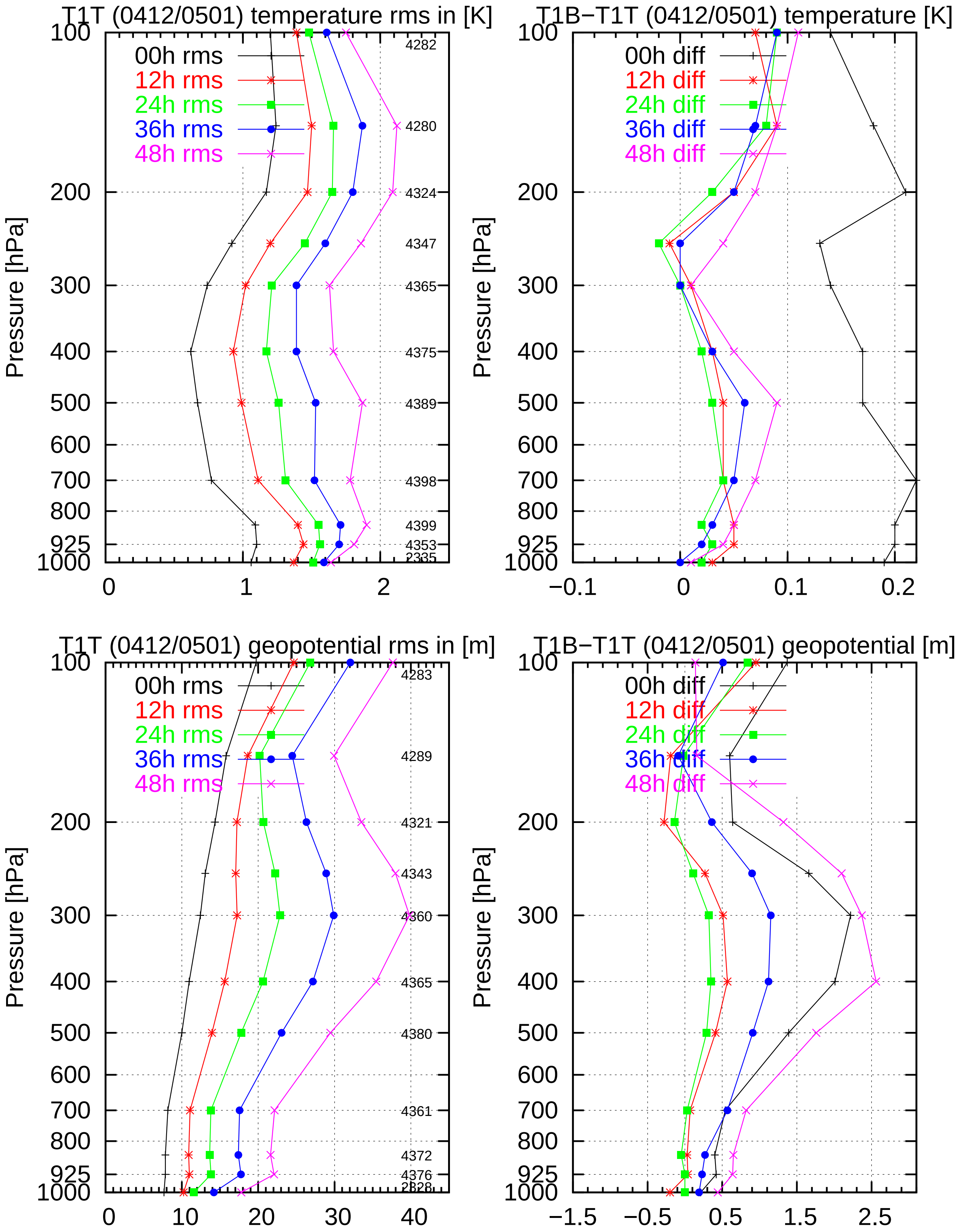

Figure 13: Rms scores for T1T (wind and temperature from radiosondes, left) and differences in rms-scores between T1B (all AIREPs) and T1T (right) at analysis time and for the 12, 24, 36 and 48 hour forecasts as a function of pressure in the December 2004/January 2005 period. Top row is for temperature and bottom row is for geopotential. Positive values in the difference plots indicate T1T has better rms-scores.

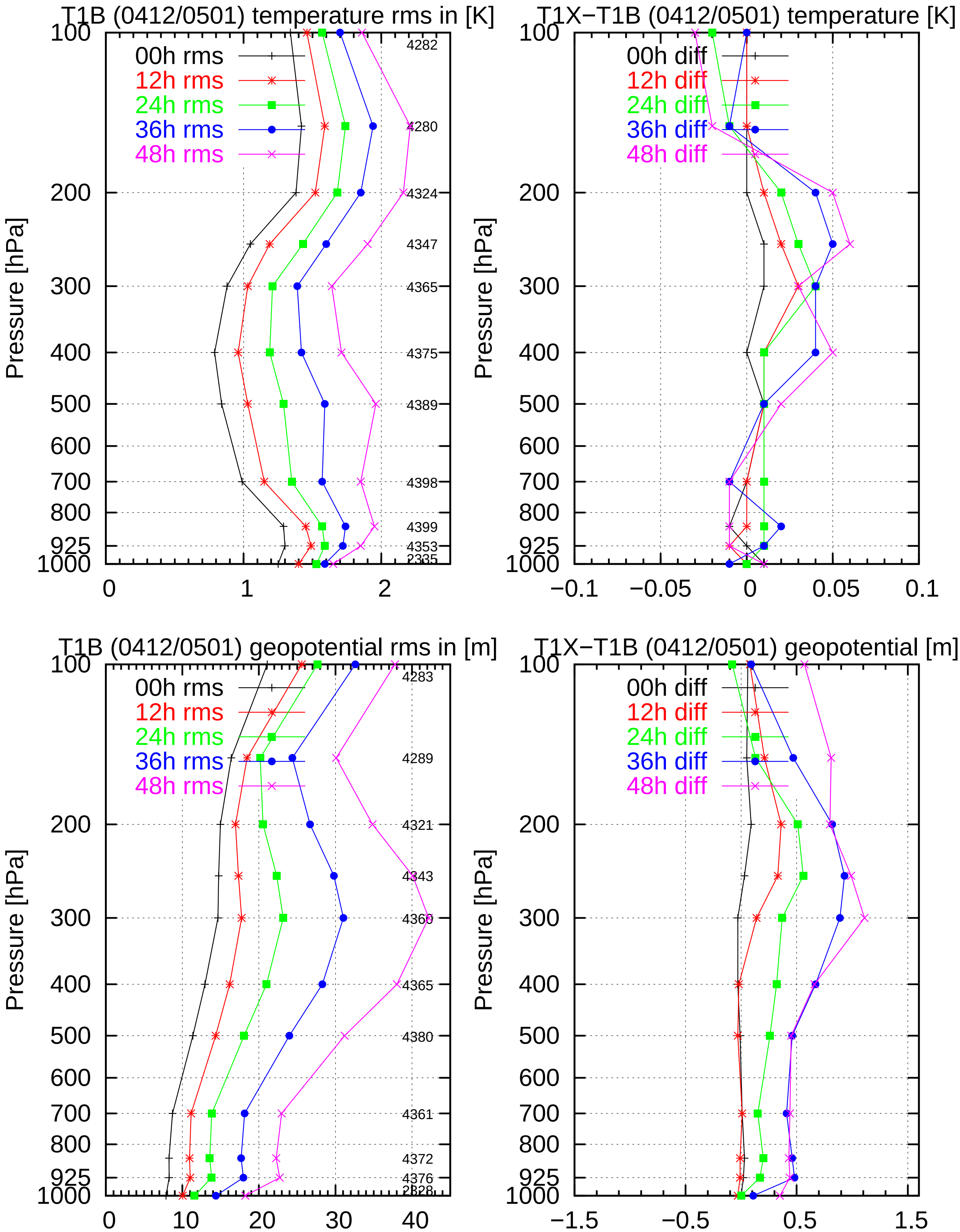

Figure 14: Rms scores for T1B (all AIREPs, left) and differences in rms-scores between T1X (all E-AMDAR) and T1B (right) at analysis time and for the 12, 24, 36 and 48 hour forecasts as a function of pressure in the December 2004/January 2005 period. Top row is for temperature and bottom row is for geopotential. Positive values in the difference plots indicate T1B has better rms-scores.

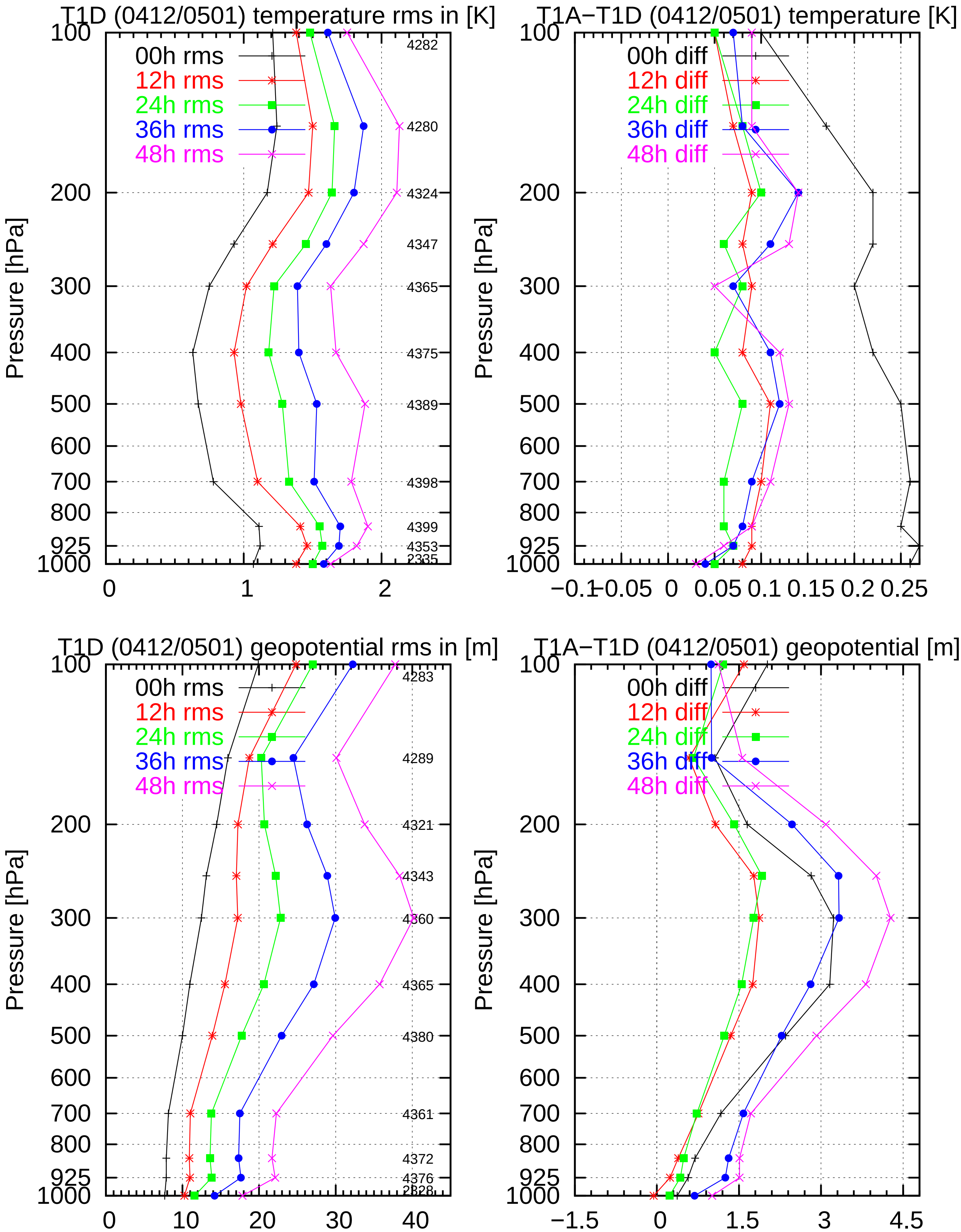

Figure 15: Rms scores for T1D (all TEMPs, left) and differences in rms-scores between T1A (baseline experiment) and T1D (right) at analysis time and for the 12, 24, 36 and 48 hour forecasts as a function of pressure in the December 2004/January 2005 period. Top row is for temperature and bottom row is for geopotential. Positive values in the difference plots indicate T1D has better rms-scores.

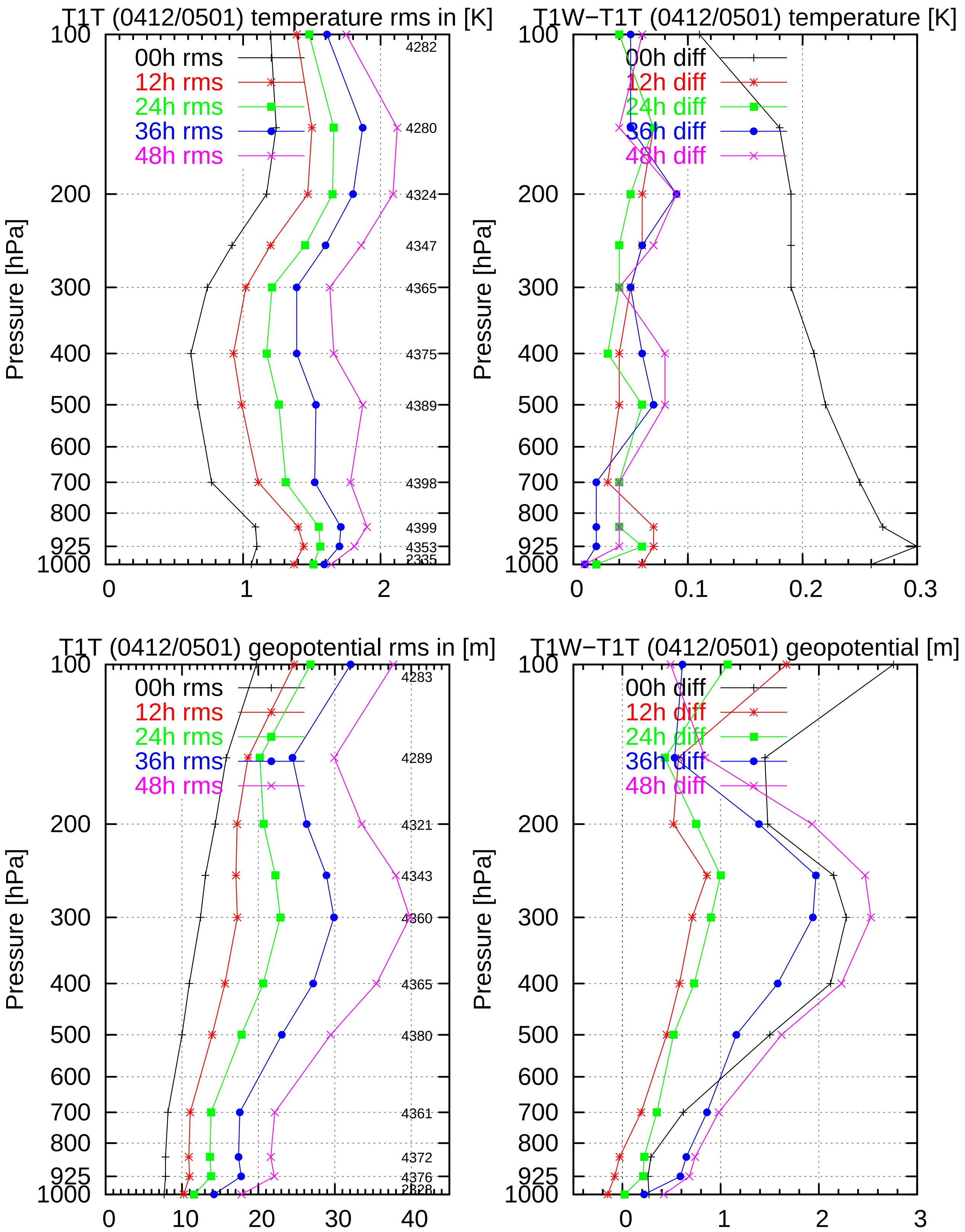

Figure 16: Rms scores for T1T (baseline + additional radiosonde wind and temperature data, left) and differences in rms-scores between T1W (baseline + additional radiosonde wind data) and T1T (right) at analysis time and for the 12, 24, 36 and 48 hour forecasts as a function of pressure in the December 2004/January 2005 period. Top row is for temperature and bottom row is for geopotential. Positive values in the difference plots indicate T1T has better rms-scores.

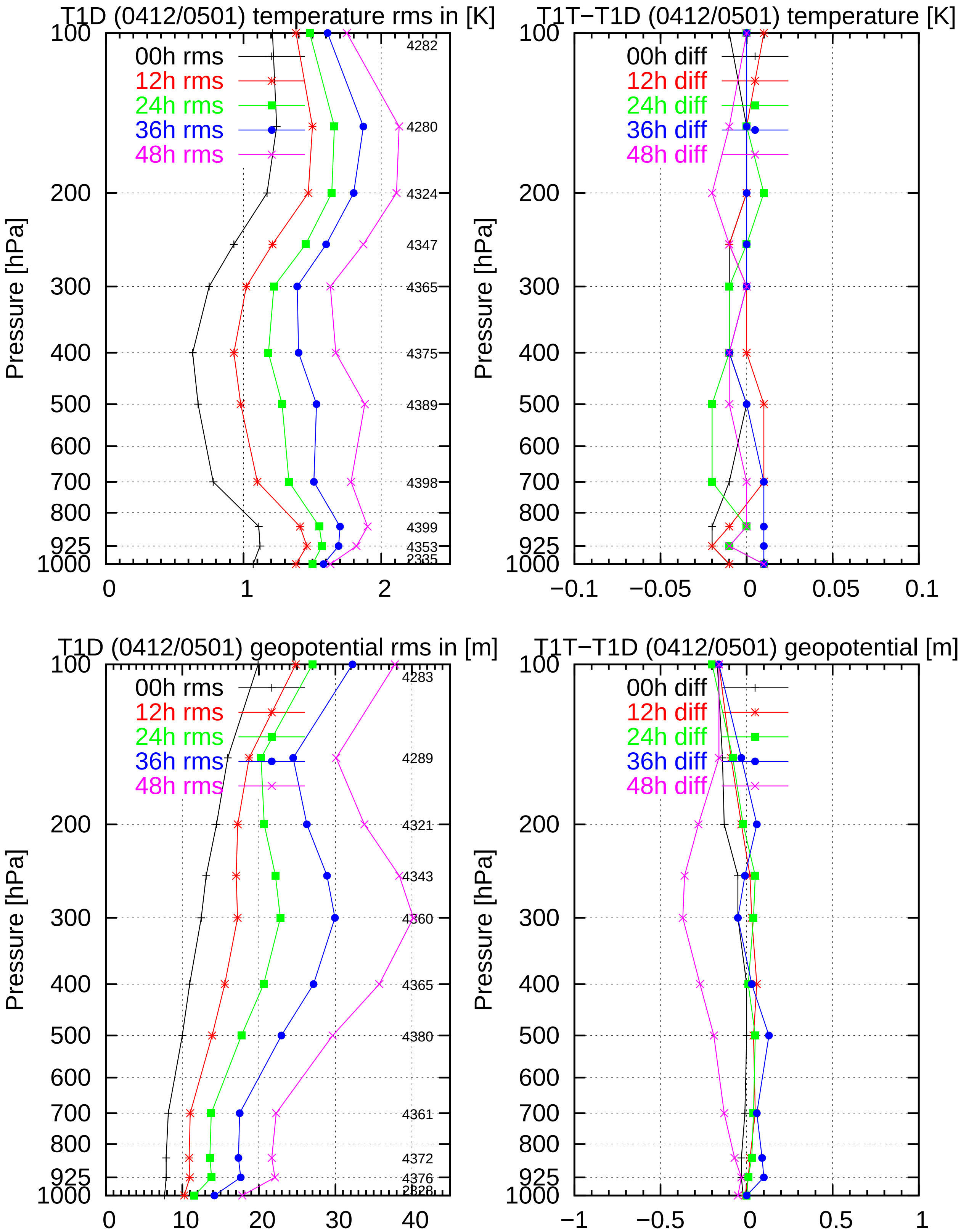

Figure 17: Rms scores for T1D (all radiosonde data, left) and differences in rms-scores between T1T (baseline + additional radiosonde wind and temperature data) and T1D (right) at analysis time and for the 12, 24, 36 and 48 hour forecasts as a function of pressure in the December 2004/January 2005 period. Top row is for temperature and bottom row is for geopotential. Positive values in the difference plots indicate T1D has better rms-scores.

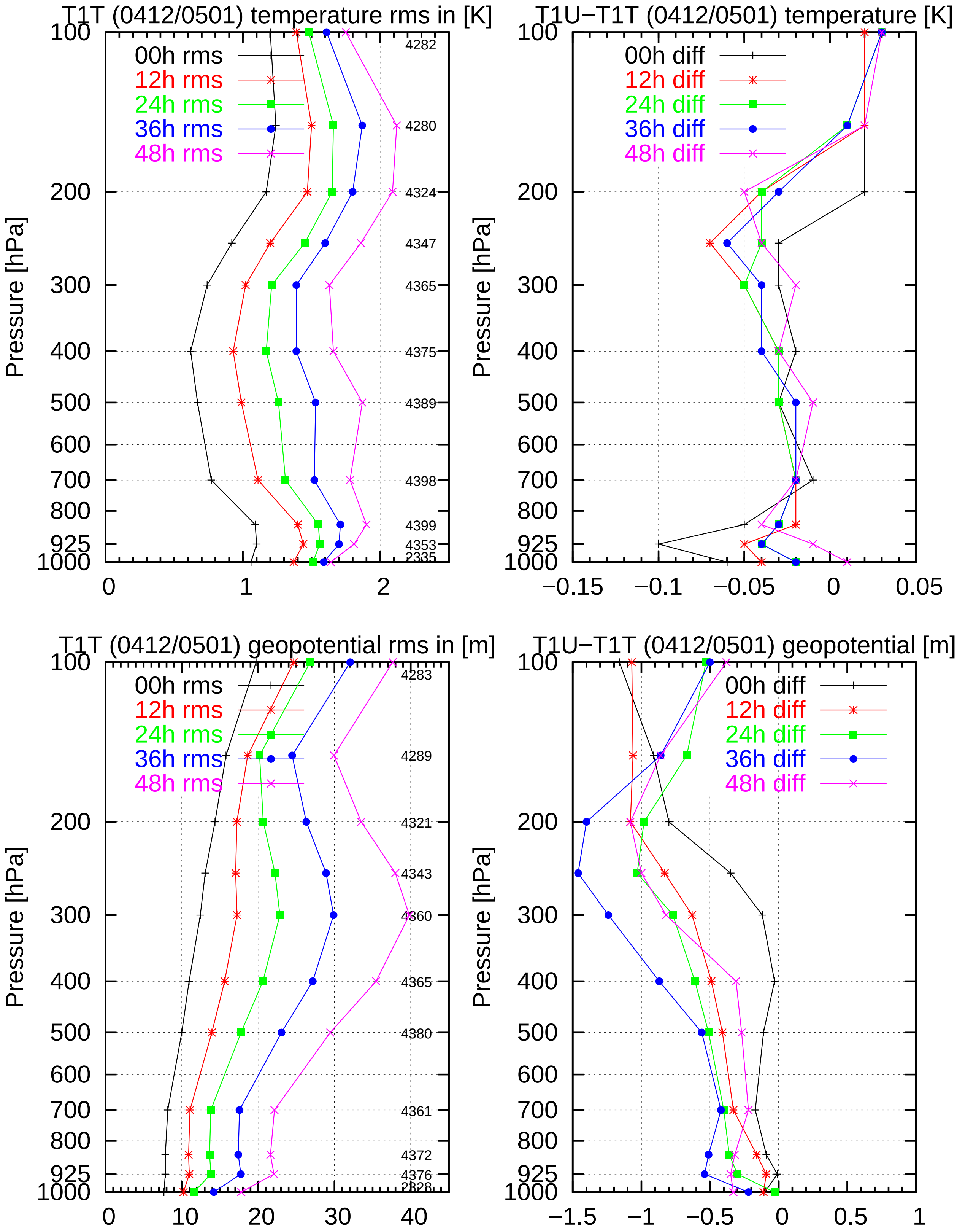

Figure 18: Rms scores for T1T (baseline + additional radiosonde wind and temperature data) and differences in rms-scores between T1U (baseline + additional radiosonde and aircraft wind and temperature data) and T1T (right) at analysis time and for the 12, 24, 36 and 48 hour forecasts as a function of pressure in the December 2004/January 2005 period. Top row is for temperature and bottom row is for geopotential. Positive values in the difference plots indicate T1T has better rms-scores.

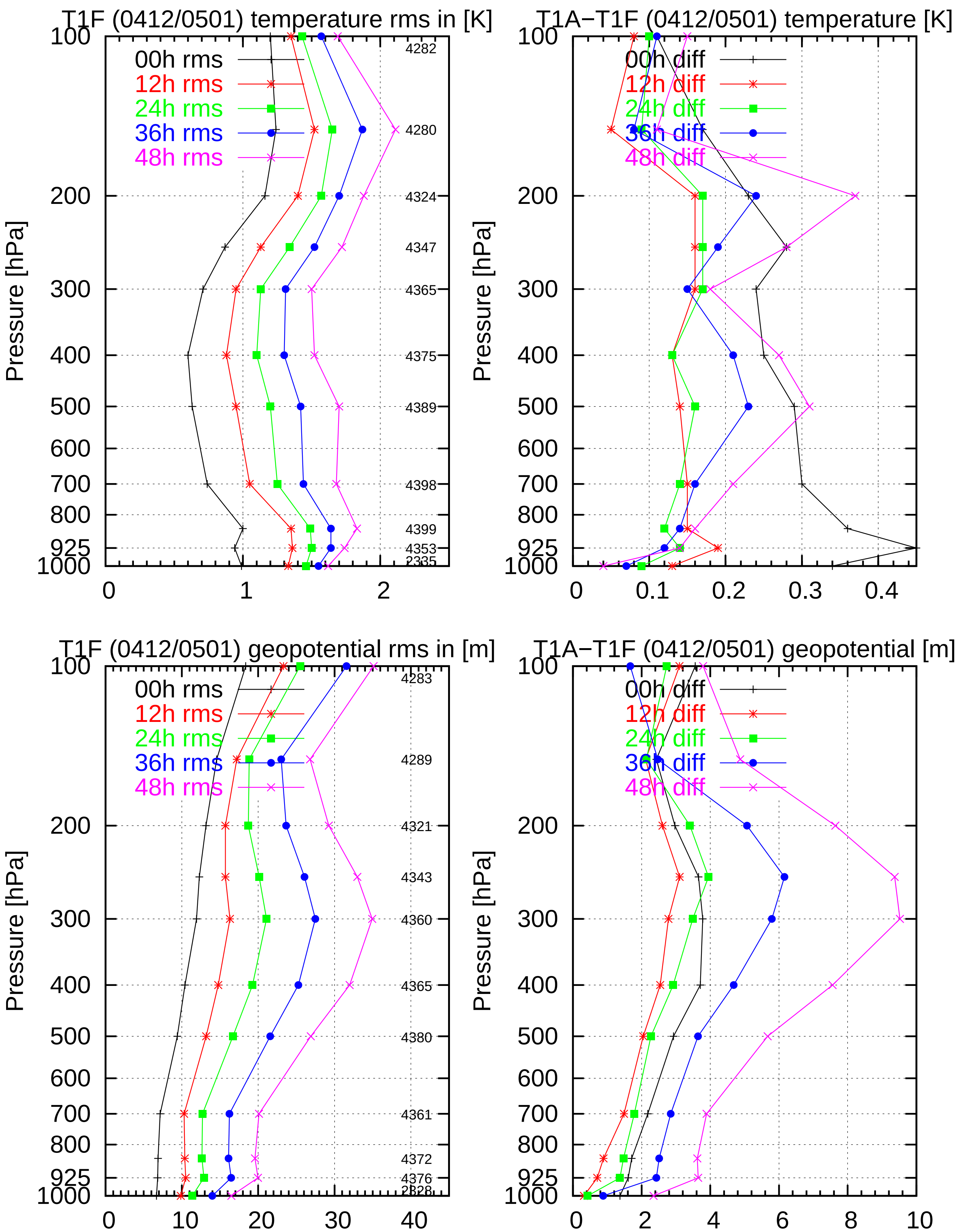

Figure 19: Rms scores for T1F (full system, left) and differences in rms-scores between T1A (baseline experiment) and T1F (right) at analysis time and for the 12, 24, 36 and 48 hour forecasts as a function of pressure in the December 2004/January 2005 period. Top row is for temperature and bottom row is for geopotential. Positive values in the difference plots indicate T1F has better rms-scores.

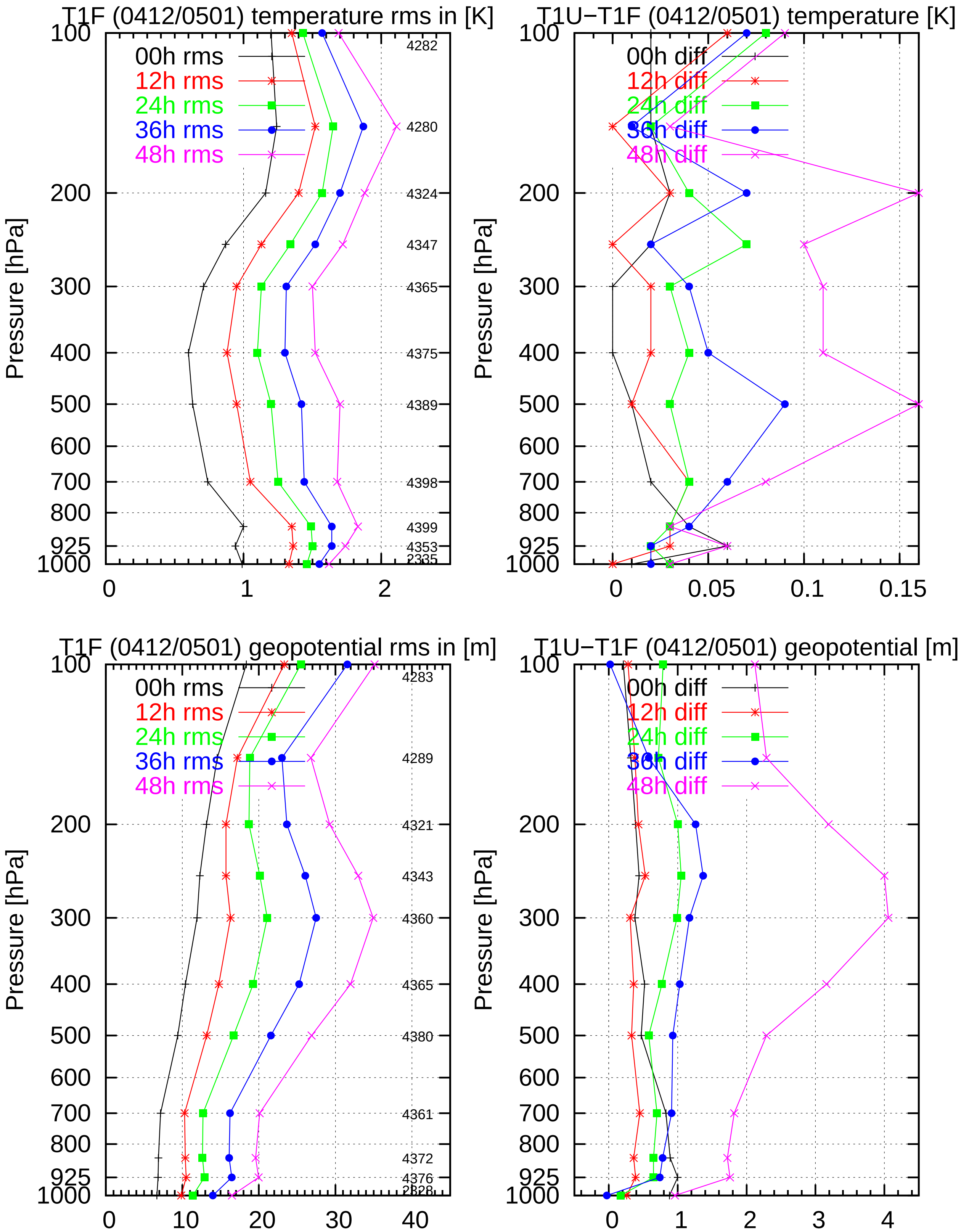

Figure 20: Rms scores for T1F (full system, left) and differences in rms-scores between T1U (baseline + additional radiosonde and aircraft wind and temperature data) and T1F (right) at analysis time and for the 12, 24, 36 and 48 hour forecasts as a function of pressure in the December 2004/January 2005 period. Top row is for temperature and bottom row is for geopotential. Positive values in the difference plots indicate T1F has better rms-scores.

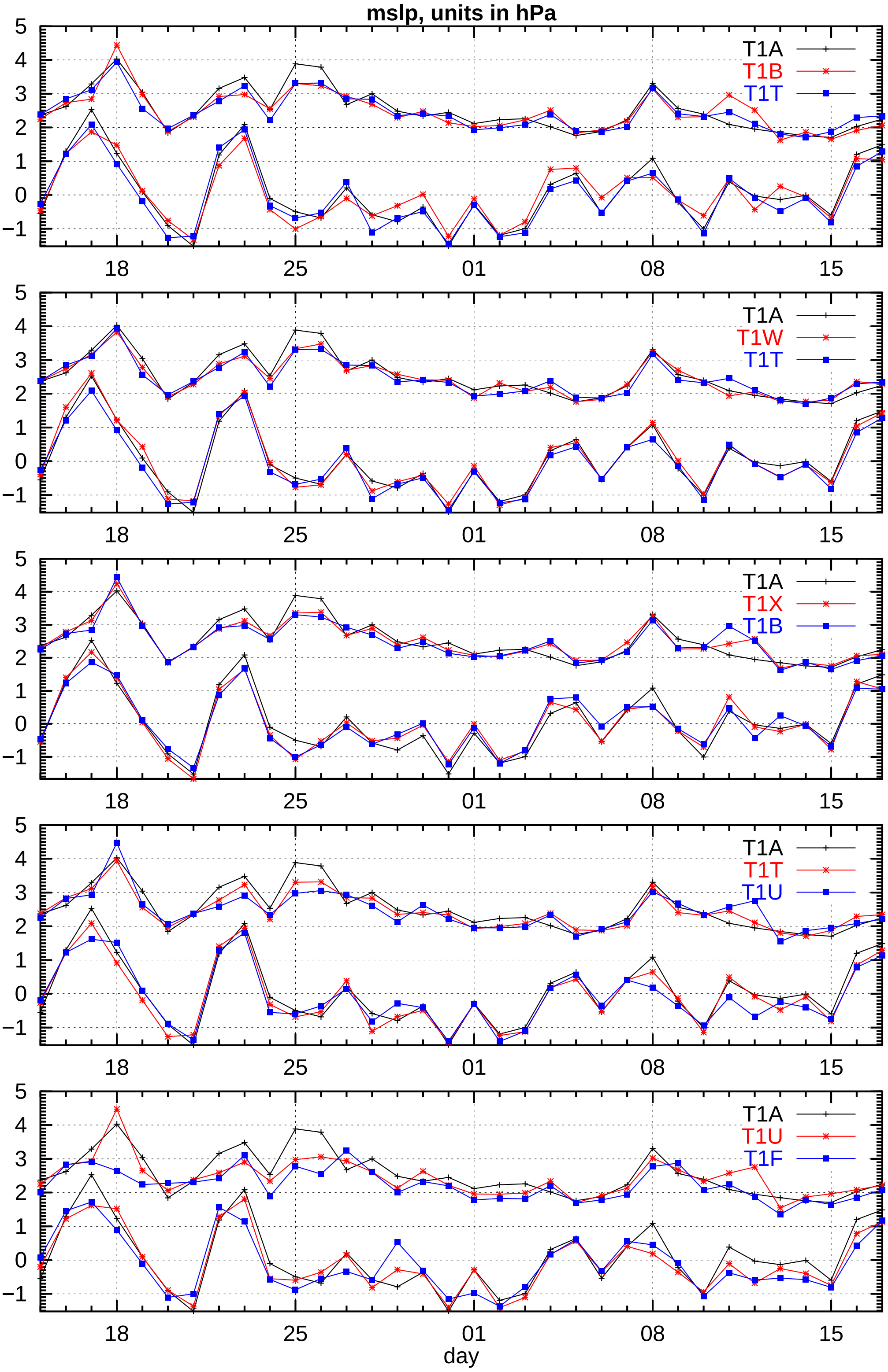

Figure 21: Daily bias and standard deviation scores for 48 h forecasts of mslp for the period December 15, 2004, to January 15, 2005.

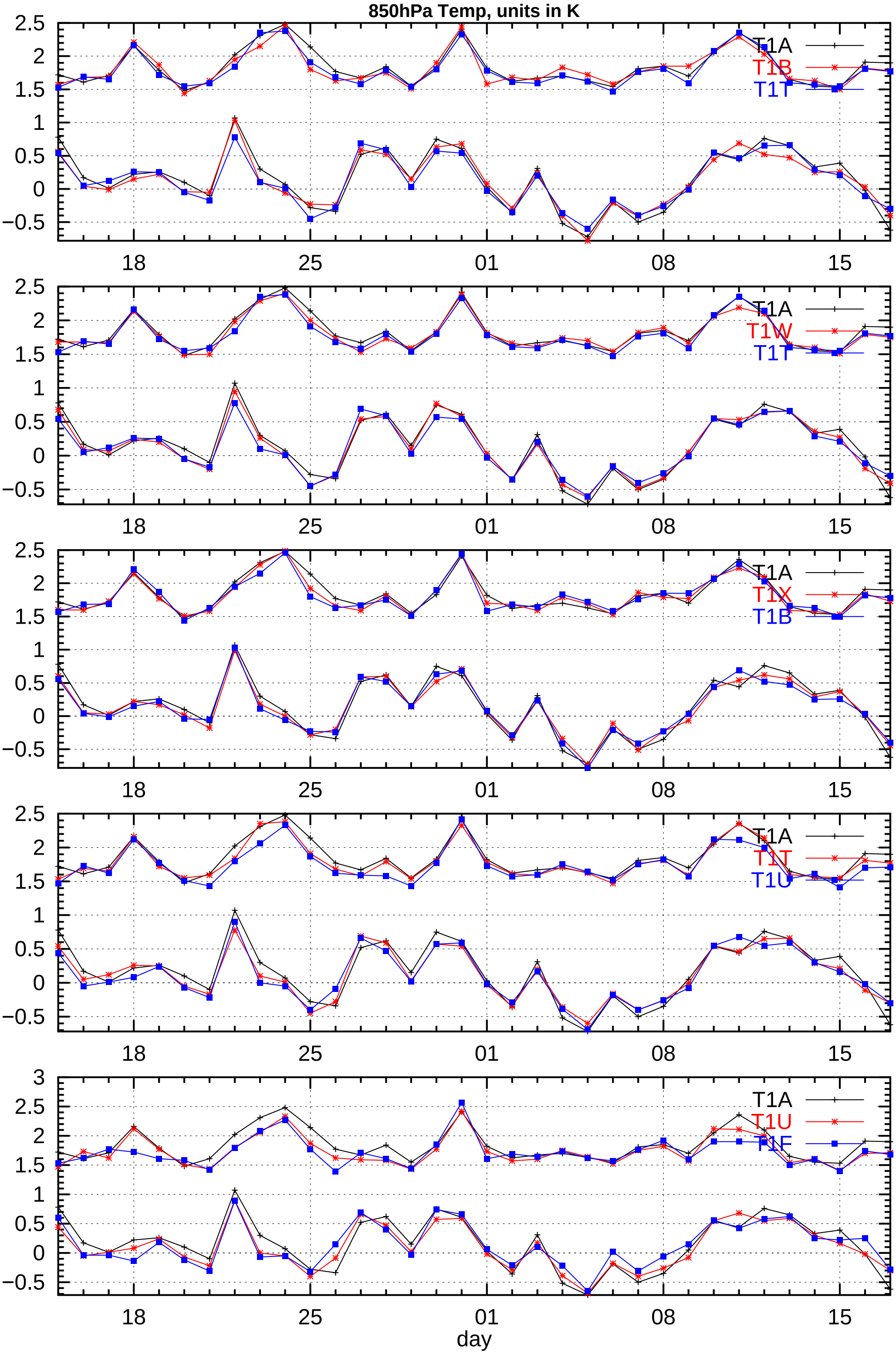

Figure 22: Daily bias and standard deviation scores for 48 h forecasts of 850 hPa temperature for the period December 15, 2004, to January 15, 2005.

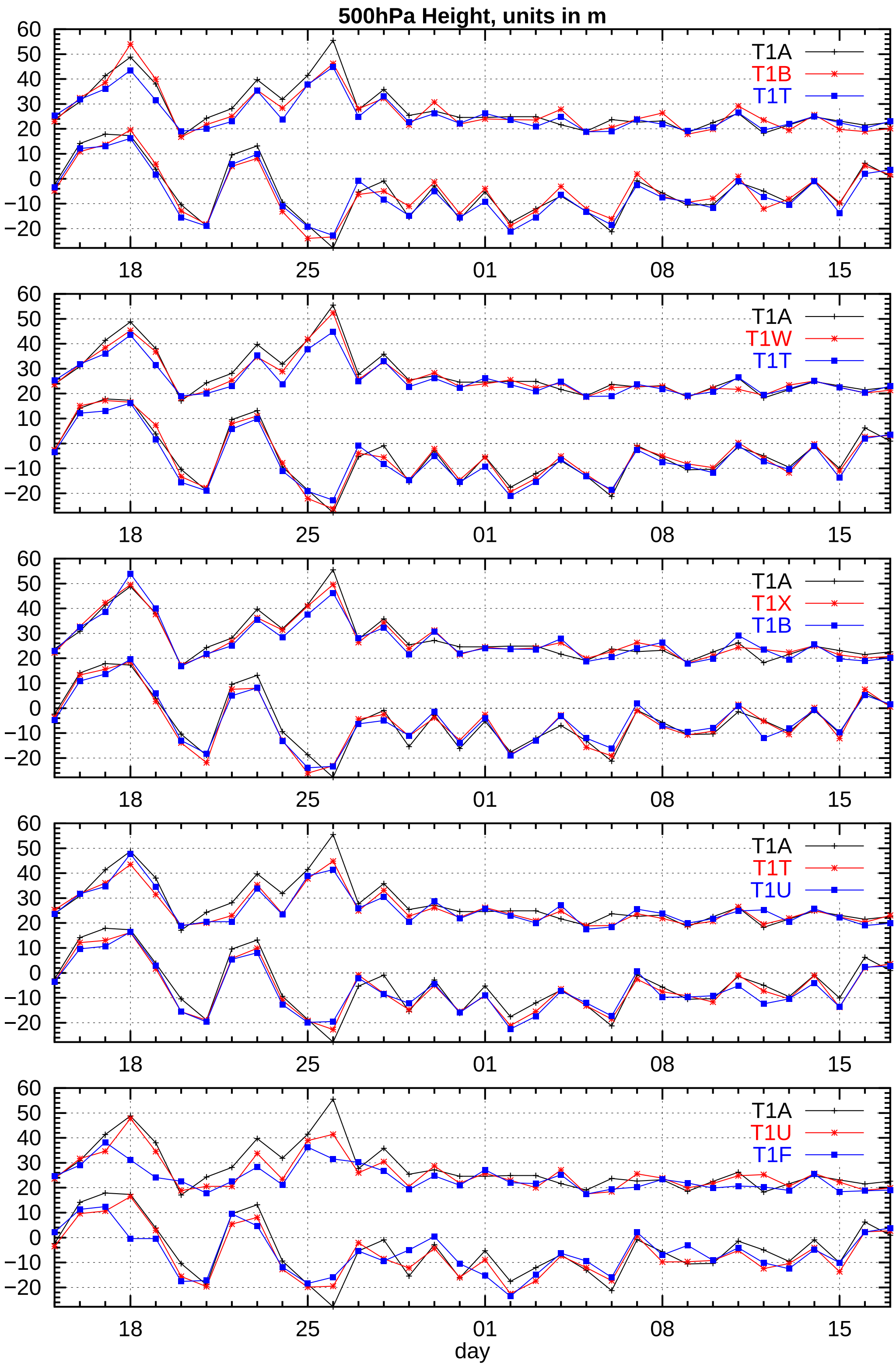

Figure 23: Daily bias and standard deviation scores for 48 h forecasts of 500 hPa geopotential height for the period December 15, 2004, to January 15, 2005.

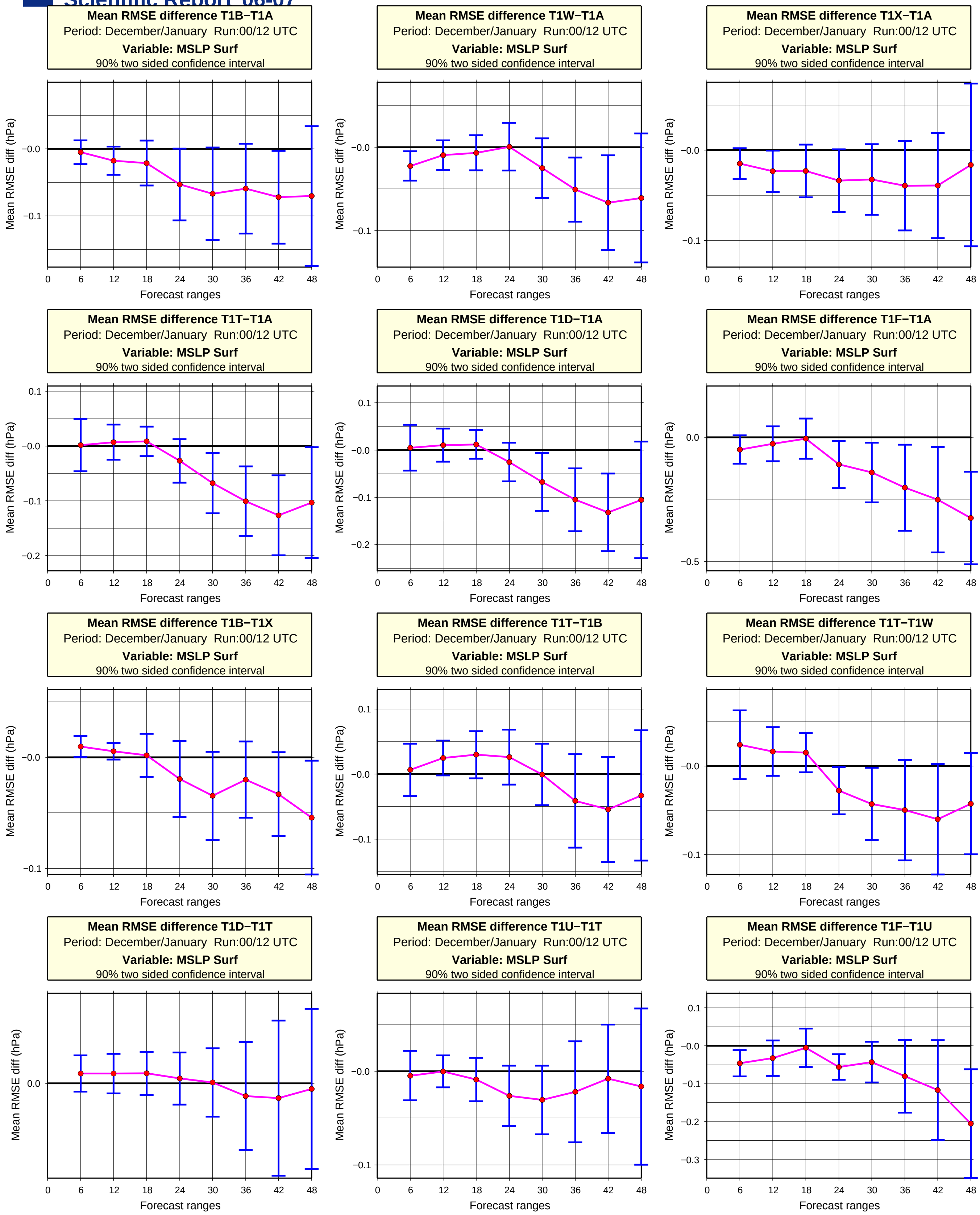

Figure 24: Significance test based on daily rms scores of mslp for 00 UTC and 12 UTC runs. 90 % two sided confidence interval. The first model run is better than the second run if the mean is negative. (T1F: all observations used; T1A: baseline run; T1B: T1A + aircraft; T1W: T1A + wind from other radiosondes; T1T: T1A + wind and temperature data from other radiosondes; T1D: T1A + data from all other radiosondes; T1X: T1A + E-AMDAR data; T1V: T1A + wind profiler data).

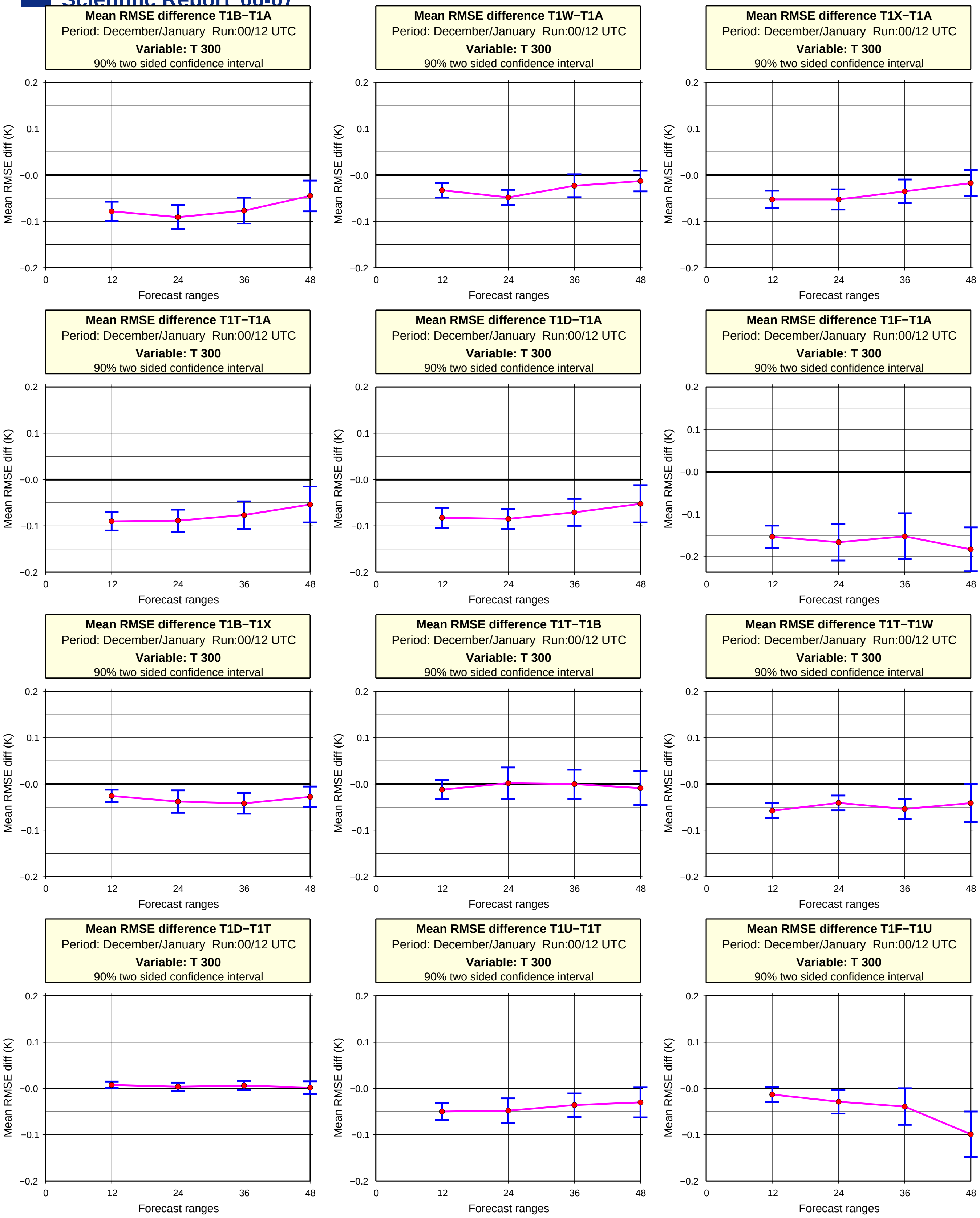

Figure 25: Significance test based on daily rms scores of 300 hPa temperature. 90 % two sided confidence interval. The first model run is better than the second run if the mean is negative. (T1F: all observations used; T1A: baseline run; T1B: T1A + aircraft; T1W: T1A + wind from other radiosondes; T1T: T1A + wind and temperature data from other radiosondes; T1D: T1A + data from all other radiosondes; T1X: T1A + E-AMDAR data; T1V: T1A + wind profiler data; T1U: T1T + all aircraft data).

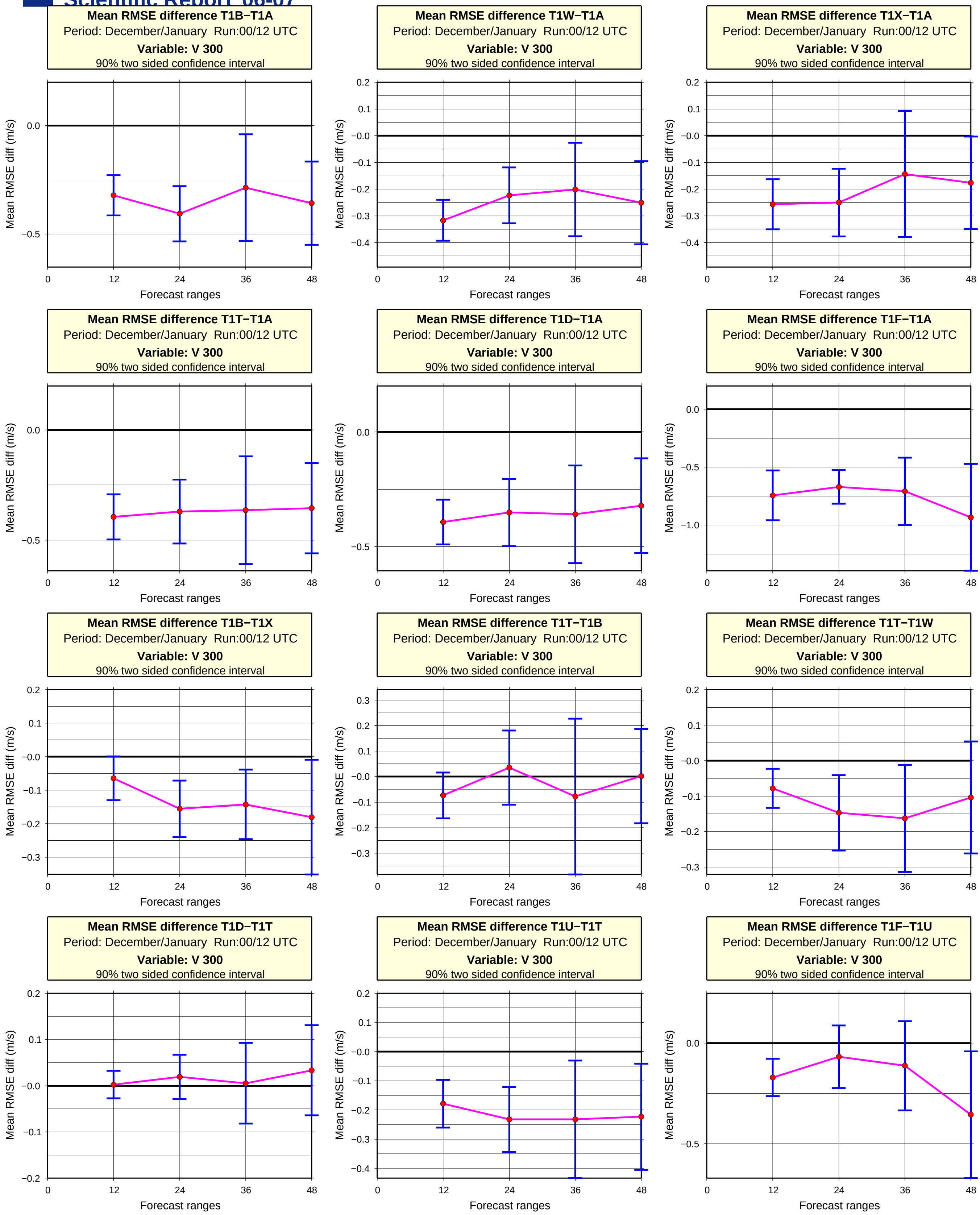

Figure 26: Significance test based on daily scores of 300 hPa wind speed. 90 % two sided confidence interval. The first model run is better than the second run if the mean is negative. (T1F: all observations used; T1A: baseline run; T1B: T1A + aircraft; T1W: T1A + wind from other radiosondes; T1T: T1A + wind and temperature data from other radiosondes; T1D: T1A + data from all other radiosondes; T1X: T1A + E-AMDAR data; T1V: T1A + wind profiler data; T1U: T1T + all aircraft data).

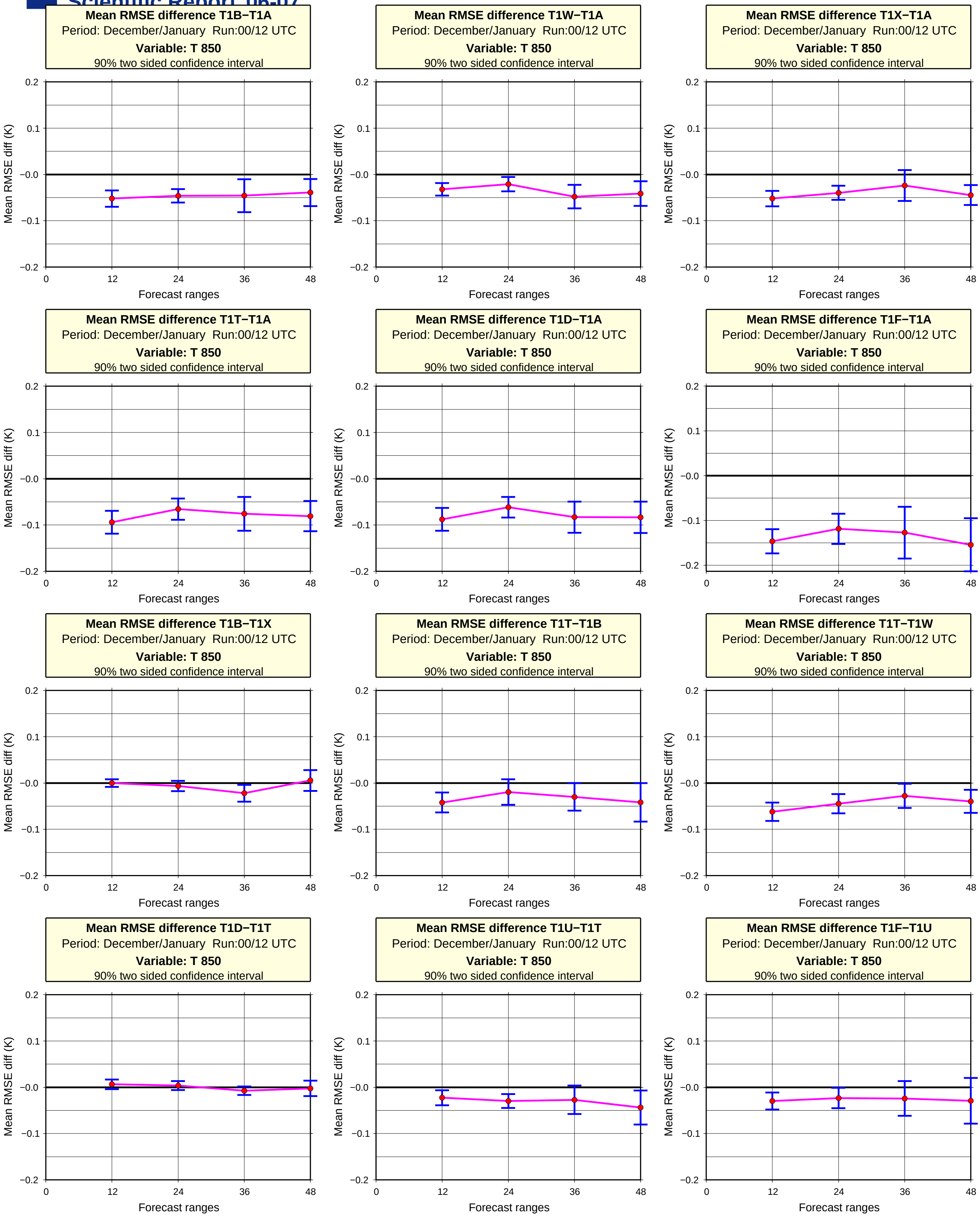

Figure 27: Significance test based on daily scores of 850 hPa temperature. 90 % two sided confidence interval. The first model run is better than the second run if the mean is negative. (T1F: all observations used; T1A: baseline run; T1B: T1A + aircraft; T1W: T1A + wind from other radiosondes; T1T: T1A + wind and temperature data from other radiosondes; T1D: T1A + data from all other radiosondes; T1X: T1A + E-AMDAR data; T1V: T1A + wind profiler data; T1U: T1T + all aircraft data).

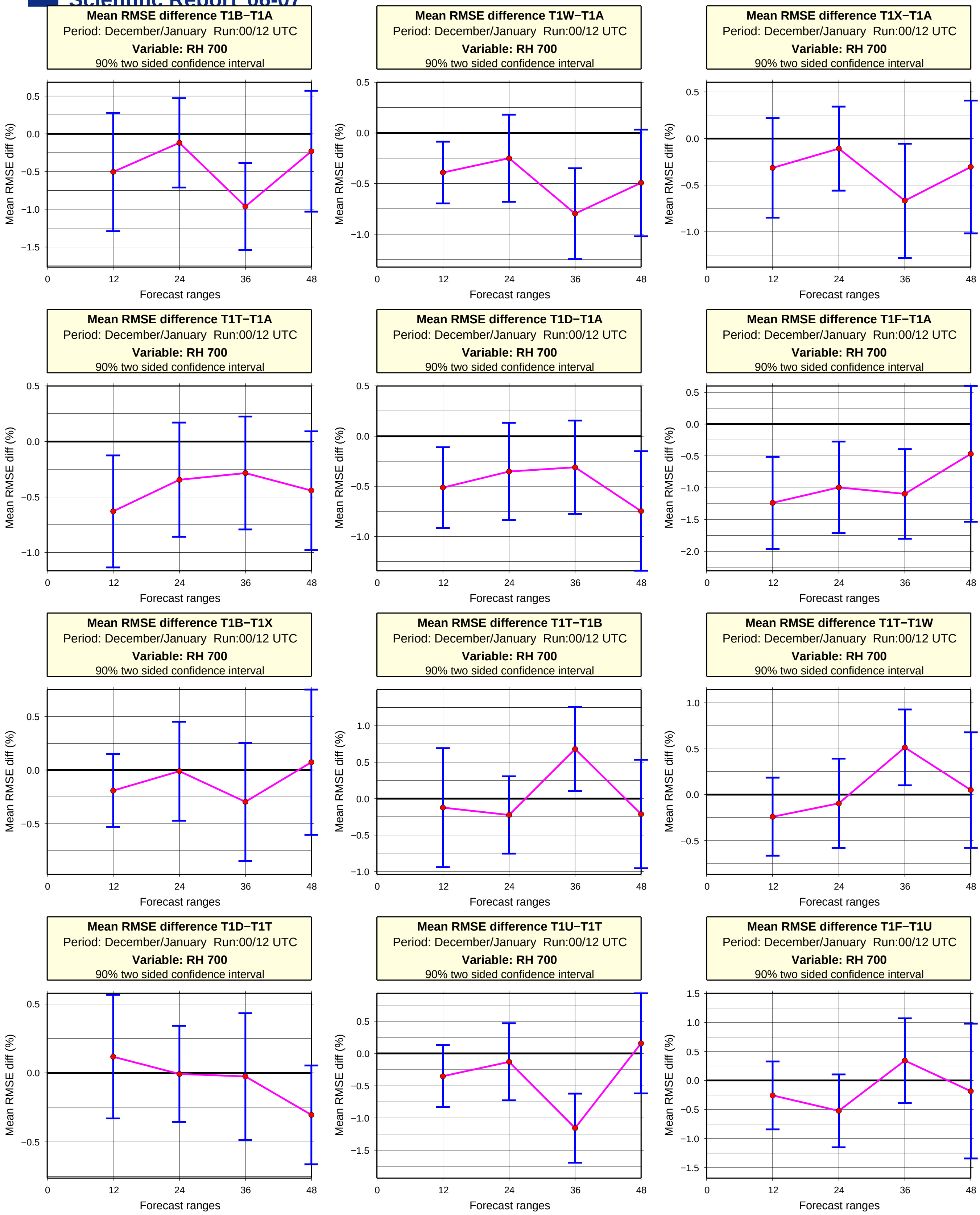

Figure 28: Significance test based on daily scores of 700 hPa relative humidity. 90 % two sided confidence interval. The first model run is better than the second run if the mean is negative. (T1F: all observations used; T1A: baseline run; T1B: T1A + aircraft; T1W: T1A + wind from other radiosondes; T1T: T1A + wind and temperature data from other radiosondes; T1D: T1A + data from all other radiosondes; T1X: T1A + E-AMDAR data; T1V: T1A + wind profiler data; T1U: T1T + all aircraft data)

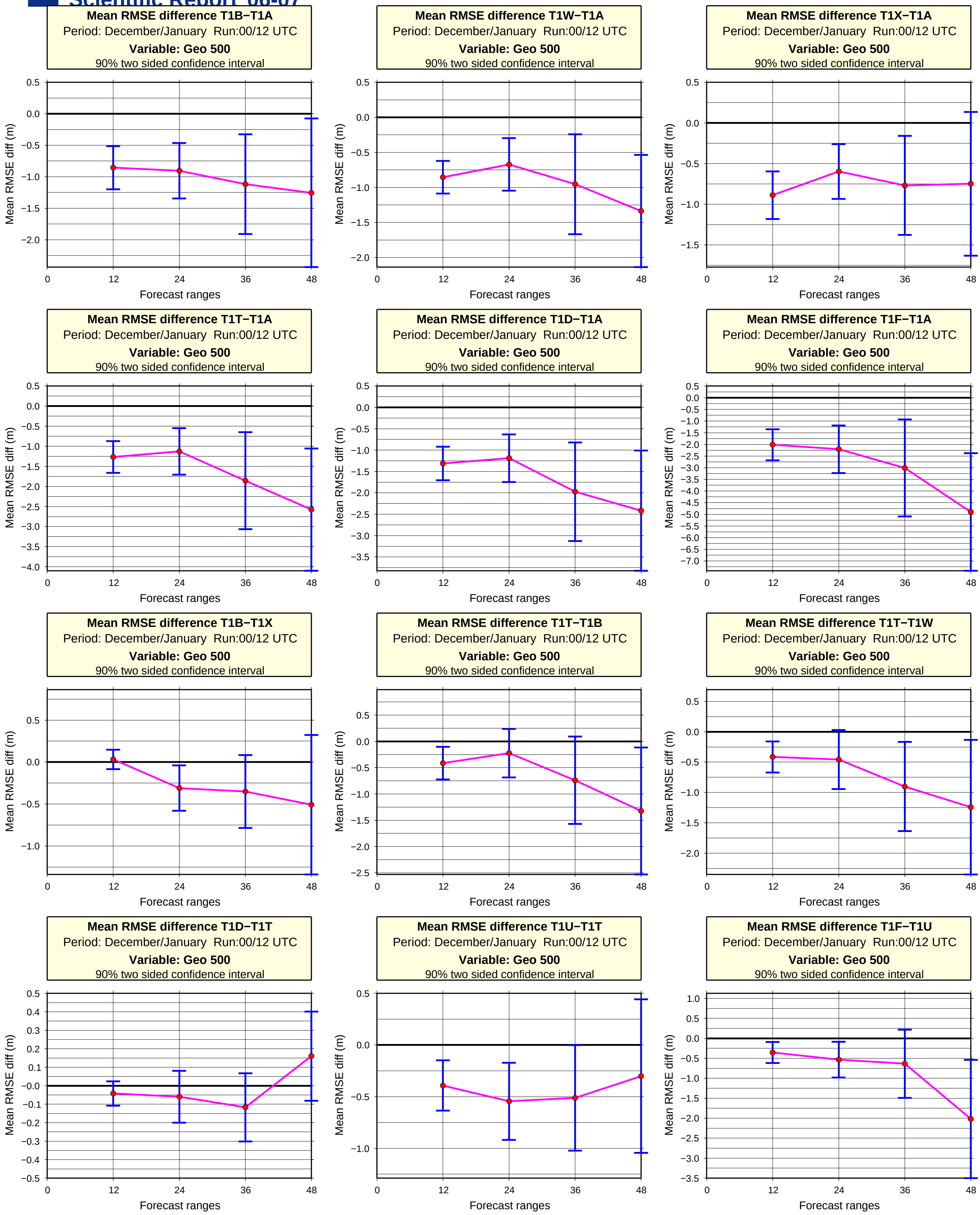

Figure 29: Significance test based on daily scores of 500 hPa geopotential height. 90 % two sided confidence interval. The first model run is better than the second run if the mean is negative. (T1F: all observations used; T1A: baseline run; T1B: T1A + aircraft; T1W: T1A + wind from other radiosondes; T1T: T1A + wind and temperature data from other radiosondes; T1D: T1A + data from all other radiosondes; T1X: T1A + E-AMDAR data; T1V: T1A + wind profiler data; T1U: T1T + all aircraft data)

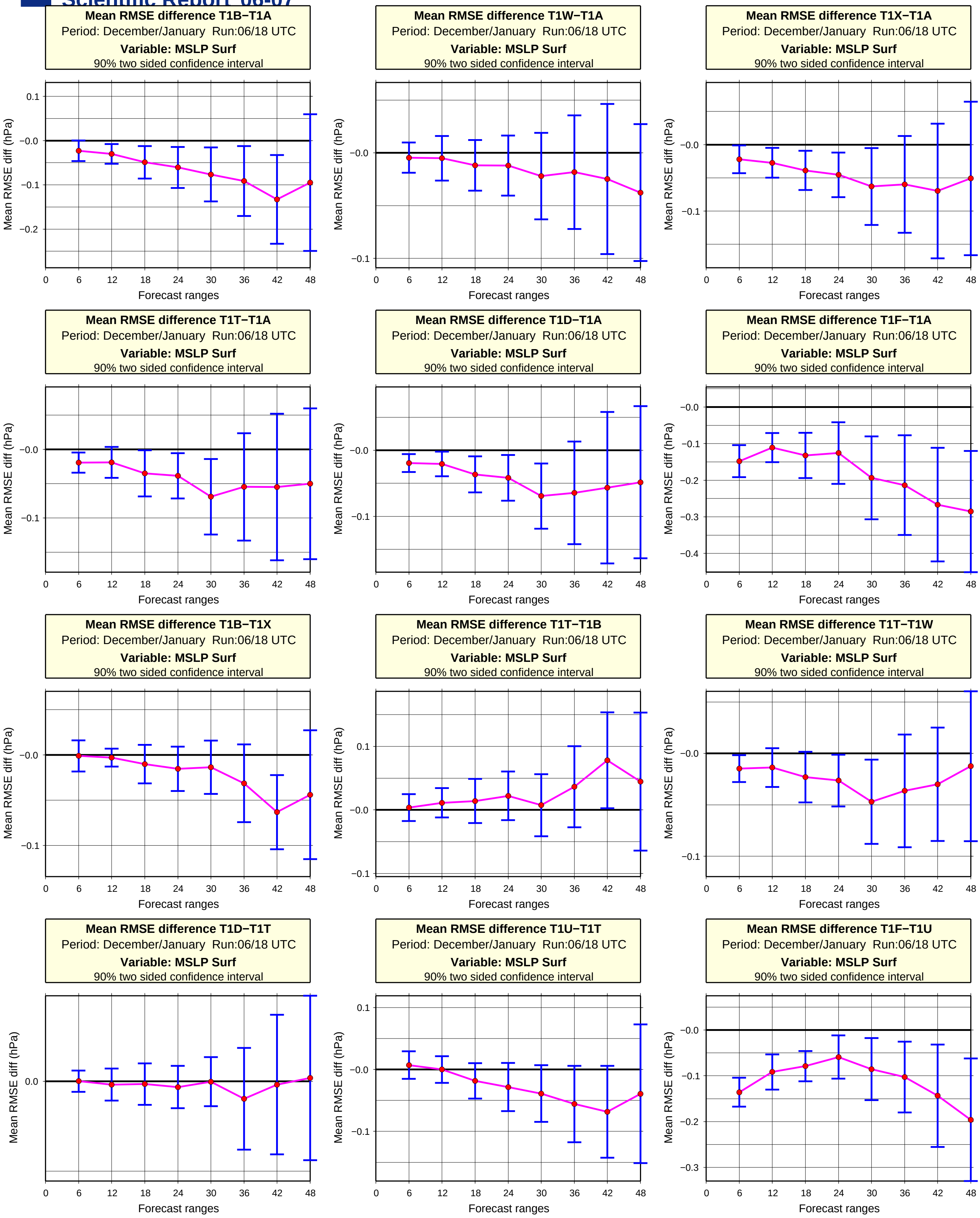

Figure 30: Significance test based on daily scores of mslp for 06 UTC and 18 UTC runs. 90 % two sided confidence interval. The first model run is better than the second run if the mean is negative. (T1F: all observations used; T1A: baseline run; T1B: T1A + aircraft; T1W: T1A + wind from other radiosondes; T1T: T1A + wind and temperature data from other radiosondes; T1D: T1A + data from all other radiosondes; T1X: T1A + E-AMDAR data; T1V: T1A + wind profiler data).

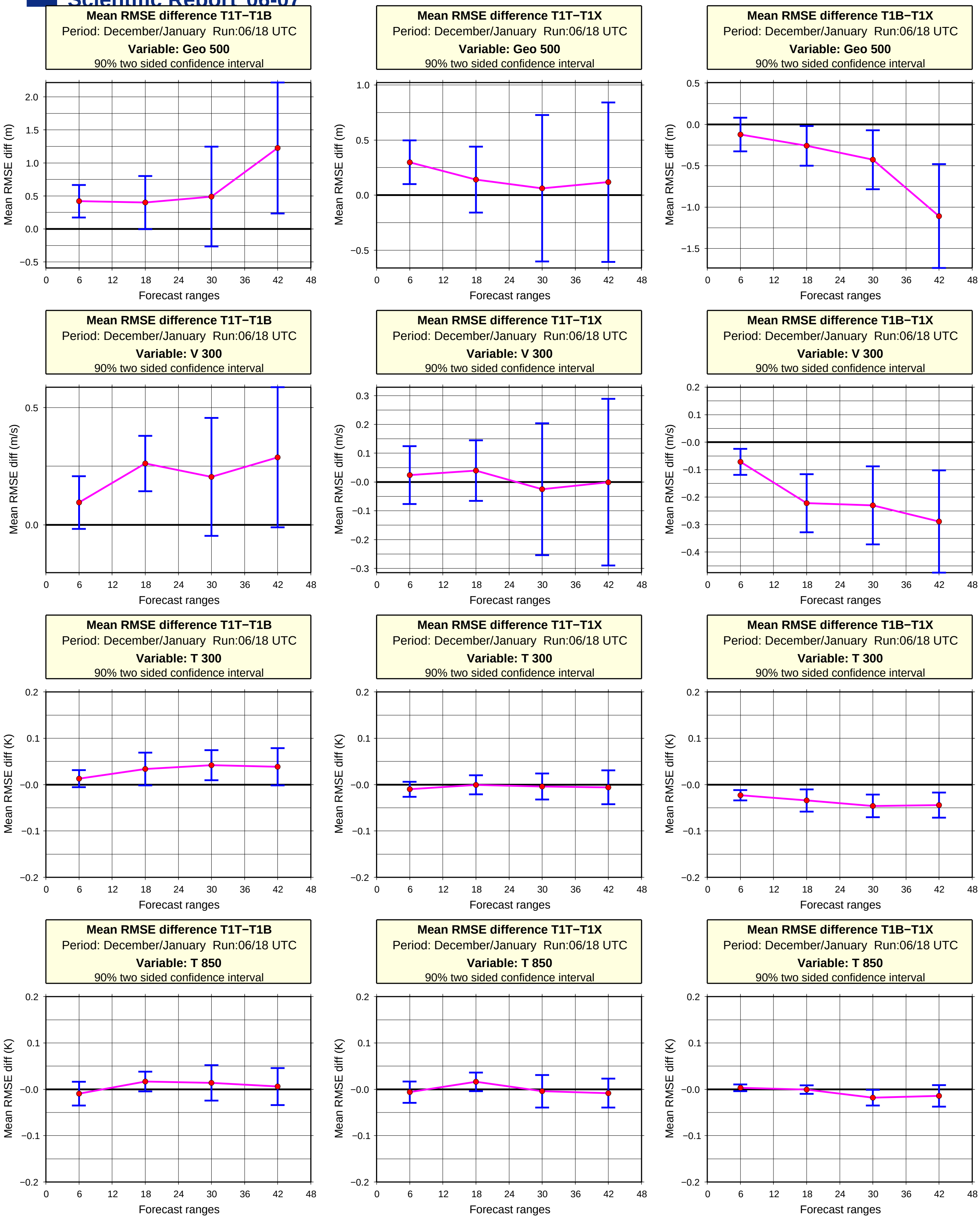

Figure 31: Significance test based on daily scores of selected parameters for 06 UTC and 18 UTC runs only. 90 % two sided confidence interval. The first model run is better than the second run if the mean is negative. Top row is for 500 hPa geopotential height, second row from top is for 300 hPa wind speed, third row is for 300 hPa temperature and bottom row is for 850 hPa temperature. (T1B: baseline + aircraft; T1T: baseline + wind and temperature data from non-GUAN radiosonde; T1X: baseline + E-AMDAR data).

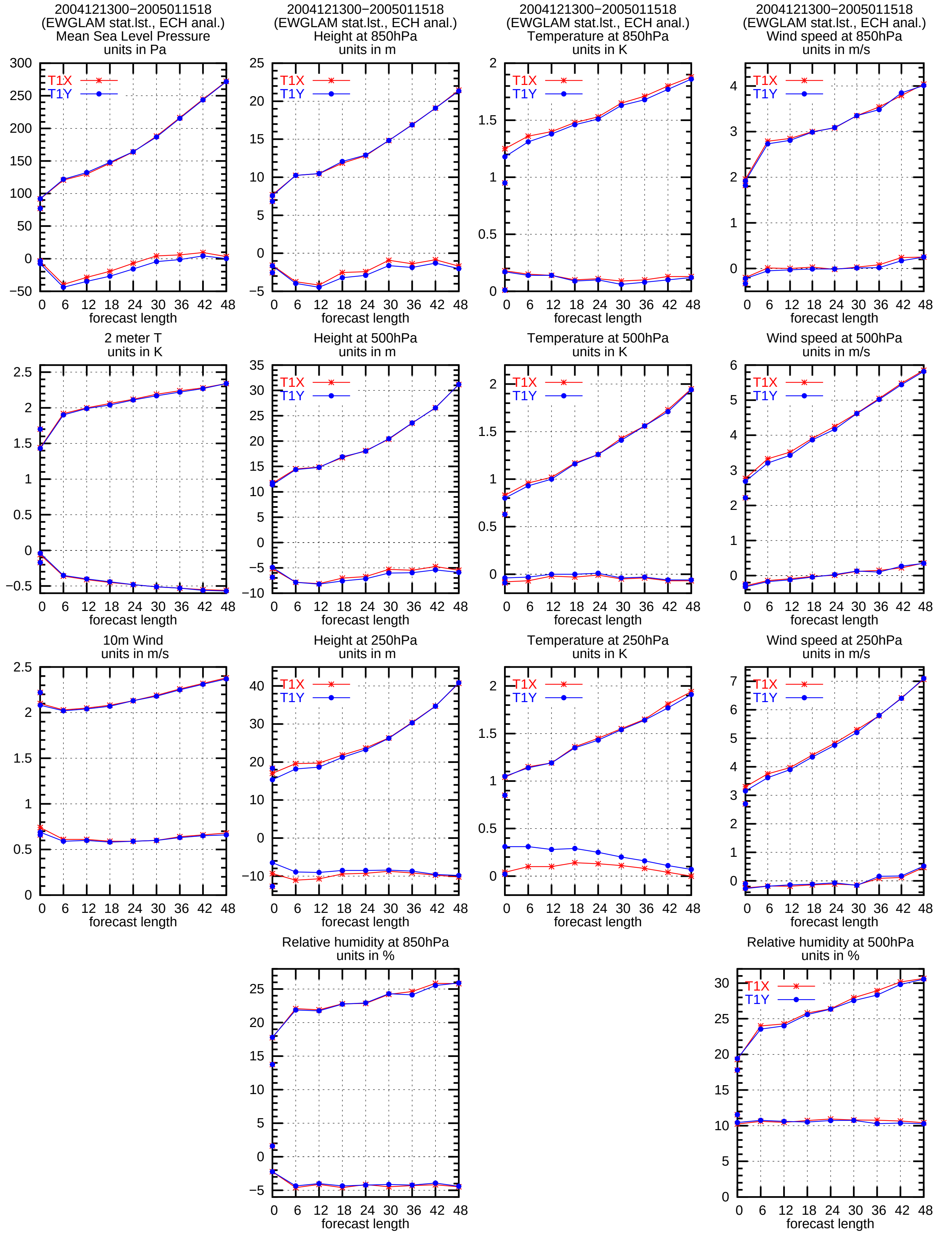

Figure 32: Obs-verification of the 'baseline plus operational E-AMDAR wind and temperature data' (T1X) run and the 'baseline plus E-AMDAR (including data from the ECMWF archive)' (T1Y) run. EWGLAM station list.

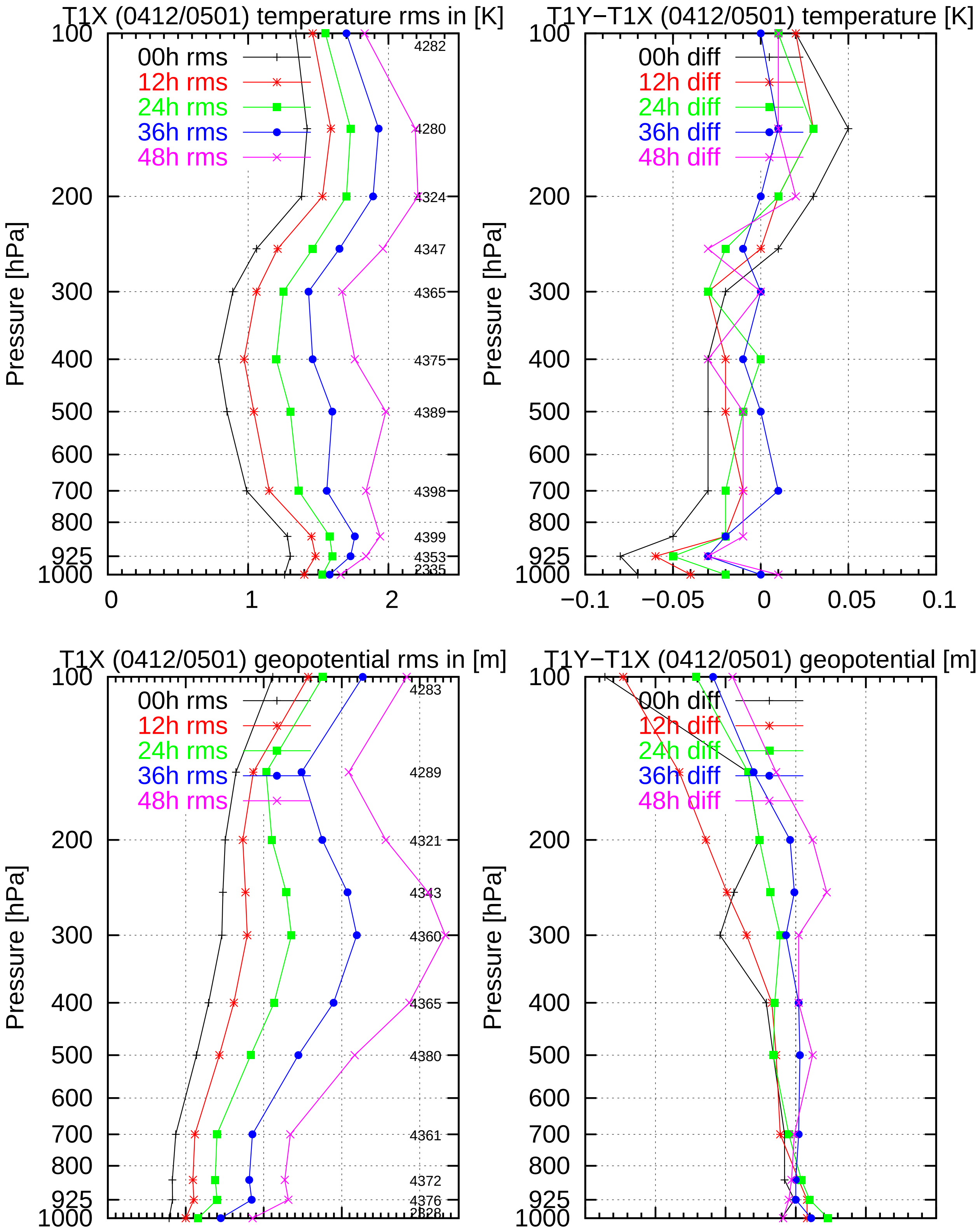

Figure 33: Rms scores for T1X (baseline plus operational E-AMDAR wind and temperature data) and differences in rms-scores between T1Y (baseline + additional aircraft wind and temperature data from E-AMDAR including data from the ECMWF archive) and T1X (right) at analysis time and for the 12, 24, 36 and 48 hour forecasts as a function of pressure in the December 2004/January 2005 period. Top row is for temperature and bottom row is for geopotential. Positive values in the difference plots indicate T1Y has better rms-scores.

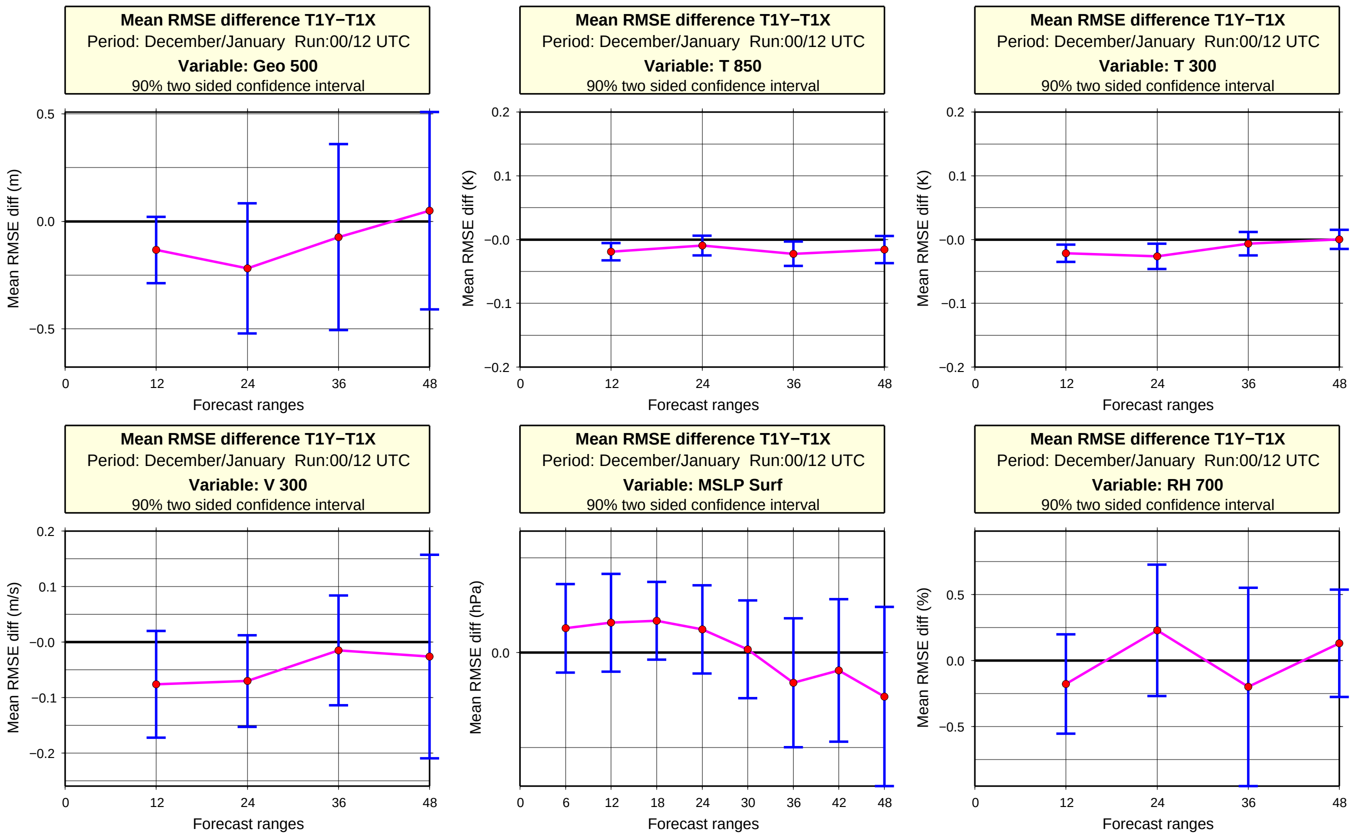

Figure 34: Significance test based on daily scores of selected parameters for T1Y and T1X. 90 % two sided confidence interval. The T1Y experiment is better than the T1X experiment if the mean is negative. Top row is for 500 hPa geopotential height and temperature and 300 hPa temperature, second row from top is for 300 hPa wind speed, mslp and 700 hPa relative humidity. (T1X: baseline + E-AMDAR data from DMI operations. T1X: baseline + E-AMDAR from DMI operations and from the ECMWF archive).

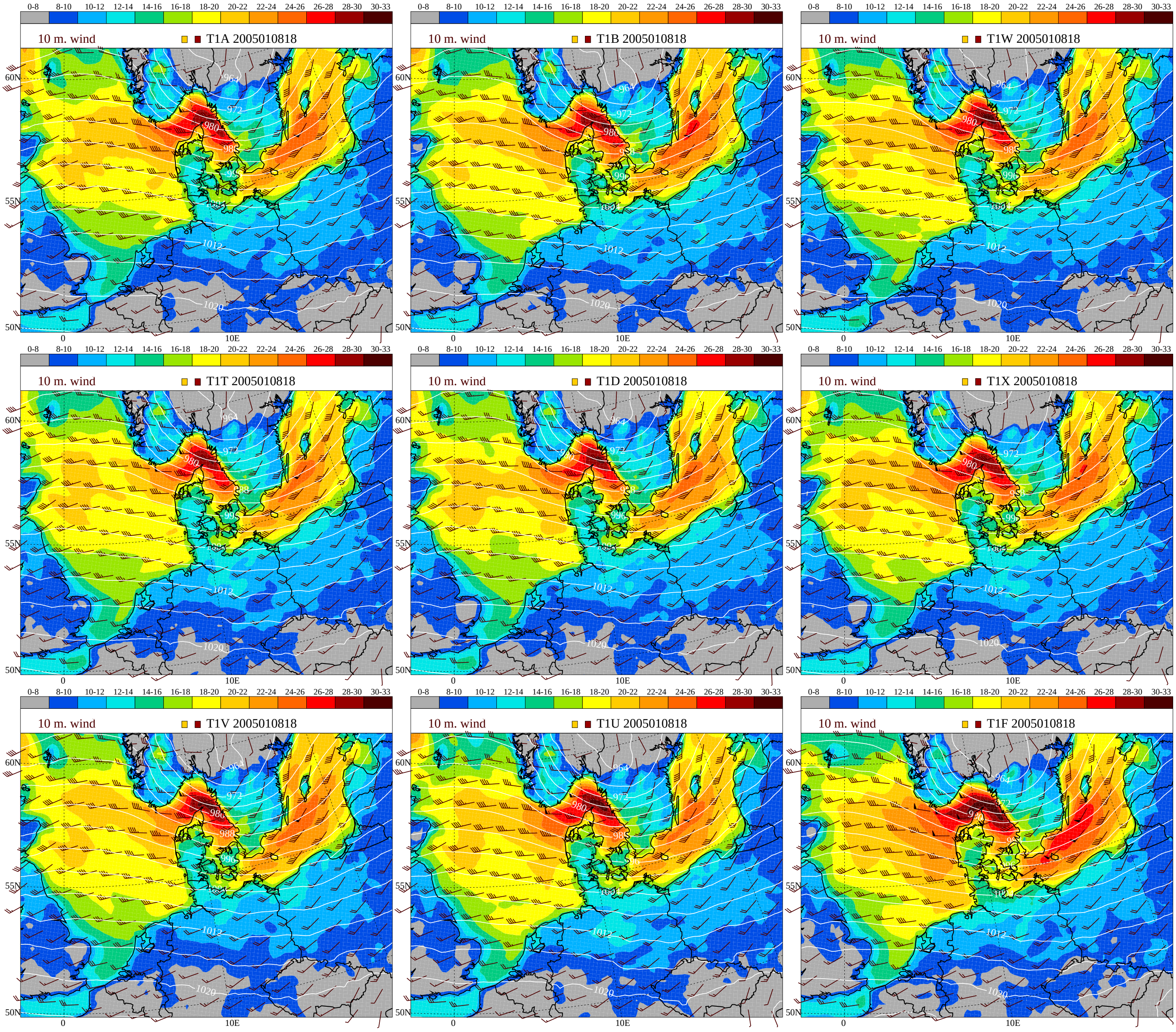

Figure 35: Analyses valid at 18 UTC January 8, 2005. (T1F: all observations used; T1A: baseline run; T1B: T1A + aircraft; T1W: T1A + wind from other radiosondes; T1T: T1A + wind and temperature data from other radiosondes; T1D: T1A + data from all other radiosondes; T1X: T1A + E-AMDAR data; T1V: T1A + wind profiler data; T1U: T1T + all aircraft data).

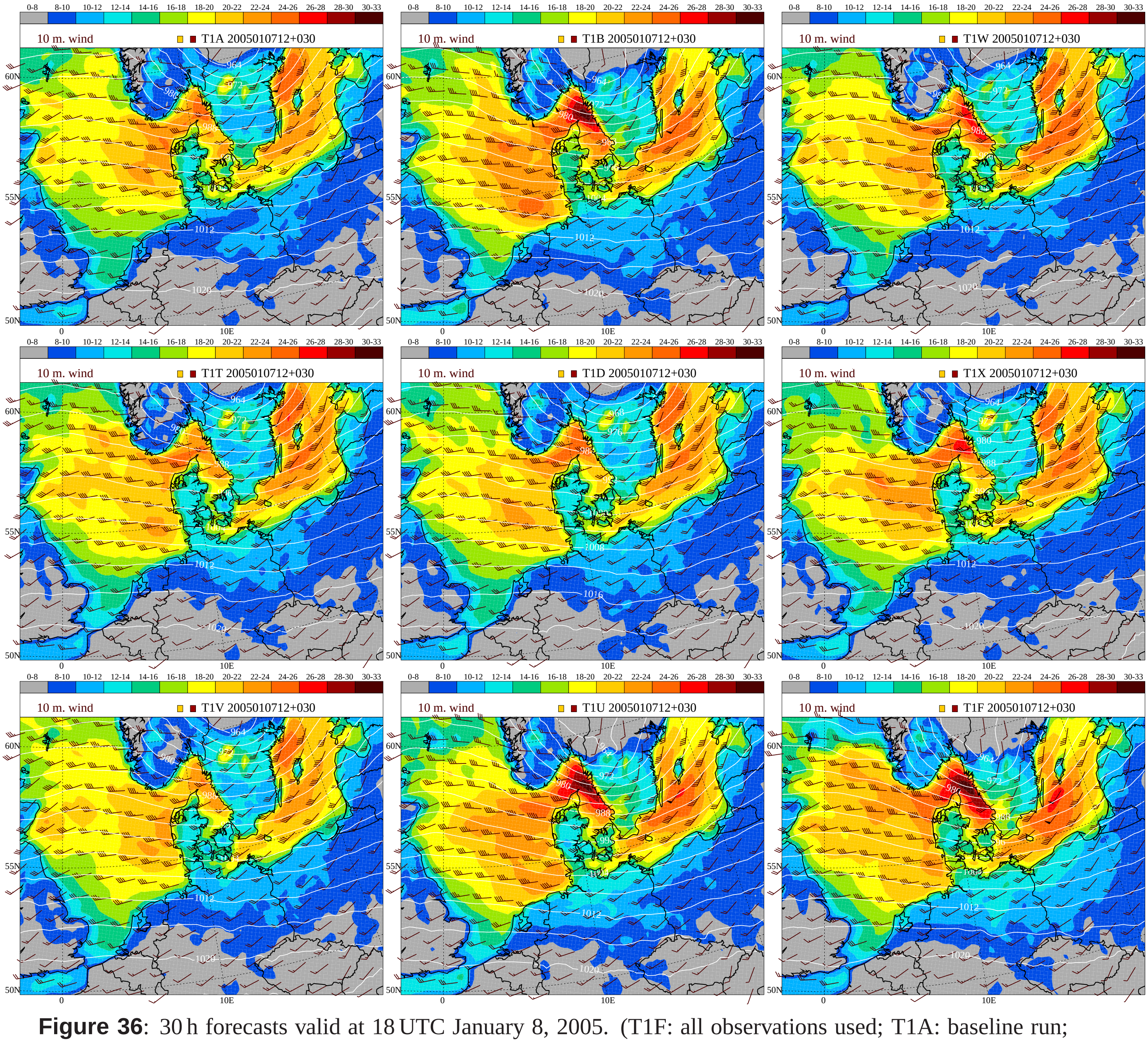

Figure 36: 30 h forecasts valid at 18 UTC January 8, 2005. (T1F: all observations used; T1A: baseline run; T1B: T1A + aircraft; T1W: T1A + wind from other radiosondes; T1T: T1A + wind and temperature data from other radiosondes; T1D: T1A + data from all other radiosondes; T1X: T1A + E-AMDAR data; T1V: T1A + wind profiler data; T1U: T1T + all aircraft data).

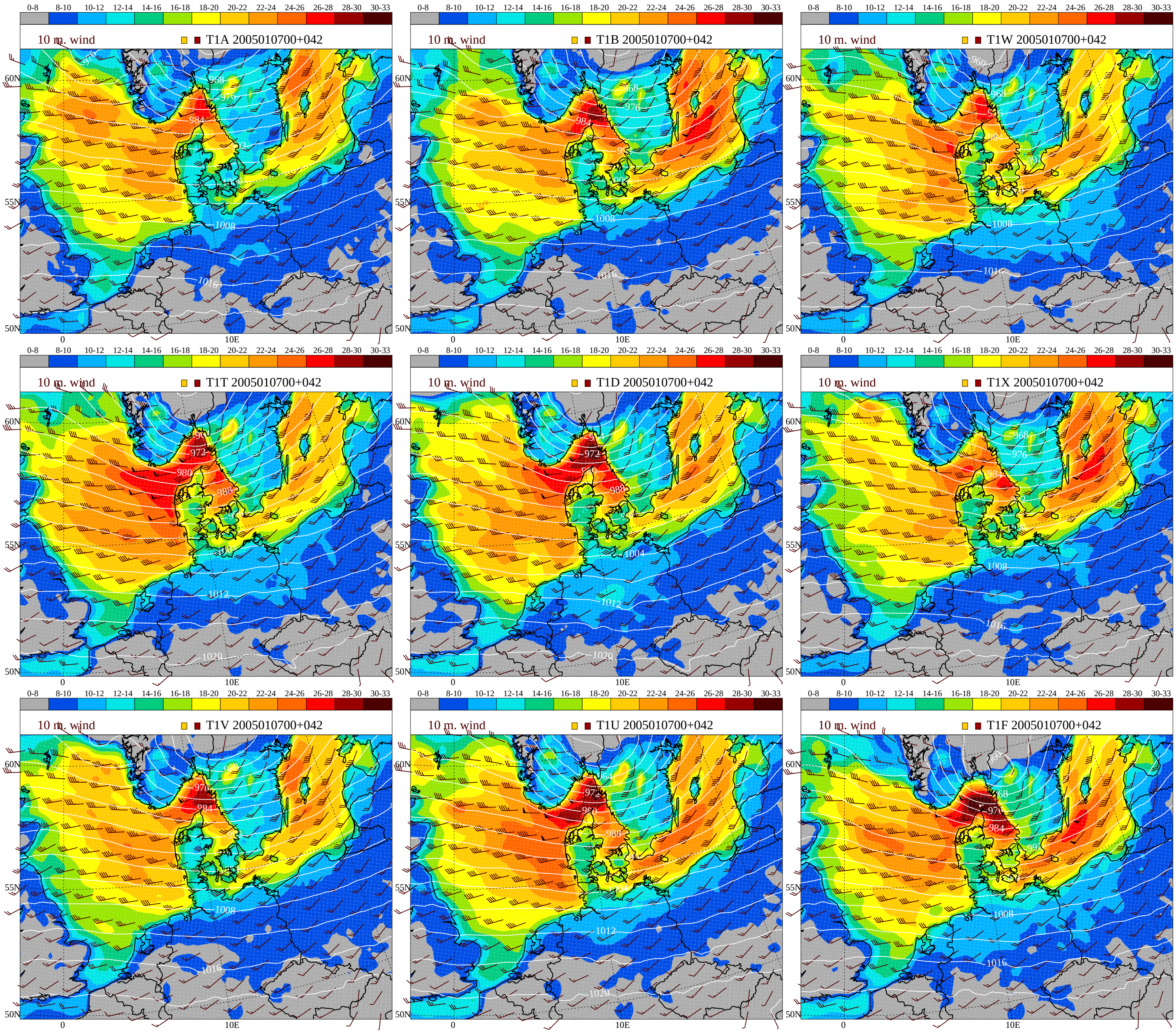

Figure 37: 42 h forecasts valid at 18 UTC January 8, 2005. (T1F: all observations used; T1A: baseline run; T1B: T1A + aircraft; T1W: T1A + wind from other radiosondes; T1T: T1A + wind and temperature data from other radiosondes; T1D: T1A + data from all other radiosondes; T1X: T1A + E-AMDAR data; T1V: T1A + wind profiler data; T1U: T1T + all aircraft data).

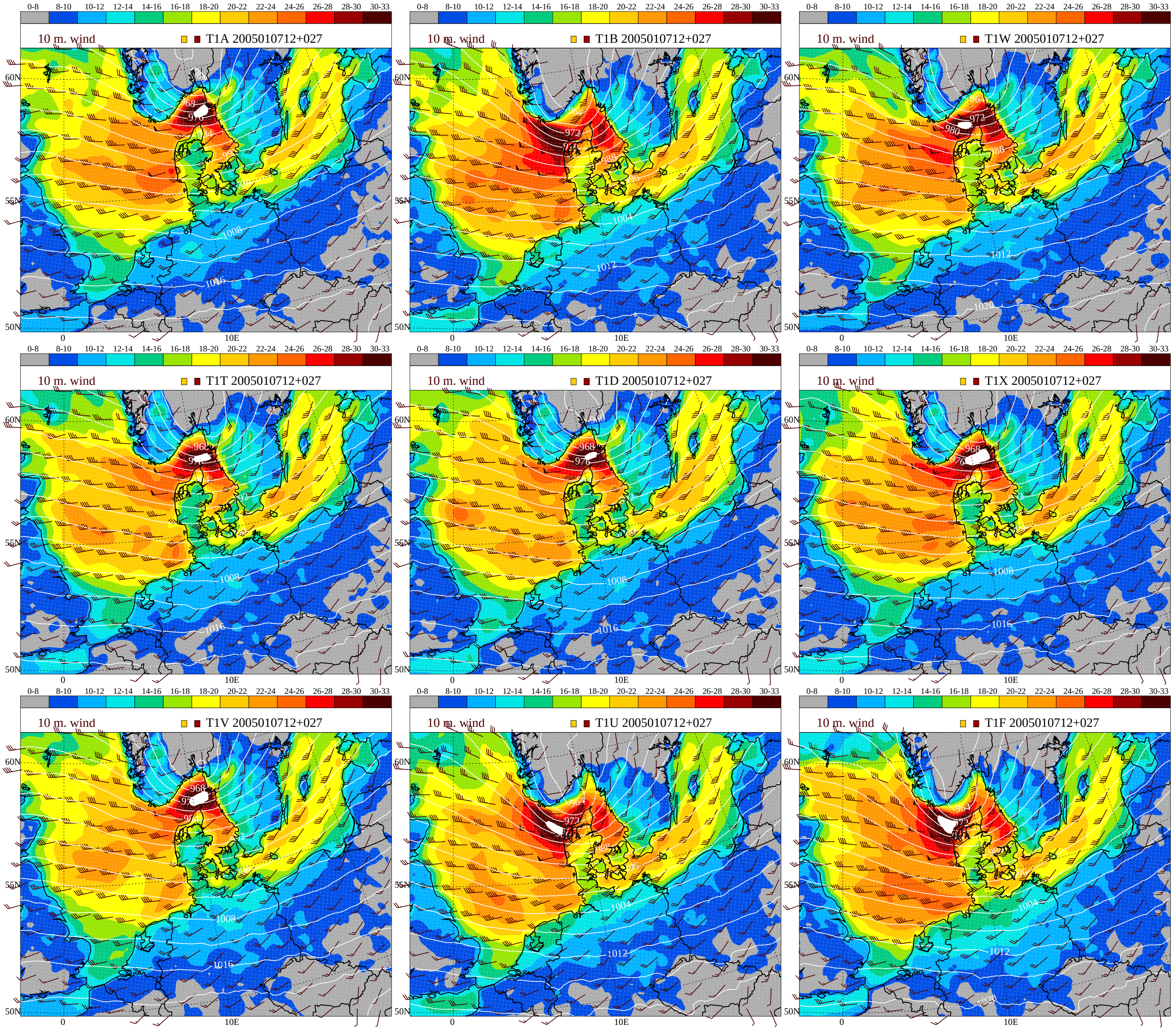

Figure 38: 27 h forecasts valid at 15 UTC January 8, 2005. (T1F: all observations used; T1A: baseline run; T1B: T1A + aircraft; T1W: T1A + wind from other radiosondes; T1T: T1A + wind and temperature data from other radiosondes; T1D: T1A + data from all other radiosondes; T1X: T1A + E-AMDAR data; T1V: T1A + wind profiler data; T1U: T1T + all aircraft data).

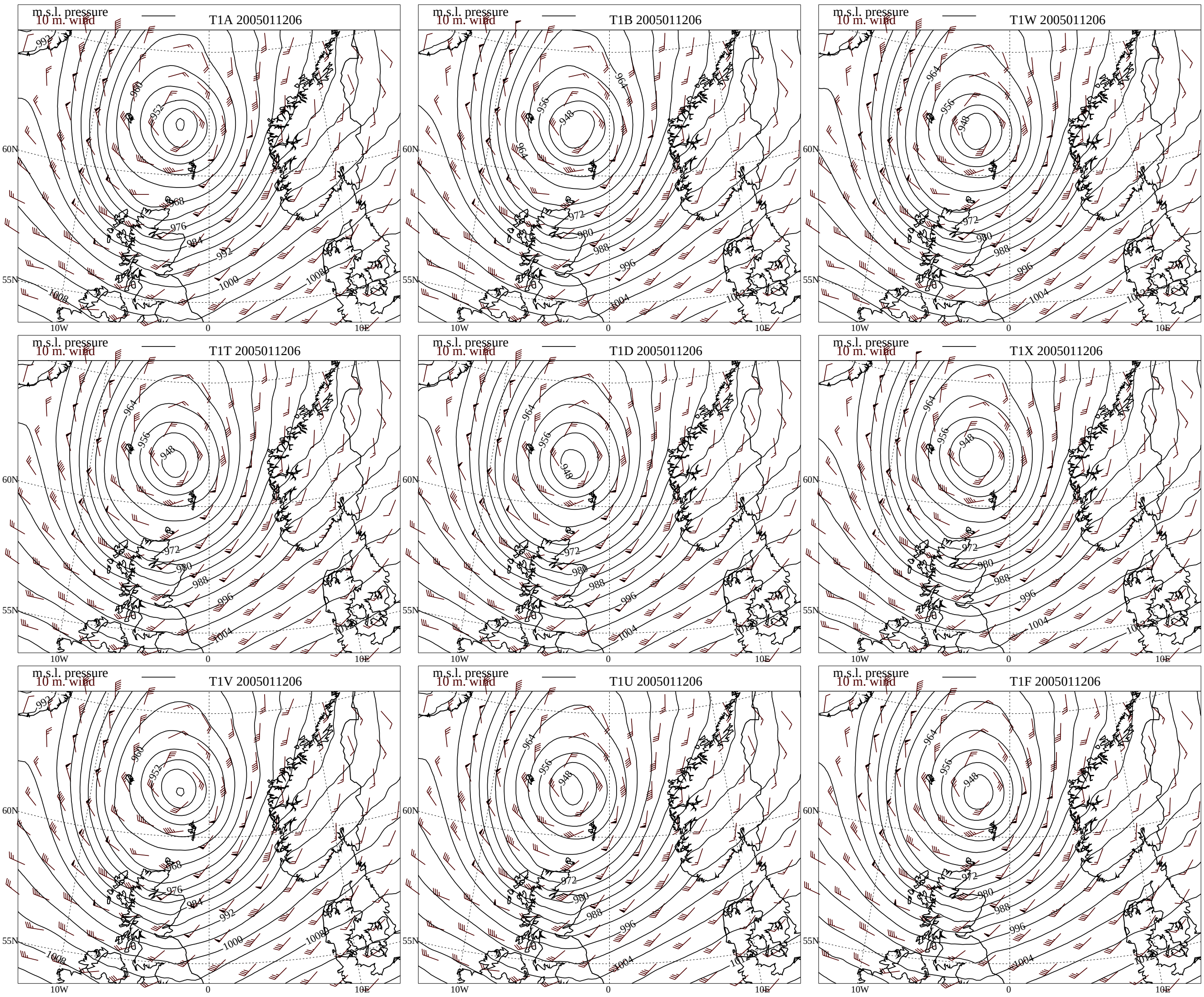

Figure 39: Analyses valid at 06 UTC January 12, 2005. T1B: T1A + aircraft; T1W: T1A + wind from other radiosondes; T1T: T1A + wind and temperature data from other radiosondes; T1D: T1A + data from all other radiosondes; T1X: T1A + E-AMDAR data; T1V: T1A + wind profiler data; T1U: T1T + all aircraft data). Mslp contours for every 4 hPa.

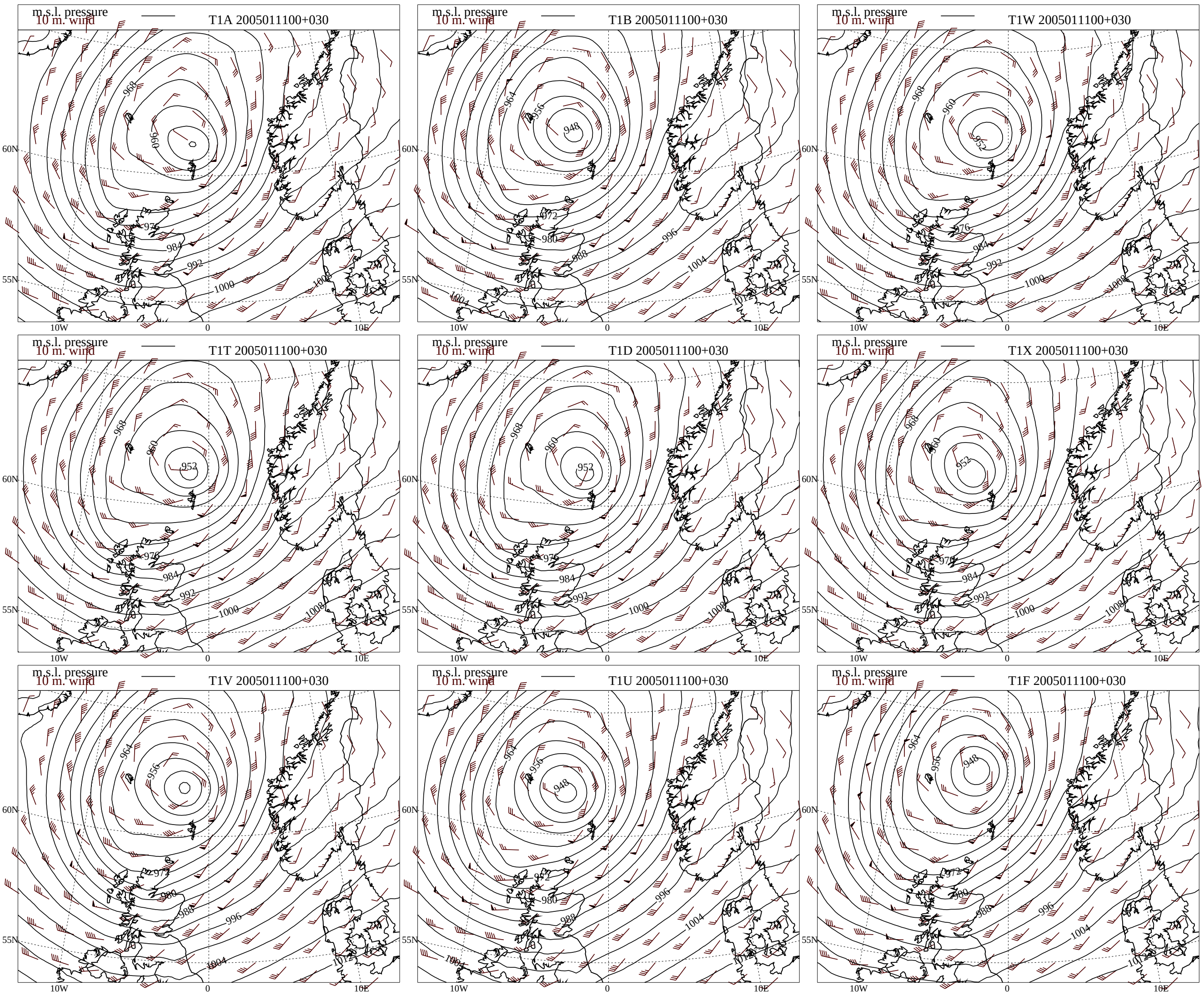

Figure 40: 30 h forecasts valid at 06 UTC January 12, 2005. (T1F: all observations used; T1A: baseline run; T1B: T1A + aircraft; T1W: T1A + wind from other radiosondes; T1T: T1A + wind and temperature data from other radiosondes; T1D: T1A + data from all other radiosondes; T1X: T1A + E-AMDAR data; T1V: T1A + wind profiler data; T1U: T1T + all aircraft data). Mslp contours for every 4 hPa.

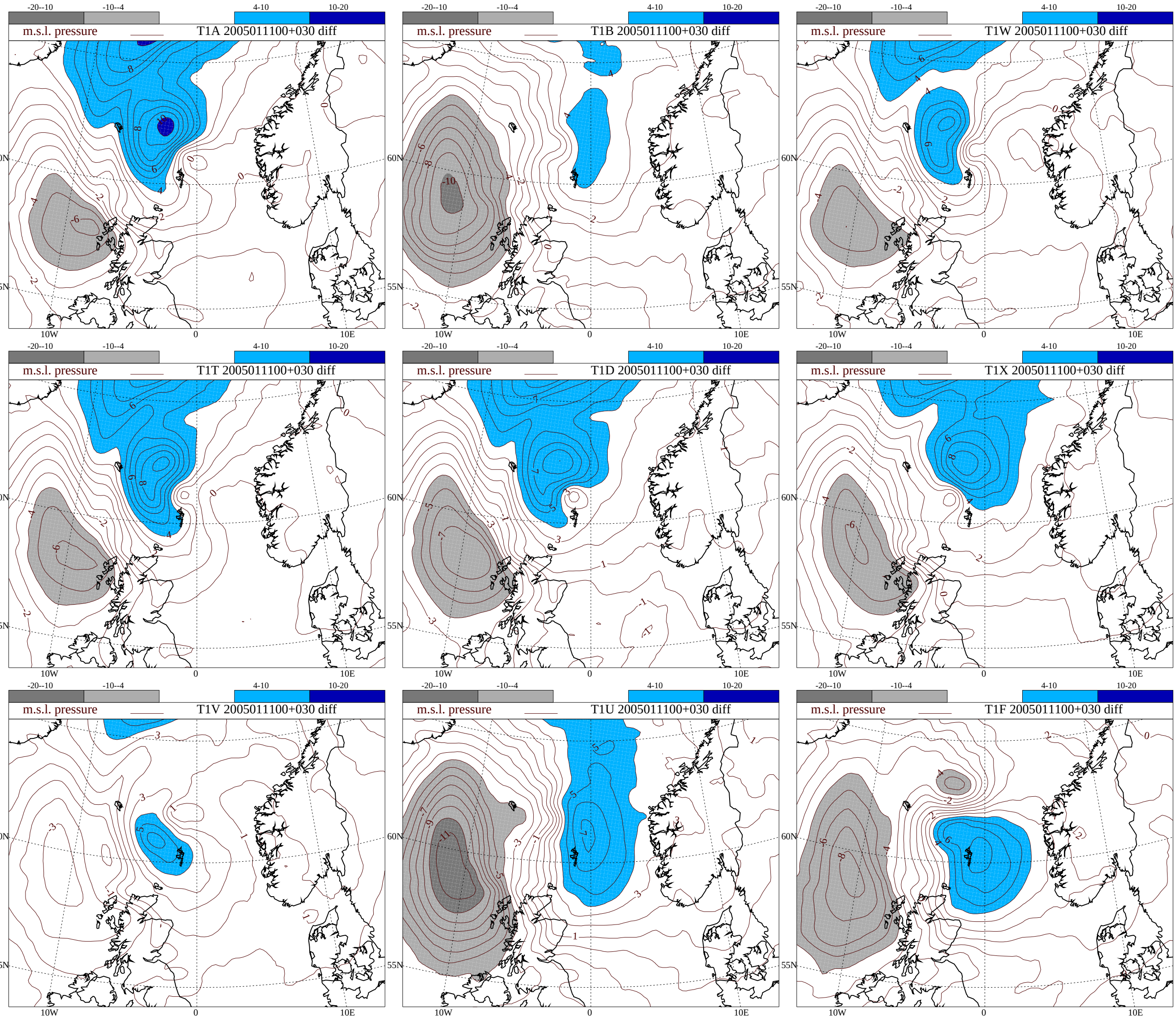

Figure 41: 30 h forecast differences against the T1F analysis valid at 06 UTC January 12, 2005. (T1F: all observations used; T1A: baseline run; T1B: T1A + aircraft; T1W: T1A + wind from other radiosondes; T1T: T1A + wind and temperature data from other radiosondes; T1D: T1A + data from all other radiosondes; T1X: T1A + E-AMDAR data; T1V: T1A + wind profiler data; T1U: T1T + all aircraft data). Mslp contours for every 1 hPa. Light grey areas for values between -4 hPa and -10 hPa, dark grey areas for values between -10 hPa and -20 hPa, light blue areas for values between 4 hPa and 10 hPa, and dark blue areas for values between 10 hPa and 20 hPa.

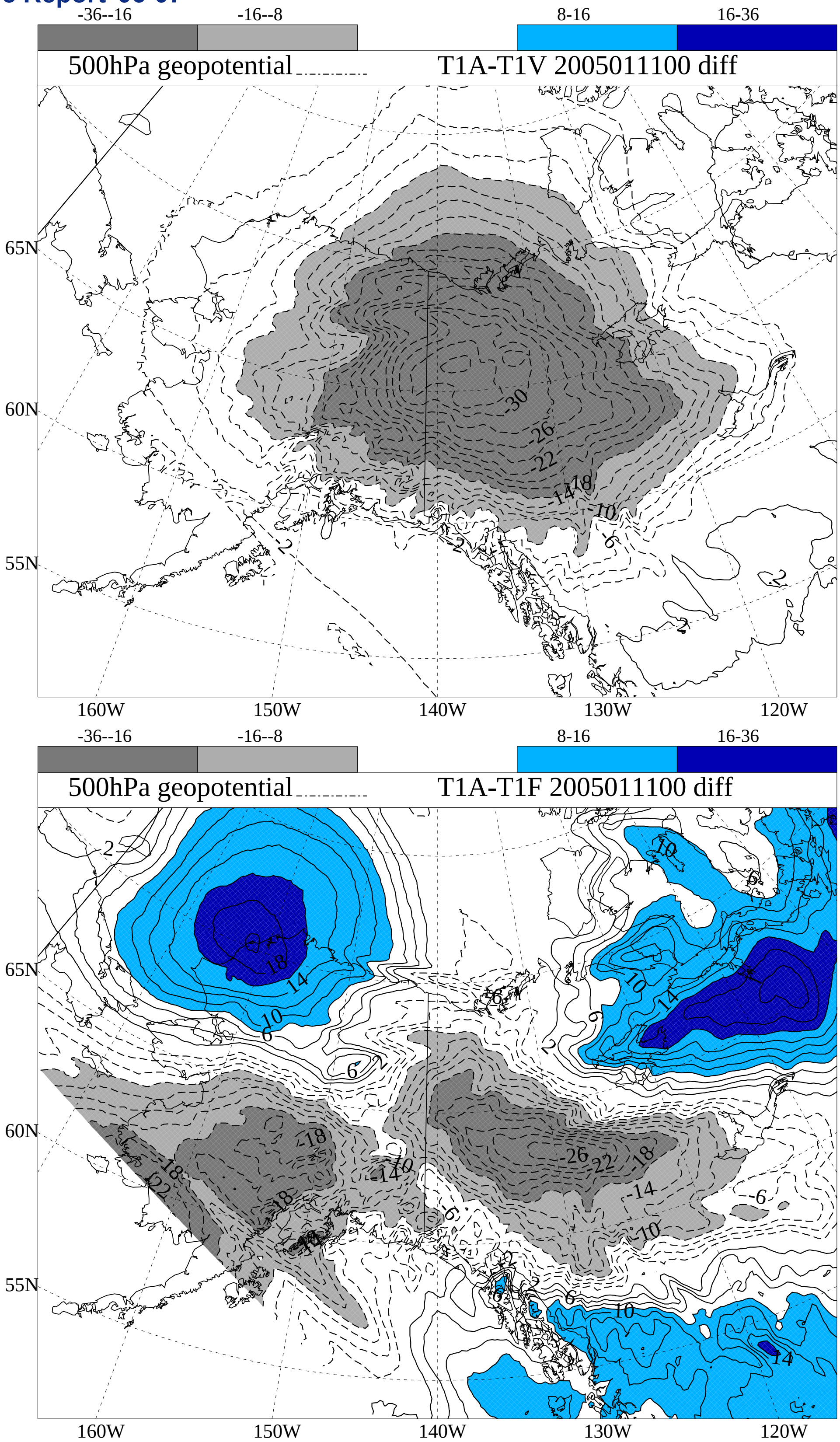

Figure 42: Initialised analyses differences between T1A and T1V (upper) and between T1A and T1F (lower) for 500 hPa geopotential height valid at 00 UTC January 11, 2005. The area is centered close to Alaska. (T1F: all observations used; T1A: baseline run; T1V: T1A + wind profiler data). Geopotential height contours for every 2 m. Light grey areas for values between −16 m and −8 m, dark grey areas for values between −36 m and −16 m, light blue areas for values between 8 m and 16 m, and dark blue areas for values between 16 m and 36 m. The edge of the DMI-HIRLAM-T15 area is clearly seen in the lower plot in the lower left corner.

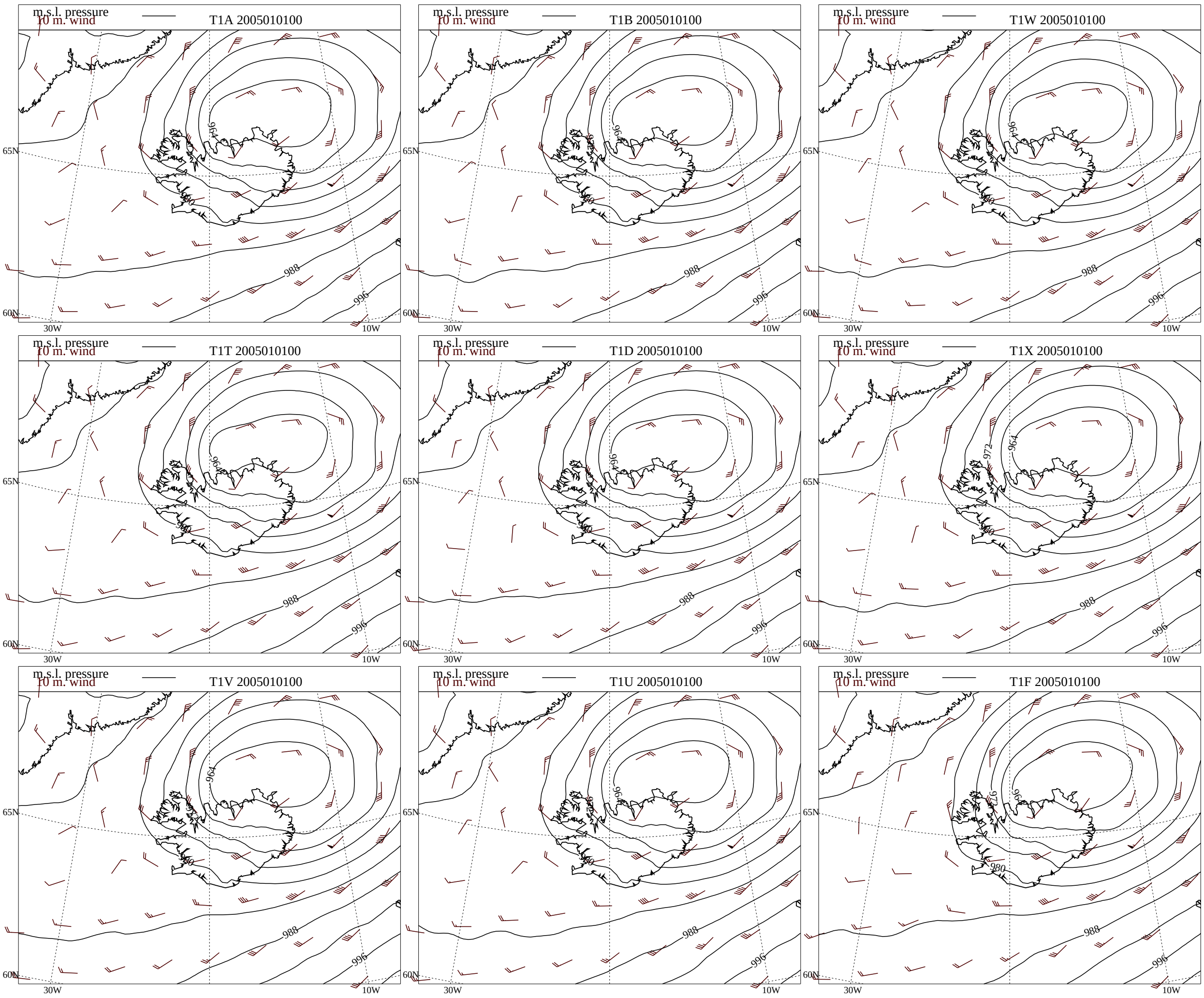

Figure 43: Analyses valid at 00 UTC January 1, 2005 for a selected region around Iceland. (T1F: all observations used; T1A: baseline run; T1B: T1A + aircraft; T1W: T1A + wind from other radiosondes; T1T: T1A + wind and temperature data from other radiosondes; T1D: T1A + data from all other radiosondes; T1X: T1A + E-AMDAR data; T1V: T1A + wind profiler data; T1U: T1T + all aircraft data). Mslp contours for every 4 hPa.

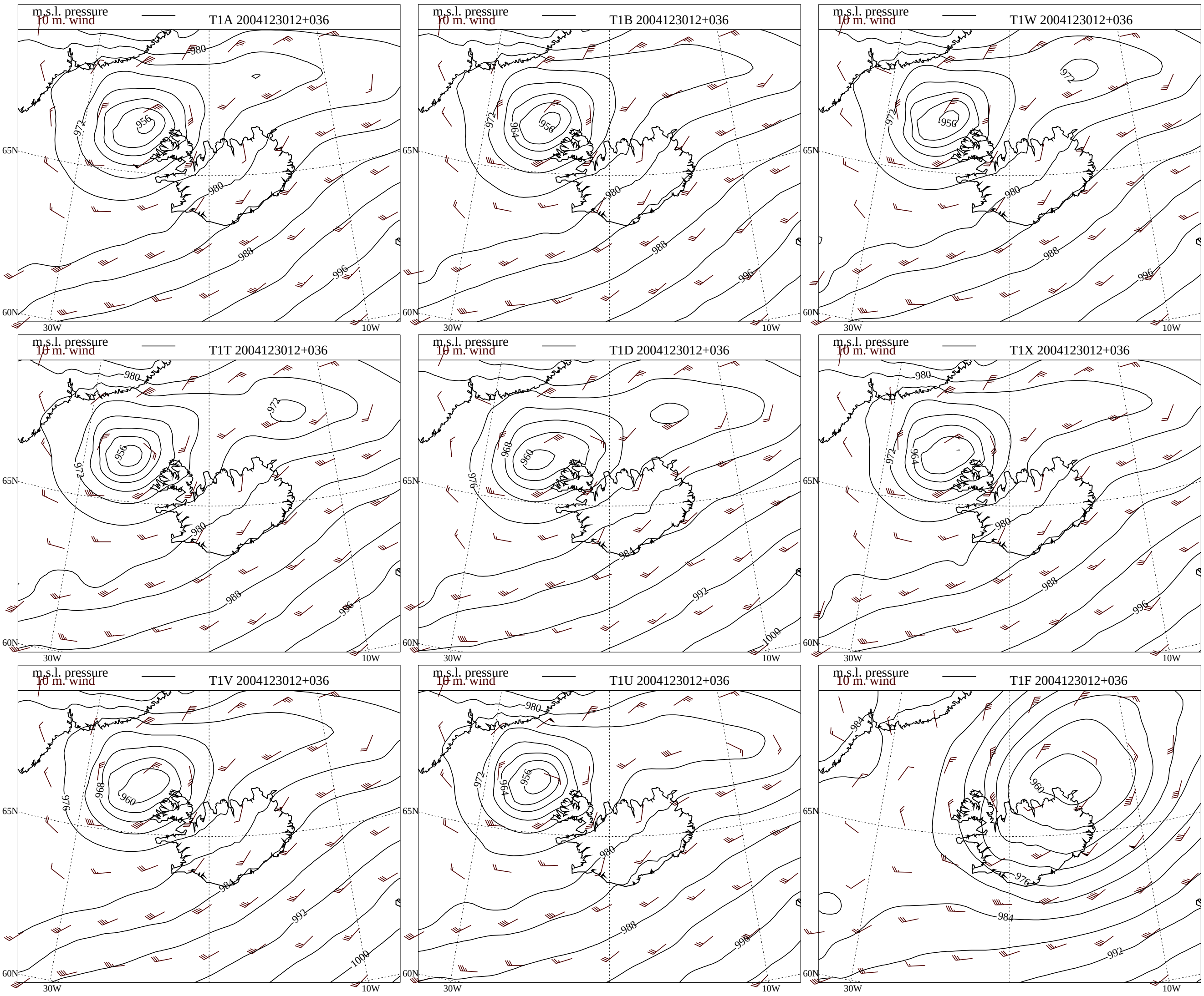

Figure 44: 36 h forecasts valid at 00 UTC January 1, 2005 for a selected region around Iceland. (T1F: all observations used; T1A: baseline run; T1B: T1A + aircraft; T1W: T1A + wind from other radiosondes; T1T: T1A + wind and temperature data from other radiosondes; T1D: T1A + data from all other radiosondes; T1X: T1A + E-AMDAR data; T1V: T1A + wind profiler data; T1U: T1T + all aircraft data). Mslp contours for every 4 hPa.

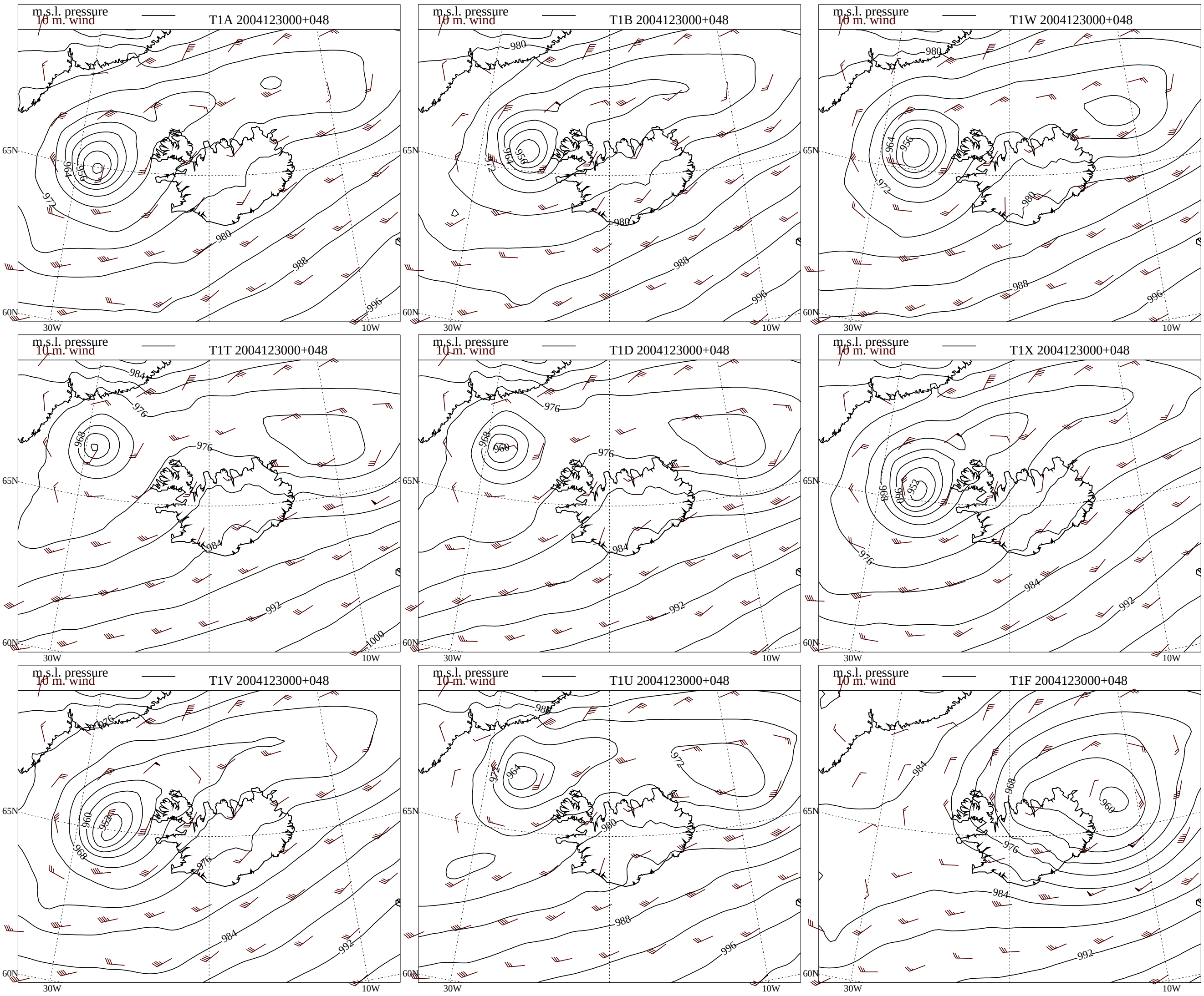

Figure 45: 48 h forecasts valid at 00 UTC January 1, 2005 for a selected region around Iceland. (T1F: all observations used; T1A: baseline run; T1B: T1A + aircraft; T1W: T1A + wind from other radiosondes; T1T: T1A + wind and temperature data from other radiosondes; T1D: T1A + data from all other radiosondes; T1X: T1A + E-AMDAR data; T1V: T1A + wind profiler data; T1U: T1T + all aircraft data). Mslp contours for every 4 hPa.

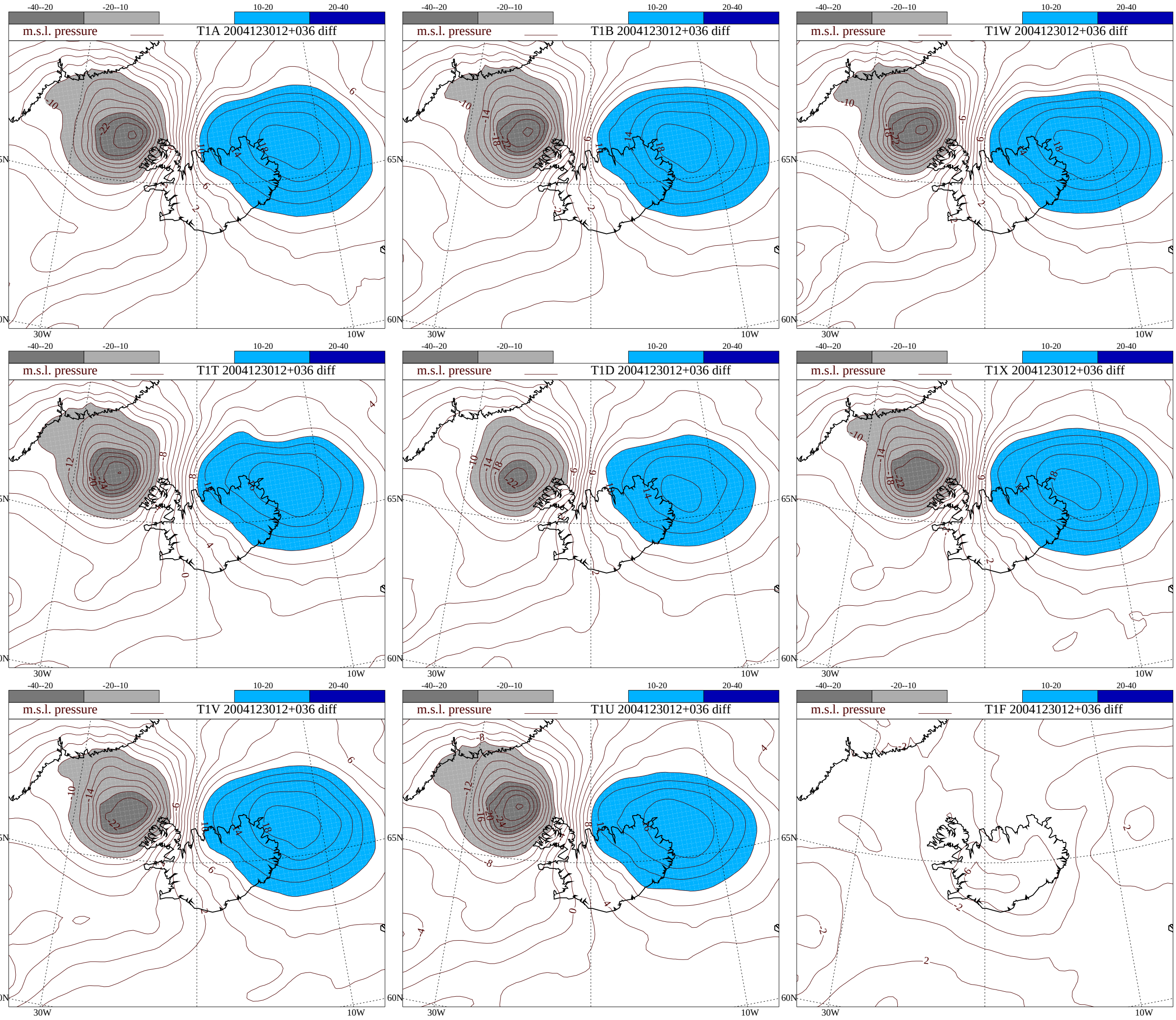

Figure 46: 36 h forecast differences against the T1F analysis valid at 00 UTC January 1, 2005 for a selected region around Iceland. (T1F: all observations used; T1A: baseline run; T1B: T1A + aircraft; T1W: T1A + wind from other radiosondes; T1T: T1A + wind and temperature data from other radiosondes; T1D: T1A + data from all other radiosondes; T1X: T1A + E-AMDAR data; T1V: T1A + wind profiler data; T1U: T1T + all aircraft data). Mslp contours for every 2 hPa. Light grey areas for values between -10 hPa and -20 hPa, dark grey areas for values between -20 hPa and -40 hPa, light blue areas for values between 10 hPa and 20 hPa, and dark blue areas for values between 20 hPa and 40 hPa.

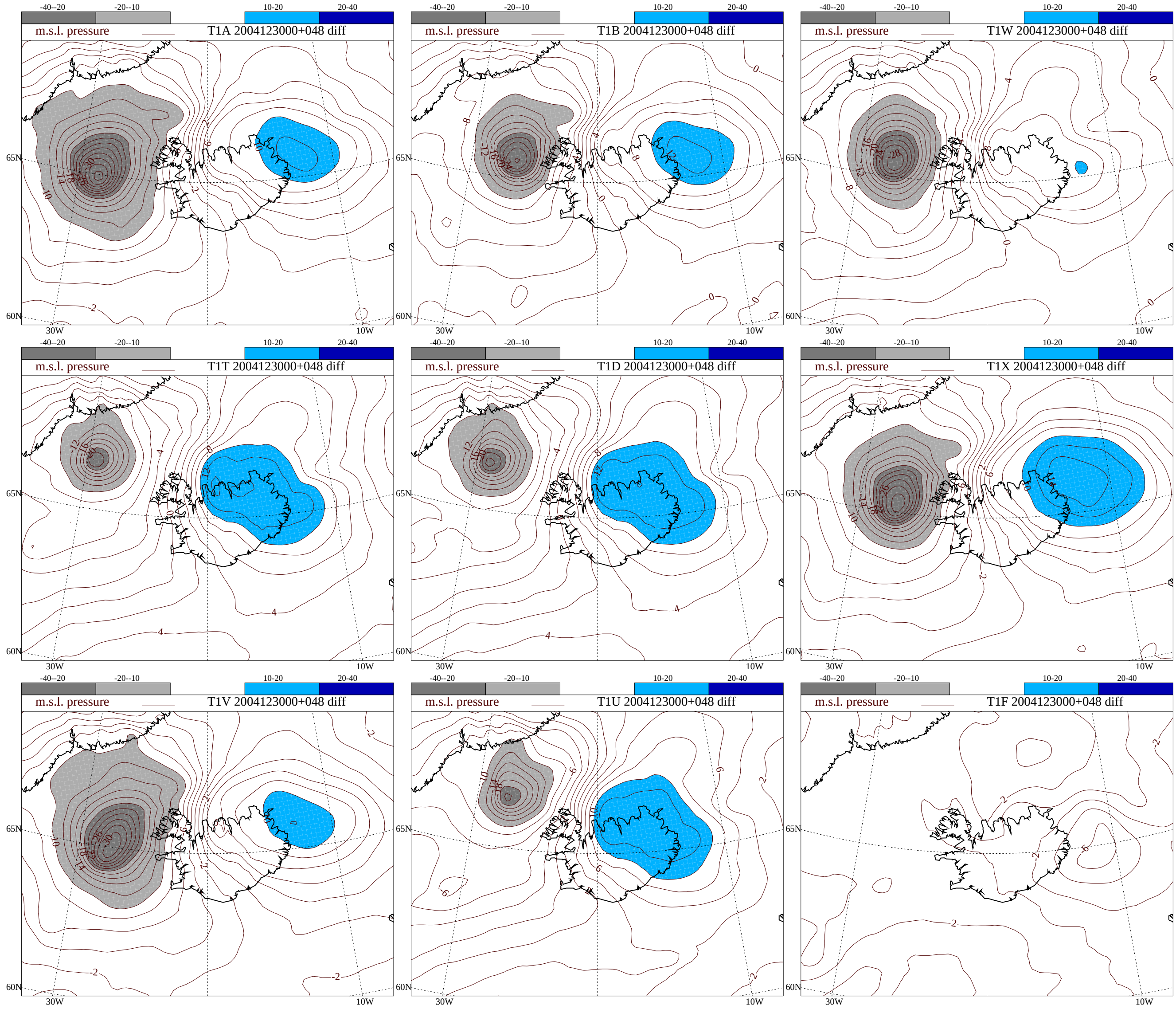

Figure 47: 48 h forecast differences against the T1F analysis valid at 00 UTC January 1, 2005 for a selected region around Iceland. (T1F: all observations used; T1A: baseline run; T1B: T1A + aircraft; T1W: T1A + wind from other radiosondes; T1T: T1A + wind and temperature data from other radiosondes; T1D: T1A + data from all other radiosondes; T1X: T1A + E-AMDAR data; T1V: T1A + wind profiler data; T1U: T1T + all aircraft data). Mslp contours for every 2 hPa. Light grey areas for values between -10 hPa and -20 hPa, dark grey areas for values between -20 hPa and -40 hPa, light blue areas for values between 10 hPa and 20 hPa, and dark blue areas for values between 20 hPa and 40 hPa.

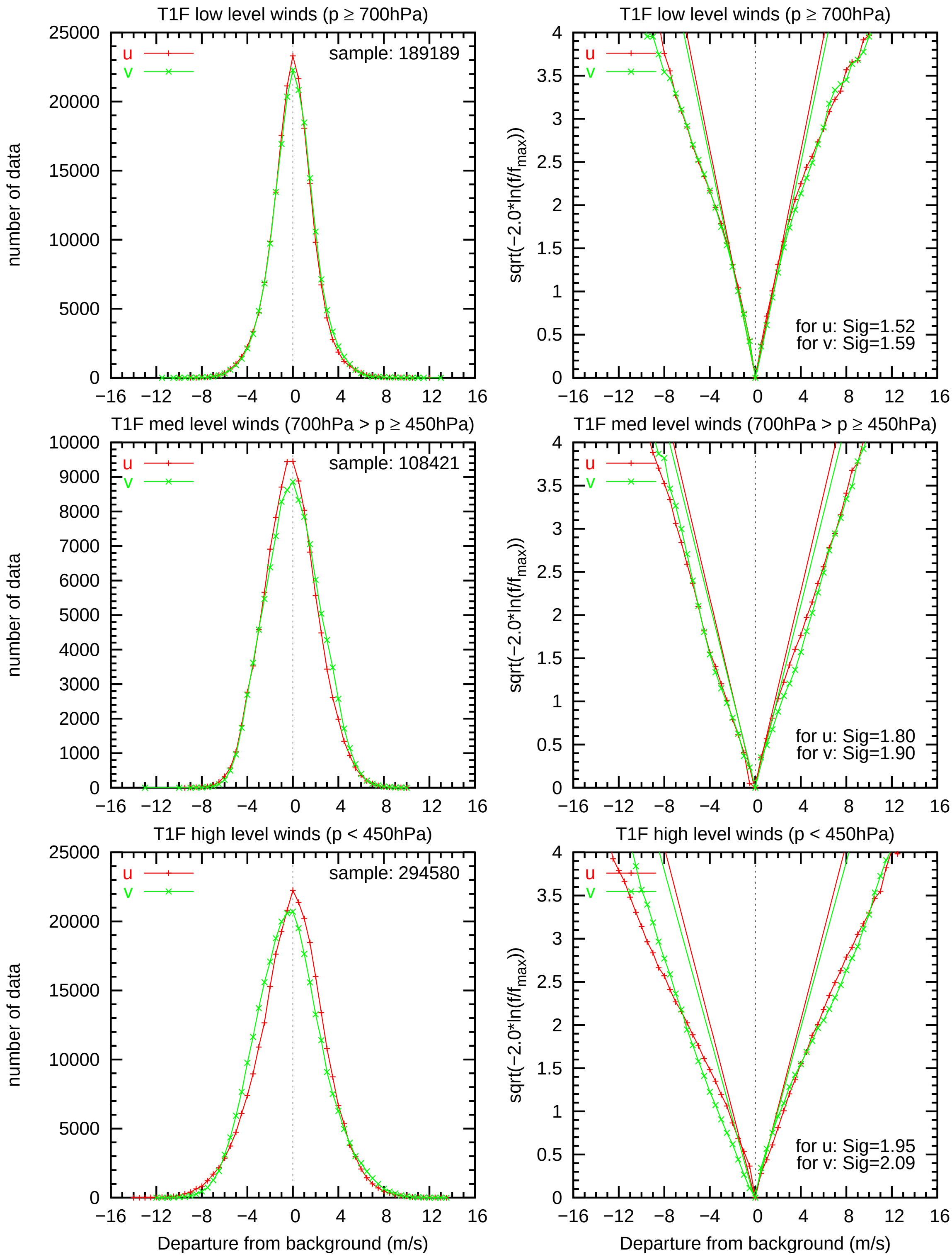

Figure 48: Distribution of Meteosat-8 AMV wind speed innovations (differences between the model first guess wind speeds and observed wind speeds) for the control run (T1F). The transformation $\sqrt{-2\ln(f/f_{\max})}$ make a Gaussian distribution linear on each side of 0.

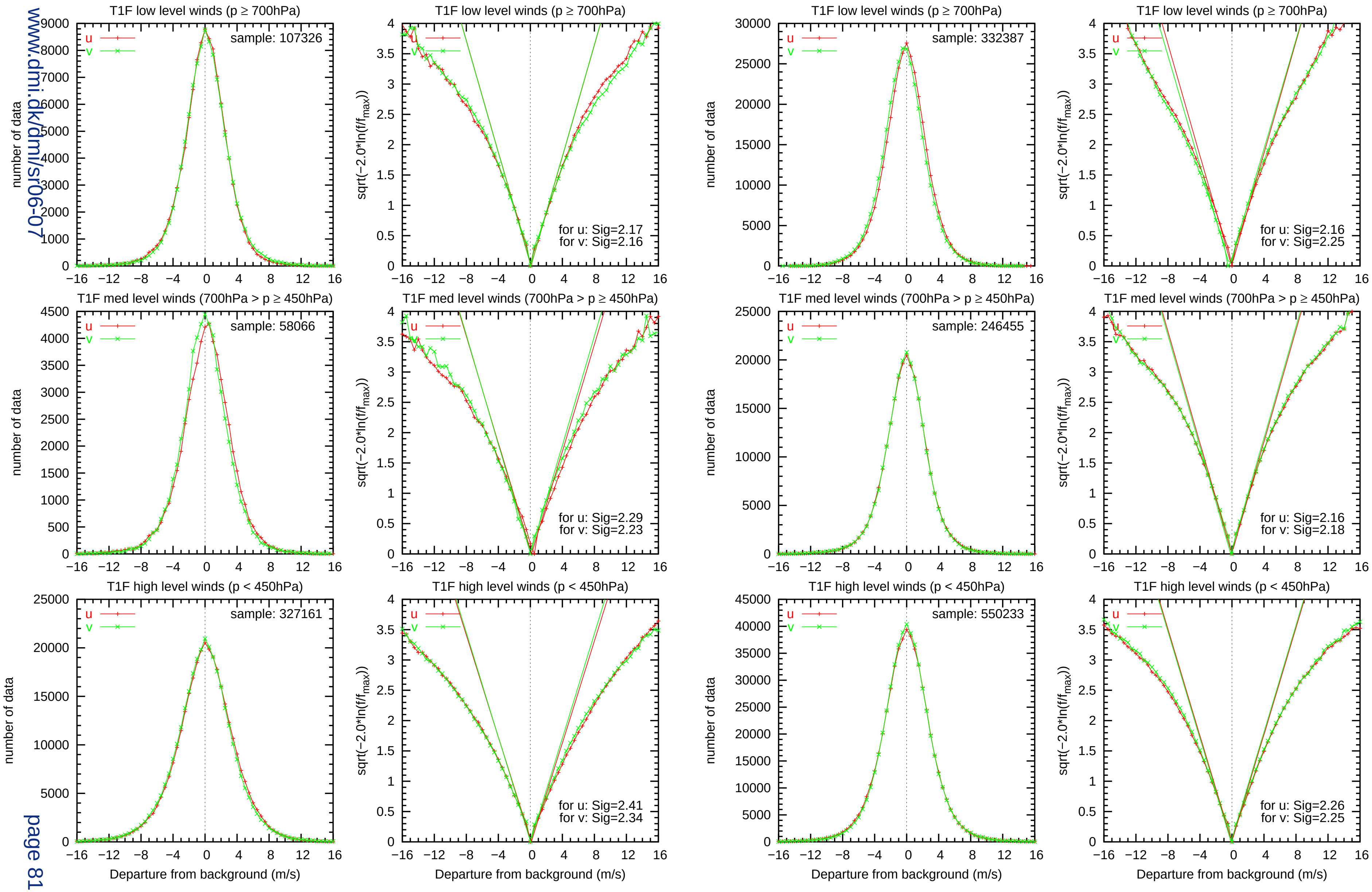

Figure 49: Distribution of radiosonde wind speed innovations (differences between the model first guess wind speeds and observed wind speeds) (left) and aircraft wind innovations (right) for the control run (T1F). The transformation $\sqrt{-2\ln(f/f_{\max})}$ make a Gaussian distribution linear on each side of 0.

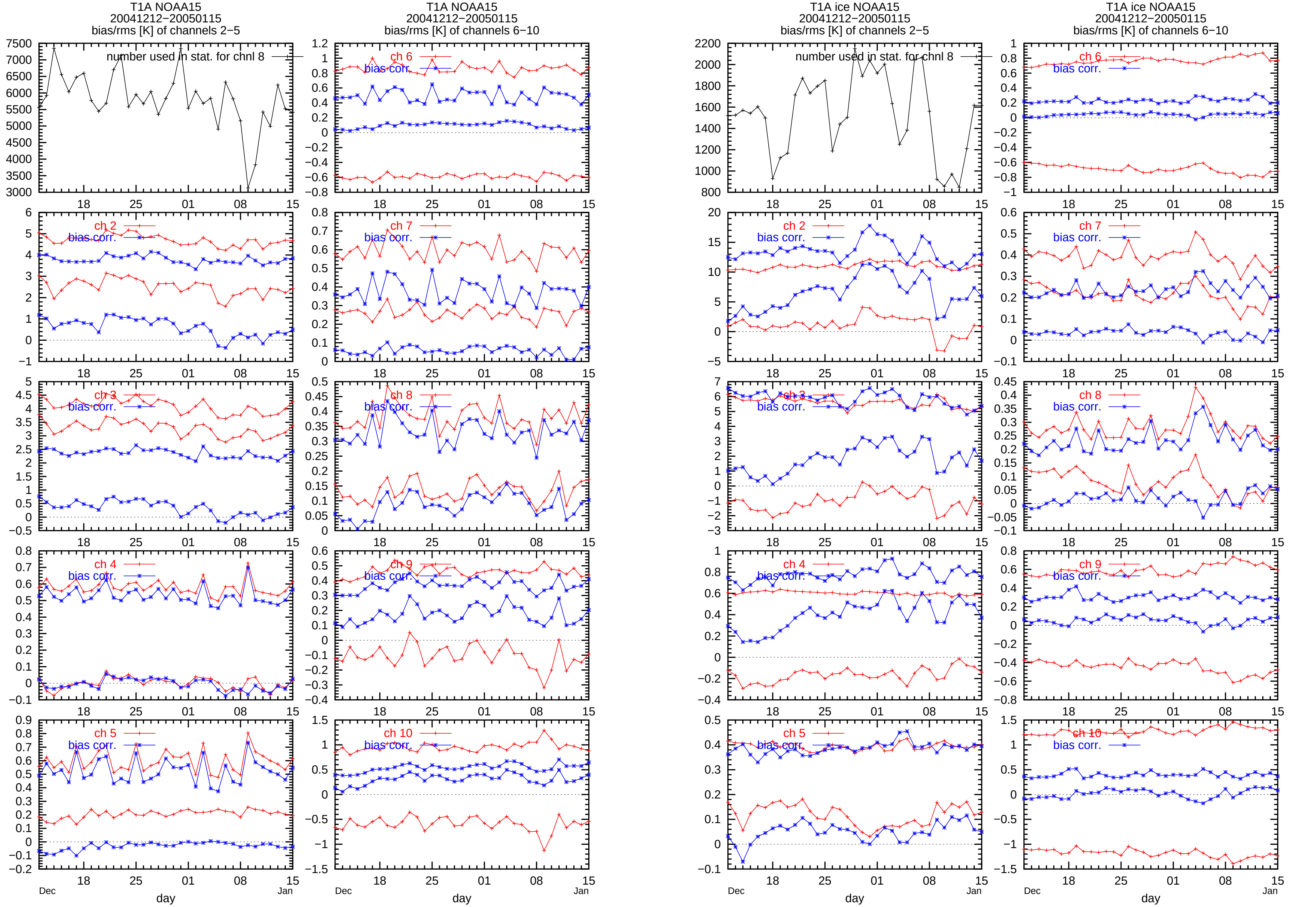

Figure 50: Daily bias- and rms-values (level 1c brightness temperature departure (in K)) for NOAA15 AMSU-A channels 2-10 in the December 2004/January 2005 period for the T1A (baseline) run. Red values for uncorrected and blue for bias corrected values. Left is for data over open sea and right is for data over sea ice. Channels 4-10 are used over open sea and channels 6-10 are used over sea-ice.

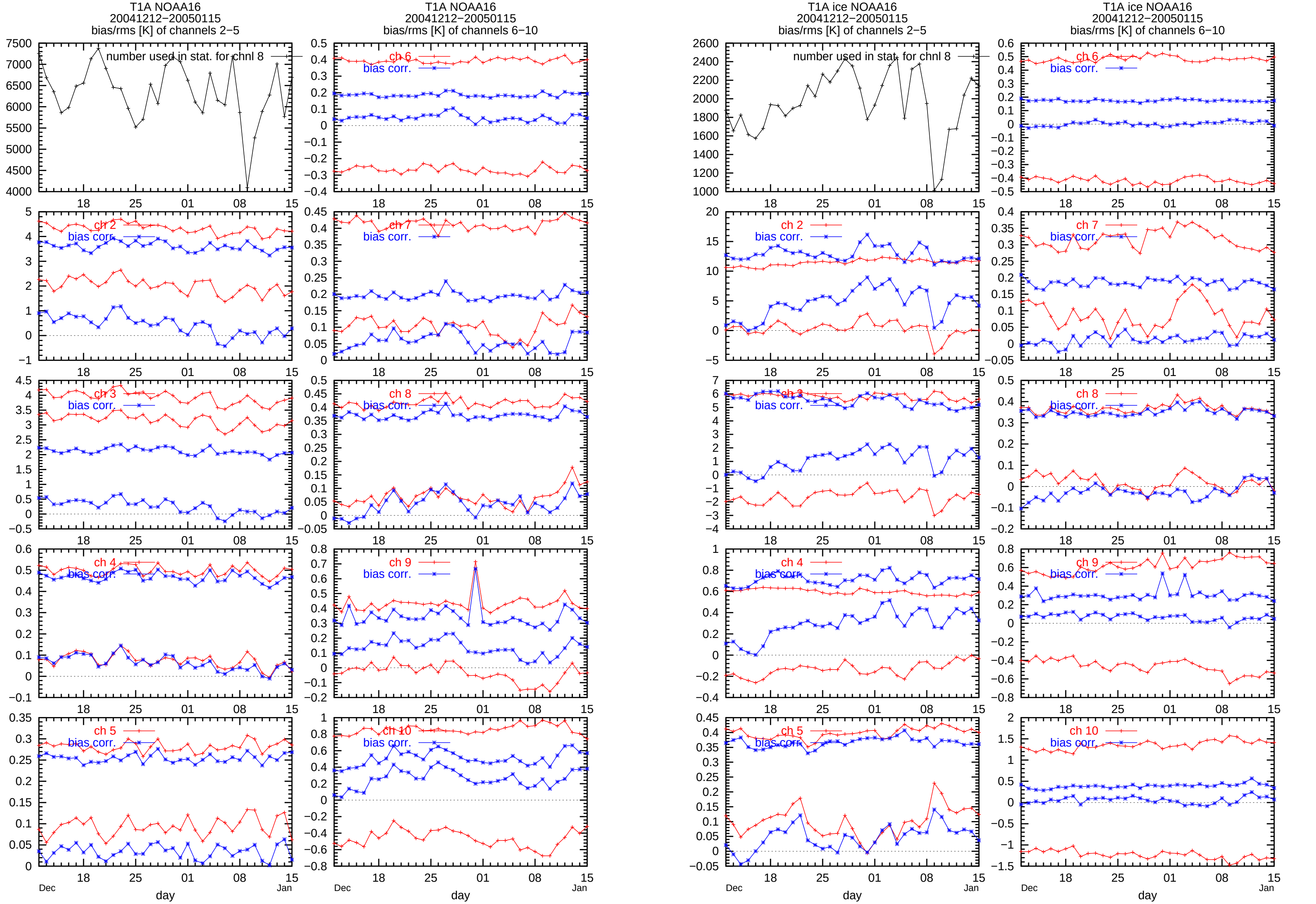

Figure 51: Daily bias- and rms-values (level 1c brightness temperature departure (in K)) for NOAA16 AMSU-A channels 2-10 in the December 2004/January 2005 period for the T1A (baseline) run. Red values for uncorrected and blue for bias corrected values. Left is for data over open sea and right is for data over sea ice. Channels 4-10 are used over open sea and channels 6-10 are used over sea-ice.

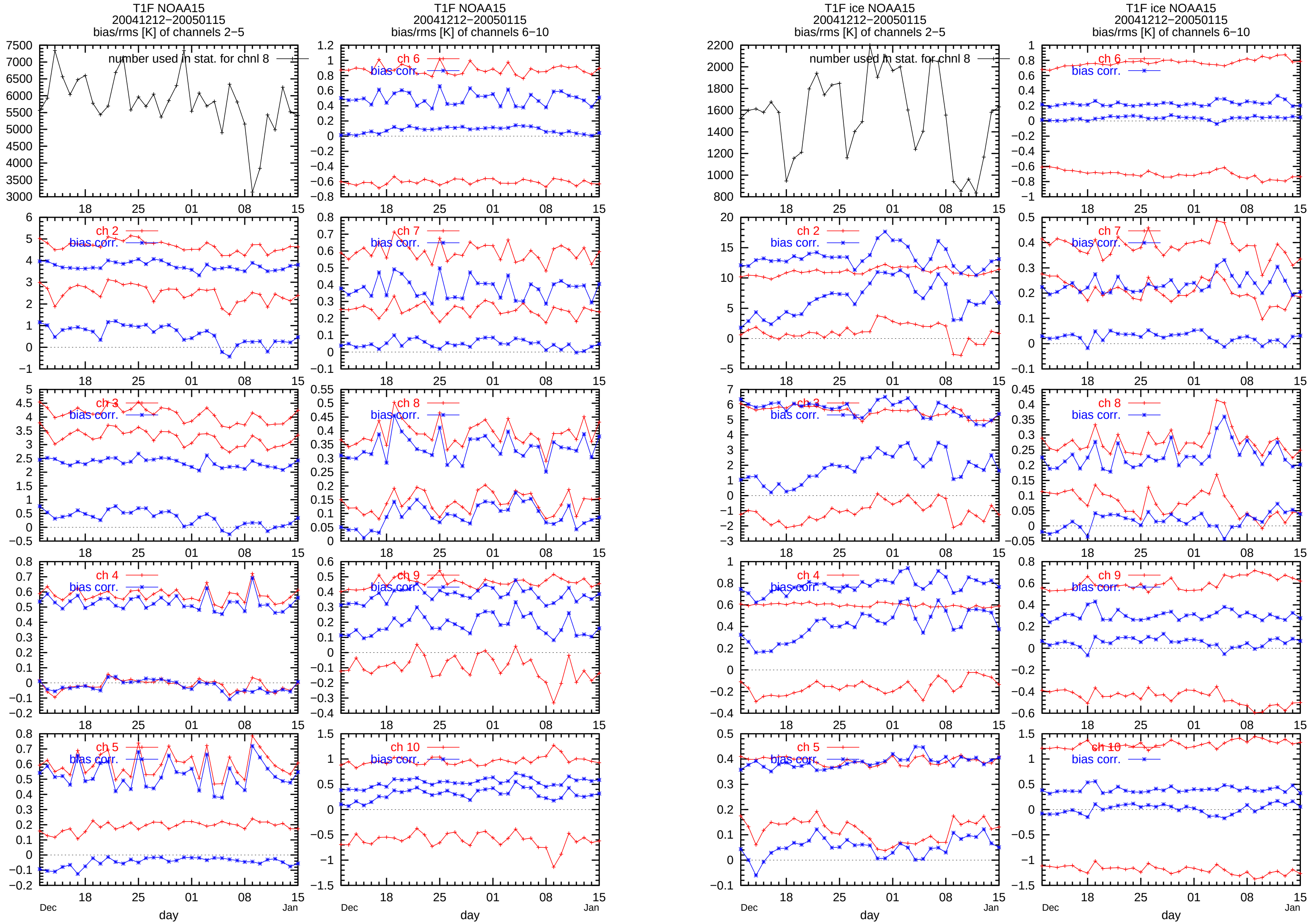

Figure 52: Daily bias- and rms-values (level 1c brightness temperature departure (in K)) for NOAA15 AMSU-A channels 2-10 in the December 2004/January 2005 period for the T1F (full observing system) run. Red values for uncorrected and blue for bias corrected values. Left is for data over open sea and right is for data over sea ice. Channels 4-10 are used over open sea and channels 6-10 are used over sea-ice.

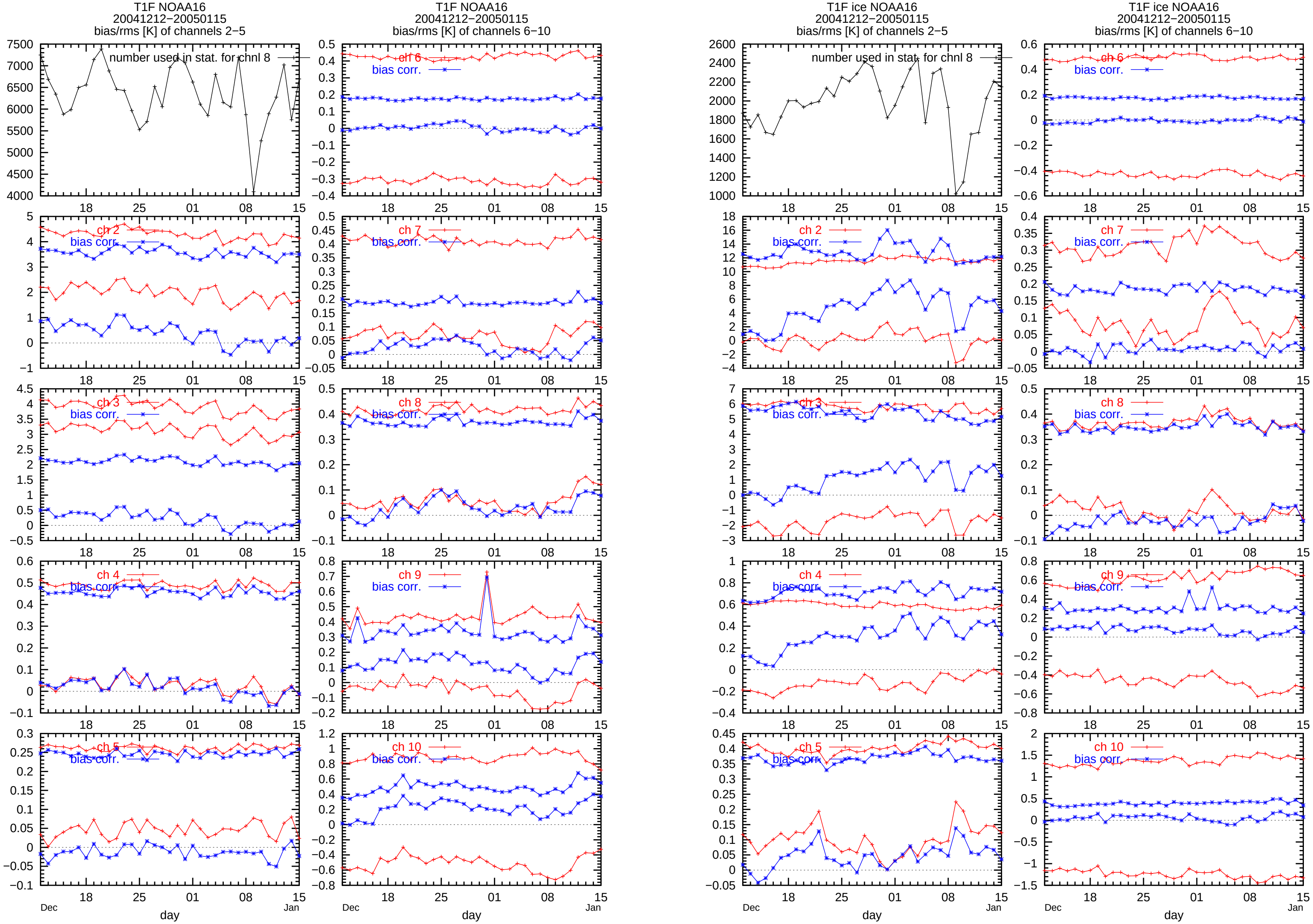

Figure 53: Daily bias- and rms-values (level 1c brightness temperature departure (in K)) for NOAA16 AMSU-A channels 2-10 in the December 2004/January 2005 period for the T1F (full observing system) run. Red values for uncorrected and blue for bias corrected values. Left is for data over open sea and right is for data over sea ice. Channels 4-10 are used over open sea and channels 6-10 are used over sea-ice.

Previous Reports

Previous reports from the Danish Meteorological Institute can be found at:
`http://www.dmi.dk/dmi/dmi-publikationer.htm`